Dynamic Analysis for Railway Tunnel at Karakore

Tequamework Assefa

A Thesis Submitted to
The School of Civil and Environmental Engineering

Presented in Fulfillment of the Requirements for the Degree of Master of Science
(Civil and Environmental Engineering)

ADDIS ABABA UNIVERSITY
Addis Ababa, Ethiopia

2017

Addis Ababa University

Addis Ababa Institute of Technology

School of Civil and Environmental Engineering

This is to certify that the thesis presented by Tequamework Assefa, entitled: *Dynamic Analysis for Railway Tunnel at Karakore* and submitted in partial fulfillment of the requirements for the degree of Master of Sciences (Civil and Environmental Engineering) complies with the regulations of the University and meets the accepted standards with respect to Originality and quality.

To be signed by the Examining Committee:

Internal Examiner_____ Signature_____ Date_____

External Examiner_____ Signature_____ Date_____

Chair Person _____ Signature_____ Date_____

Advisor_____ Signature_____ Date_____

_____

School or Center Chair Person

DECLARATION

I certify that research work titled "Dynamic Analysis for Railway Tunnel at Karakore" is my own work. The work has not been presented elsewhere for assessment and award of any degree or diploma. Where material has been used from other sources it has been properly acknowledged/ referred.

Name: Tequamework Assefa

Signature: _____

Place: Addis Ababa University

Addis Ababa Institute of Technology

School of Civil and Environmental Engineering

Graduate Studies

Railway Engineering

Date: _____

ABSTRACT

In this research thesis an attempt is made to contribute towards a better understanding of seismic response of deep tunnel using the specific case of the railway tunnel at Karakore, located in one of the active seismic zones of Ethiopia known as escarpment seismic zone.

Since stresses due to seismic action on underground structures depend on the seismic ground deformation, the characteristics of ground deformation induced by ground shaking need to be clarified. Therefore, to model the existing situation in a better way and to have good results regarding the deformations induced by the seismic action, finite element analysis has been conducted using the PLAXIS software.

The effect of vertically propagating shear wave has been considered as it is expected to be the destructive type of wave for the tunnel under consideration.

Probabilistic seismic hazard analysis and deaggregation has been done so as to obtain the most likely scenario of earthquake causing peak ground acceleration with 10% and 2% probability of exceedance in 50 years. Peak ground acceleration of 0.36g and 0.87g has been obtained from seismic hazard analysis, for 10% and 2% probability of exceedance, respectively. Two pairs of design ground motion; one with magnitude of 5.6 and radius of 20km and the other with magnitude of 5.7 and radius of 33km has been the result of deaggregation process.

Ground motion from PEER ground motion database has been selected using the design ground motion having a magnitude of 5.6 and radius of 20km, shear wave velocity and fault mechanism of the area. The selected ground motion data points have been scaled to the peak ground acceleration specified for the site with the 10% probability of exceedance. Full dynamic analysis has been performed to refine the seismic analysis using numerical method.

Transversal deformation has been the focus of this analysis and since 2D analysis has been performed, longitudinal deformation has not been considered except for the analytical case.

Besides incremental stresses due to earthquake has been calculated assuming linear superposition of dynamic stresses on static stresses.

The incremental stresses and strains due to earthquake are compared with unreinforced concrete support capacity and found above the threshold values.

ACKNOWLEDGMENT

First, I would like to thank Ethiopian Railway Corporation (ERC) for sponsoring my study.

I want to pass my gratitude to my thesis advisor, Dr.-Ing. Henok Fikre, for his continuous support, unlimited consultating hours and patience. I am also grateful to Dr.-Ing. Asrat Worku for his advice.

I would also like to thank Dr Atalay Ayele from the Institute of Geophysics, Space Science and Astronomy, Ato Biruk, Ato Abiy and Ato Abebe from ERC for their help in collecting secondary data.

I also appreciate the material and technical support of Ato Demeke Andarge, Ato Mintesinot Abera and Ato Mintesinot Tesema.

Finally, I would like to express my very intense gratitude to Dr.-Ing. Belethe Birhanu for his appreciable support, continuous discussions and encouragement and to my mother W/ro Genet Abebe for her unlimited encouragement, financial and moral support.

TABLE OF CONTENTS

LIST OF TABLES

LIST OF FIGURES

ABBREVIATIONS

α - Activity rate while using natural logarithm

α_{cc} - Coefficient to account for long term effects

β - Ratio of small to large magnitude while using natural logarithm

β_2 - Coefficient used in developing loading criteria for ODE

ε_a - Axial strain (Longitudinal deformation)

ε_{ab} -Combined axial and curvature strain in longitudinal direction

ε_{allow} - Allowable concrete strain

ε_b - Curvature strain (Longitudinal deformation)

ε_m - Bending moment induced strain (Transversal deformation)

ε_T - Thrust induced strain (Transversal deformation)

γ - Unit weight

γ_c - Partial factor for concrete

γ_{max} - Maximum free field shear strain

λm - Rate of earthquakes with magnitudes greater than m

ρ - Density

ρ_{sat} -Saturated density

σ - Intra-event aleatory uncertainty

σ_{MT} - Stress from M_{max} and T_{max}

σ_{ex} - Extrados stress

σ_{in} - Intrados stress

ø - Angle of incidence

ø_c - Critical angle of incidence

ø_m - Angle of internal friction

ζ - Maximum shear stress

ν - Poisson’s ratio

ν_l - Poisson's ratio of the lining

ν_m - Poisson’s ratio of the medium

ΔD - Diametrical change

ΔD_{ssi} - Diametrical change accounting soil structure interaction

Δm - Interval range of earthquake magnitude

ΔR - Interval range of distance

a - Activity rate while using logarithm of base 10

a_g - Design ground acceleration on type A ground

A_c - Cross-section area of tunnel lining

A1, A2, A3, A4, A5 - Support classes

a_1 - Assigned threshold levels for linear amplifications

a_2 - Assigned threshold levels for nonlinear amplifications

A-E - Soil groups labels

b - Ratio of small to large magnitude while using logarithm of base 10

b_1 and b_2 - period-dependent coefficients

b_{lin} - Period dependent coefficient

c_1, c_2 ,c_3 - Coefficient used in distance function

c_m - Cohesion

C - Compressibility ratio

CDF - Cumulative distribution function

D_t - Tunnel diameter

D - Effects due to dead loads of structural components

D - Ground type of standard deviations of single predicted values of ln Y

DC - Dead load

e - Fractional number

e_1 - e_7 - Magnitude scaling coefficients

E - Young's Modulus

E_c - Modulus of elasticity of tunnel linning

E_m - Young's modulus of the ground

EH - Horizontal earthpressure

EQ - Effects due to design earthquake motion

ES - Earth surcharge load

EV - Vertical earth pressure

EX - Effects of static loads due to excavation

F - Flexibility ratio

FHWA - Federal Highway Administration

f_c - Concrete yield strength

f_{cd} - Design compressive strength

f_{ctd} - Design tensile strength

f_{ck} - Characteristic compressive cylinder strength

f_{ctk} - Characteristic axial tensile strength

F_D - Distance function

F_{LIN} - Linear terms

F_{NL} - Nonlinear terms

$F_X(x)$ - Cumulative distribution function for PGA

F_M - Magnitude scaling

$f_M(m)$ - Probability density function for earthquake magnitude

$F_M(m)$ - Cumulative distribution function for earthquake magnitude

$f_R(r)$ - PDF for distance

F_S - Site amplification

G - Shear modulus

GMPEs - Ground motion prediction equations

G_m - Shear modulus of the medium

H - Effects due to hydrostatic water pressure

H_i- Depth of a single soil class

h - Near-source effective depth coefficient

I_c - Moment of inertia of the tunnel section

I_{cl}- Moment of inertia (for longitudinal deformation)

I_{cx} - Moment of inertia (for transversal deformation)

K - Total scaling factor for PGA of selected ground motion

K' - Total scaling factor for PGV of selected ground motion

K_a - Longitudinal spring coefficient of medium

K_t - Transverse spring coefficient of medium

K_1 - Full slip lining response coefficient

K_2 - No slip lining response coefficient

L - Love waves

LL - Effects due to live loads

L_t - Length of tunnel

L_w - Wavelength

M_b - Bending moments

M, m - Moment magnitude

MDE - Maximum design earthquake

M_h - Hinge magnitude

m_j - Discretized magnitude

m_{min} - The smallest magnitude of earthquake

m_{max} - Upper bound of earthquake

M_{max} - Maximum bending moment

m_{max}^{obs} - The largest historical earthquake

Mref - Reference magnitude to which the magnitude dependence of the geometric spreading is referenced

N - Normal force

n_M - Increments of magnitude

n_R - Increments of distance

NS - Dummy variables used to denote normal slip fault

ODE - Operating design earthquake

P - Compressional waves

PDF - Probability density function

PEER - Pacific Earthquake Engineering Research Center

PGA - Peak ground acceleration

pga _ low - Variable assigned to transition between linear and nonlinear behaviors

pga4nl - Predicted peak ground acceleration in g for V_{ref} = 760m/s with F_s=0 and ε=0

PGV_s - Peak particle velocity

PGV_s' - Peak particle velocity of selected motion

PSHA - Probabilistic seismic hazard analysis

Q - Axial forces

r- radius of tunnel

R - Rayleigh waves

R_{hyp} - Hypocentral distance

R_{ep} - Epicentral distance

R_{eq} - Equivalent radius of tunnel

R_{inter} - Interface strength reduction factor

R_{JB} - Closest horizontal distance to the surface projection of the fault plane

r - Radius of the tunnel

R_{ref} - Reference distance at which near source predictions are pegged

RS - Dummy variables used to denote reverse slip fault

S - Shear waves

SS - Dummy variables used to denote strike-slip fault

T-04 - Tunnel 4

T- Inter-event aleatory uncertainty

t - Thickness of the tunnel lining

T_F - Fundamental period

T_{max} - Maximum thrust force

U - Dummy variable used to denote unspecified fault

U_{req} - Required structural strength capacity

USGS - US Geological Survey

V - Shear forces

V_{ref} - Specified reference velocity

V_{si} – Shear wave velocity of single soil class

V_{s30} - Shear wave velocity from the surface to 30m

X_s - Easting of source

X_t - Easting of tunnel

Y - Ground motion parameter

Y_s - Northing of source

Y_t - Northing of tunnel

Z_s - Elevation of source

Z_t - Elevation of tunnel

2D - Two dimension

3D - Three dimension

CHAPTER 1 INTRODUCTION

Facilities can be provided in underground spaces with underground structures being the main parts. Transportation facilities are one of the major underground facilities whose main structural part is tunnel.

Tunnels are underground structures in which the length is much larger than the cross-sectional dimension. They could be exposed to both static and dynamic loading. Design and analysis of tunnel linings are usually performed for the static loadings only (Shaalan et al., 2014). Loadings, which creat vibrations varying with time result in dynamic loadings. Such sources can be explosion, moving train, earthquake, pile driving and so on. Vibration from earthquake is a natural phenomenon that is so powerful to cause severe damage. Therefore, the design and analysis of tunnel linings should extend towards dynamic loadings in addition to the static ones. The dynamic analysis for this thesis would be for the dynamic stress and strain induced by earthquake on a railway tunnel.

A study conducted by Gouin (1979, cited in Kinde et al.,2011) suggests that as many as 15,000 tremors, strong enough to be felt by humans, had occurred in Ethiopia proper and the Horn of Africa in the 20th century alone. A similar study by Kebede (1966, cited in Kinde et al.,2011) indicated that there were a total of 16 recorded earthquakes of magnitude 6.5 and higher in some of Ethiopia's seismic active areas in this same century.

The 1961, magnitude 6.7, Karakore earthquake is one of the most significant earthquakes in Ethiopia. Karakore is located in the escarpment seismic zone of Ethiopia. The tunnel which is going to be analyzed in this thesis is located in this seismic zone.

Most earthquakes affect tens of square kilometers while the severest can cause destruction over areas of 2500km^2 or more(Bell, 2002). Therefore, structures built in the destructive region of earthquake require assessment of wave propagations effects.

Earthquakes of magnitude 5.0 or greater generate sufficiently large ground motions to be potentially damaging to structures (Bell, 2002).

Two levels of earthquake ground motions are commonly considered in tunnel design and analysis. They are the maximum design earthquake (MDE) and the operating design earthquake (ODE) (Hashasha et al., 2001; Pavlovic, 2005). The maximum design earthquake is the earthquake event with a return period of several thousand years and small probability of exceedance, approximately 5 % or less. The operating design earthquake is the earthquake event with recurrence interval of several hundred years and that can be reasonably expected to occur during the facility life. Public life safety and sustained functioning of the structure are the aim for the maximum design earthquake and the operating design earthquake respectively.

The geology of the area of this study through which the railway tunnel traverse is dominated by Ashangi and Kemise formation (Belay et al., 2009). The main rock type within Kemise formation is rhyolitic tuff. It consists of rhyolite, ignimbrite, tuff and ash with subordinate basalt.

The railway tunnel is about 1.5km long constructed under a mountain. The overburden along the alignment could reach up to 320m. The section of the tunnel which is going to be analyzed in the next sections is the weakest section in the entire tunnel stretch excluding the portals.

As the railway tunnel considered in this thesis is one of the major structures which are developing currently in Ethiopia, stability checking of such big structures is required. The risk due to an earthquake for such capital intensive structures need to be controlled or at least minimized as it could lead to great losses. Kinde et al. (2011) state the absence of understanding of the levels of threats incurred by seismic hazard on the serviceability of structure even among engineers. Therefore, a number studies are required to achieve better

understanding. Besides, as it is new advancement towards building such structures and since infrastructural development is advancing in the country; studies could help in raising the understanding level of the topic.

1.1. Objectives

1.1.1. General objective

The general objective of this thesis is to analyze response of tunnel for ground shaking effects due to earthquake. This will be done on railway tunnel at Karakore which is located in escarpment seismic zones of Ethiopia.

1.1.2. Specific objectives

- Calculating deformations caused by ground shaking upon the application of selected ground motion
- Comparison of calculated deformation with permissible limits
- Proposing remedial measures in case of any seismic threats on the above mentioned tunnel.

1.2. Problem statement

In Ethiopia, large scale structures weren't constructed in earthquake prone areas. However, in recent years, due to development of infrastructures in seismic areas, the effect of earthquakes started to get some attention. Up to recently, focus was mostly concentrated on buildings. Other structures need also attention as long as they are constructed in seismic areas.

The effect of seismic event on tunnel structure should be well understood first. Transient deformations due to propagating waves affect the whole length of the tunnel and it is not limited around the fault unlike permanent displacement. In addition, the return period of transient deformations is small as compared to return period of permanent displacements.

This fact makes transient deformation to be the most frequently occurring deformation as compared to permanent deformation during the life time of the structure. Therefore, even though analysis for large displacement should not be omitted, the most frequently occurring effect which influences the whole length need to be analyzed.

The movement of the ground as a result of traveling seismic waves affects the response of the structure, and this in turn affects the response of the ground. How such effect and interaction are considered is a major issue. Due to difference in properties of the tunnel and the surrounding material, differential strain with the corresponding differential stress may occur during earthquake excitation.

Loads due to seismic events are stated in deformations along the longitudinal and transverse direction of the tunnel. Calculations of the magnitude of such deformations require pertinent ground motion parameters like peak ground acceleration and velocity. These ground motion parameters together with geotechnical engineering parameters and material properties of the tunnel lining will be the major input data.

Numerical modeling is used for analyzing the tunnel. The analysis is conducted using the time history analysis approach. Stresses and strains are analyzed for drained condition with seismic load and the capacity of the structure will be checked.

1.3. Limitations

Deformations and stresses due to earthquake load have been calculated for the weakest section and for 320m high overburden pressure. These calculations were done using both numerical and analytical methods. For the dynamic loading, ground motion was selected based on probabilistic seismic hazard analysis and deaggregation results.

A single stretch between 178+807 and 178+864 of the tunnel section is taken for this analysis. Portal areas were excluded. Besides, regarding the earthquake effects, numerical analysis is done for ground shaking effects due to operating design earthquake. Structures such as ventilation shafts, stations, joints or others which create inconsistency or great difference in stiffness were excluded from this thesis. Only long term effects were considered so that drained analysis was carried out as long as the soil behavior is concerned. Some material properties are taken from the literature and existing correlations rather than from direct tests. Ground type identification was done using shear wave velocity. The analysis is conducted assuming the absence of train during the occurrence of an earthquake.

CHAPTER 2 LITERATURE REVIEW

2.1. Introduction

Usage of underground structures for transportation and utility works makes their seismic vulnerability issue sensitive. Underground structures suffer less than surface structures from earthquakes due to the confinement they attain from the medium. Generally, their seismic response (Paci,2014) is different from surface structures. It is dominated by the behavior of the medium in which they are buried, as their relative displacement with respect to the medium is small. They also have higher damping due to the confinement. Besides, their inertial force due to weight of structure is negligible when compared with the medium.

Nevertheless, significant damages were registered from some underground structures in recent large earthquakes; which can be found in literatures(Gaspari et al., 2012; Torcato,2010) .Seismic analysis of tunnels close to seismogenic faults is a complex problem, which is often neglected at the design stage for the lack of specific codes or guidelines for the design of underground structures in seismic conditions and also because, as mentioned above, underground structures are considered less vulnerable to earthquake loading(Corigliano et al. 2011).

Seismic waves can be divided broadly as body waves and surface waves. Propagation velocity of body waves is high which makes them faster than surface waves (Nikam and Bhagat , 2016). As seen by the formula provided by Wang (1993) for analytic solution, induced strain on tunnels due to wave propagation is directly proportional to peak ground acceleration and velocity while it is inversely proportional to wave propagation velocity. Therefore the ground strain produced due to propagation of body waves is much less than the one produced by surface waves which have less propagation velocity.

The body waves are classified into compressional (P) and shear (S) waves while surface waves are classified as Rayleigh (R) and love (L) waves. From the body waves, which travel

inside the ground, P waves are less destructive due to their lower amplitude. The force created by the customary vertical motion of P waves rarely exceeds the force of gravity (Boore and Joyner, 1982; Raju et al., 2004). R waves have to be considered for shallow tunnels and L waves have lesser frequency than the S waves. Therefore for deep tunnels, S wave is the strongest to create great destruction.

Horizontal loads are the concern for seismic resistance since structures are designed to resist gravity or vertical loads. In addition, body waves arrive to ground surface nearly vertically due to refraction by layering. Therefore, as compressional waves will only be responsible for vertical motion and horizontal load need to be the focus, vertically propagating shear waves should be the one to be considered (Kamatchi et al., 2013).

2.2. Effects of Earthquake on Tunnel

Transient and permanent ground deformations are the effects of earthquake on tunnels. Small strains result from transient deformations (Gaspari et al., 2012).With regard to underground structures including tunnel, the seismic effect is categorized as:

- Ground shaking
- Ground failure

Liquefaction, fault displacement, rock slides, landslides, soil subsidence and slope instability are grouped under ground failure category while ground shaking refers to deformations of ground as the result of propagated seismic wave. Most ground failures cause destruction of portals and shallow structures and result in permanent deformations (Gaspari et al., 2012). These permanent deformations are large scale deformations. If great attention is provided to slope stability, most damages from ground failure can be reduced.

If tunnel passes through fault zone, damage could occur ranging from minor cracking of lining to total collapse. Most of the time, the damage due to fault slip will be local failure (Owen and Scholl, 1981). Since fault slip can't be prevented, damage could only be

eliminated by avoiding intersection with faults. If not possible, repairs after occurrence of earthquake should be planned.

Rock fall, rock slabbing, rock fracturing, cracking, shifting of rock bolts, spalling of liner and other surfacing materials, unraveling of rock bolted system and steel set collapse can result from ground shaking.

2.3. Response of Tunnel to Earthquake Ground Motion

The tunnel response is greatly influenced by the strain and curvature caused by wave propagation. The type of wave travelling determines soil particle motions of the medium in which the tunnel is located. The following factors majorly influence the damage related to ground shaking (Lanzano, 2008):

1. The shape, dimensions and depth of the structure;
2. The properties of the surrounding soil or rock;
3. The properties of the structure; and
4. The severity of the ground shaking

The most serious direct effect of an earthquake in terms of structures is ground shaking (Bell, 2002).

Methods of analysis regarding the deforming effects of tunnel linings are provided. Earlier analyses use solution of wave equation in one dimension to determine longitudinal effects of earthquake on tunnel. However, current analyses provide recommendations regarding the deformation both along the longitudinal and transversal direction of the tunnel.

The response of tunnel to earthquake motion can be described using three primary modes of deformation; (Gaspari et al., 2012)

1. Axial compression and extension
2. Longitudinal bending
3. Ovaling or racking

Generally the additional loads due to an earthquake result in two motion components: ovalisation in the transverse direction and movement in the longitudinal direction.

2.3.1. Longitudinal deformation

Axial deformations and longitudinal bending deformations are included under the longitudinal deformation. Seismic waves producing motion parallel to tunnel axis causes axial deformation. Such waves cause alternating compression and tension as shown in Figure 2.1 (a). Figure 2.1 (b) shows waves capable of producing particles motion perpendicular to the longitudinal axis. These waves are responsible for bending deformation.

Incidence angle of wave propagation is difficult to find. Therefore in calculating induced strains, incidence angle which maximize the resulting strain will be used (Hashasha et al., 2001; Nava-Tristán et al., 2008). This is also taken as a safety margin for the uncertainties that occur in the determination of parameters.

2.3.2 Transversal deformation

Under this category ovaling deformation which is responsible for shape change is dealt with. Ovaling deformation occurs when shear waves propagate perpendicular to tunnel axis as shown in Figure 2.1 (c). Associated diametrical change can be calculated in two ways: either by considering the ground as perforated or nonperforated. Both considerations ignore the presence of the lining but usage of perforated ground requires sufficiently flexible lining.

Usually, the main criterion for lining design is the deformational effect of shear waves that propagate in the vertical direction. If the wavelength is short compared to the tunnel diameter, deformation will be asymmetric, resulting in an uneven distortion of the tunnel lining. However, if the wavelength is relatively long, as it is the common case, the problem can be treated as pseudo static, so the deformation will be approximately symmetrical but still elliptical due to the difference in field stress magnitudes in the direction of wave propagation and normal to that direction (Pavlovic, 2005).

Deformation along the longitudinal axis of tunnel is calculated based on free field theory while that of ovaling or deformation along the transversal axis is based on plain strain condition (Nava-Tristán et al.,2008). Plain strain condition is used to treat structure by two dimensional theory of elasticity. It is a strain condition in which longer dimension strains are assumed to be zero.

Longitudinal deformations result in additional cyclic stress, axial and bending stresses (Nikam and Bhagat, 2016), with alternating compressive and tensile stresses that should be summed with the static stress acting on the tunnel lining. Upon superimposing this additional stresses, the result could be compressive stress that exceeds the lining compressive capacity or tensile stress which reduce the lining's moment capacity.

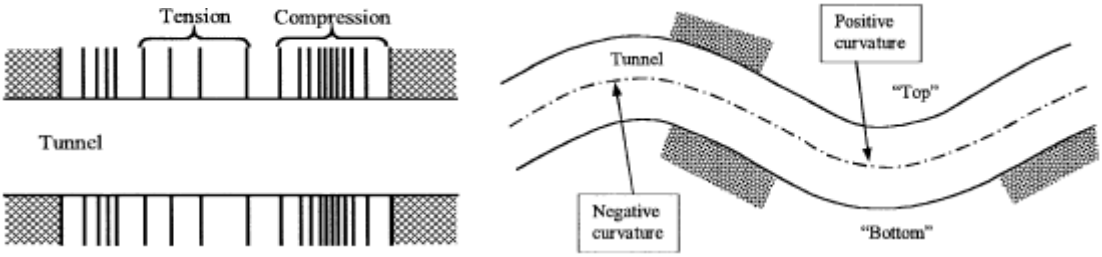

a). Compression-extension b) Longitudinal bending

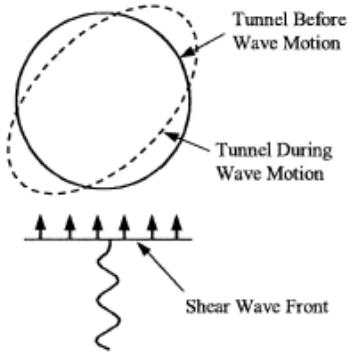

c). Ovaling of cross-section

Figure 2. 1: Deformation modes of tunnels due to seismic waves

(Hashasha et al., 2001)

When earthquake acts on structural element which comes in contact with the ground, both structural and ground displacement will be dependent on each other. This dependency is expressed using soil structure interaction (Chen & Hou, 1994) which is the process by which response of soil influences the motion of the structure and the motion of the structure influences the response of the soil. If the interaction is ignored, the case of free field deformation conforms. Free field deformation is displacement of ground caused by earthquake in the absence of a structure or excavation. This deformation provides a first order estimate of anticipated deformation. The difference in stiffness between the structure and ground leads in overestimation or underestimation of the lining deformation (Lanzano, 2008).

2.4. Ground motion analysis

As stated by the British Tunneling Society and The Institution of Civil Engineers (2004), hazards need to be identified so that danger during construction or normal operation is avoided. Seismic hazard is one of them.

For the seismic design of underground tunnel facilities, one of the main tasks is to define the design earthquake(s), the corresponding ground motion levels and other associated seismic hazards. The process by which design ground motion parameters are established for a seismic analysis is termed the *seismic hazard analysis.* Past earthquake data, earthquake source characteristics and attenuation relationships are important factors for seismic hazard analysis (Vipin et al., 2009).

Seismic source identification, evaluation of potential and intensity of the ground motion at project site are the major results of seismic hazard analysis. Establishing of fault type, geographic location, depth, size and orientation are included in source identification while evaluation of earthquake magnitude with rate of occurrence is included under seismic potential evaluation.

Identification of capable seismic sources together with evaluation of the seismic potential of each source may be referred to as *seismic source characterization*. Once the seismic sources are characterized, intensity of ground motions at the project site from these sources must be characterized. The Federal Highway Administration (FHWA) (2009) states three general ways by which the intensity of ground motions at a project site is assessed in practice. They are, in order of complexity: (1) use of existing hazard analysis results published by credible agencies such as the US Geological Survey (USGS) and some State agencies; (2) project-specific and site-specific deterministic seismic hazard evaluation; and (3) project-specific and site-specific probabilistic seismic hazard evaluation.

As Morales-Esteban et al.(2012:1) noted: "*In some regions, with a vast history of large earthquakes, such as Japan and California, a wide network of recording stations is available and provides many records for large earthquakes, for different types of soils and for a wide range of distances. In regions of minor seismicity, the network of recording stations is not so wide, or is not old enough, so that the number of records is insufficient. For the analysis of minor seismicity activity regions, records from other regions are used, or artificial accelerograms are generated.* "

The intensity of ground shaking due to earthquakes is a function of seismic source (earthquake size, focal mechanism), seismic wave propagation from the source to the site (focal distance, physical properties of the medium along the ray path), and local site effects (local geology)(Ardeleanu et al., 2012).

Peak ground motion parameters are able to describe the severity of ground shaking. Effective wave propagation velocity, peak ground particle velocity and peak ground particle acceleration are the major ground motion parameters required for seismic analysis. The characteristic parameter of the soil movement used is usually the peak ground acceleration (PGA).

2.4.1. Approaches to developing ground motions

The two basic approaches to developing ground motions that are commonly used in practice are deterministic and probabilistic methods (FHWA, 2009; Morales-Esteban et al., 2012).

2.4.1.1. Deterministic methods

The first methods to establish the seismic hazard of an area or a location were deterministic (Morales-Esteban et al., 2012). In this method, the largest earthquake that can affect the location is estimated while the rest of earthquakes are not considered. This method helps to evaluate worst case scenarios at a given site.

2.4.1.2. Probabilistic methods

The probabilistic methods sum up the contribution of all the possible earthquakes that can affect a location, and consider recurrence laws for them. As a result, the probability of exceeding every value of a parameter of the soil movement expected at the location, during a period of time, is estimated (Baker 2008; Morales-Esteban et al., 2012).

2.5. Approach to seismic analysis and design of tunnels

Ground deformation approach (Gaspari et al., 2012) is the main procedure used to design and analyze the seismic effect on underground tunnel structure. Due to the movement caused by the seismic motion, it is assumed that the tunnel structure conforms to the motion of the ground. This scenario holds true if the tunnel is sufficiently flexible as compared to the media. When tunnels are buried in soft media, the tunnel response will be affected by the soil structure interaction.

As Gaspari et al. (2012:2) noted: "*For small to moderate ground motion, the tunnel strain can be taken equal to the ground strain. However, for large ground motion the tunnel or immersed tube strain is limited by the slippage that occurs at the pipe-soil interface.*"

Strains and deformations characterize seismic loading on tunnels. There are two design approaches (Gaspari et al., 2012; Pescara et al., 2011) used to compute deformations and corresponding forces imposed on the tunnel due to the seismic waves.

- Free field deformation approach; and
- Soil structure interaction approach

2.5.1. Free field deformation method

In this method, when computing the ground deformations, the presence of the structure and disturbance due to excavation are neglected. This means that soil structure interaction will not be taken into consideration. First order, most conservative and upper bound estimate of deformation values are obtained (Gaspari et al., 2012). It is advantageous due to its least amount of input requirements.

This approach is mainly used for analyses of tunnels rather than design of tunnels. However, it is limited to tunnel structure which is flexible as compared to the ground so that the assumption that tunnel deformation conforms to ground deformation will hold true.

2.5.2. Soil structure interaction approach

In this approach, the presence of the structure is considered since it alters the response of the structure for the imposed deformation. Rather than conforming to the deformation of the ground, the tunnel starts to resist (Gaspari et al., 2012). Soil stresses have an interaction with stresses in the lining so as to maintain equilibrium. The stress state depends on the soil structure interaction so that it will be related to relative stiffness ratio between the tunnel and the soil. Therefore, both the tunnel and ground stiffness should be taken into consideration for analyzing such conditions. Spring coefficients (K_a or K_t) and sectional modulus (E_cA_c or E_cI_c) are representative of ground and tunnel stiffness respectively.

The derivations of these spring coefficients differ from those for the conventional beam on elastic foundation problems in that (Wang, 1993):

- The spring coefficients should be representative of the dynamic modulus of the ground under seismic loads.
- The derivations should consider the fact that loading felt by the surrounding soil (medium) is alternately positive and negative due to the assumed sinusoidal seismic wave.

For preliminary design, it appears that the expressions suggested by St. John and Zahrah (1987) serve the purpose:

$$k_t = k_a = \frac{16\pi G_m (1-\nu_m) d}{(3-4\nu_m) L_w} \tag{2.1}$$

Where G_m = shear modulus of the medium

ν_m = Poisson's ratio of the medium

d = diameter (or equivalent diameter) of the tunnel

L_w = wavelength

The moment of inertia of cracked section or segmental lining with joints is reduced from the values obtained by calculations. Therefore for analysis, it is better to use effective values (FHWA, 2009; Wang and Munfakh, 2001) which take this reduction into considerations.

When subjected to the axial and curvature deformations (longitudinal deformation) caused by the traveling waves in the ground, the tunnel will experience the following sectional forces (Wang, 1993) as shown in Figure 2.2 (a).

• Axial forces, Q, on the cross-section due to the axial deformation

• Bending moments, M_b, and shear forces, V, on the cross-section due to the curvature deformation.

Sectional forces due to transversal deformations are shown in Figure 2.2(b).

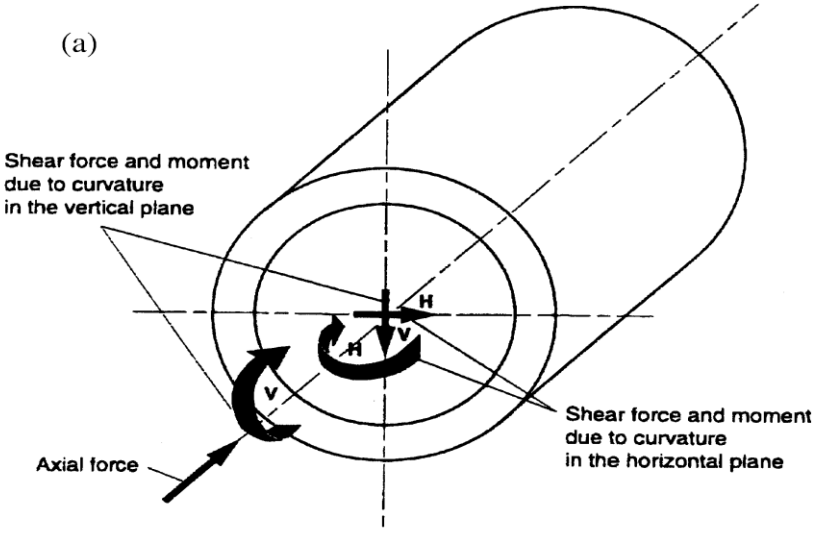

(a) Induced forces and moments caused by waves propagating along tunnel axis

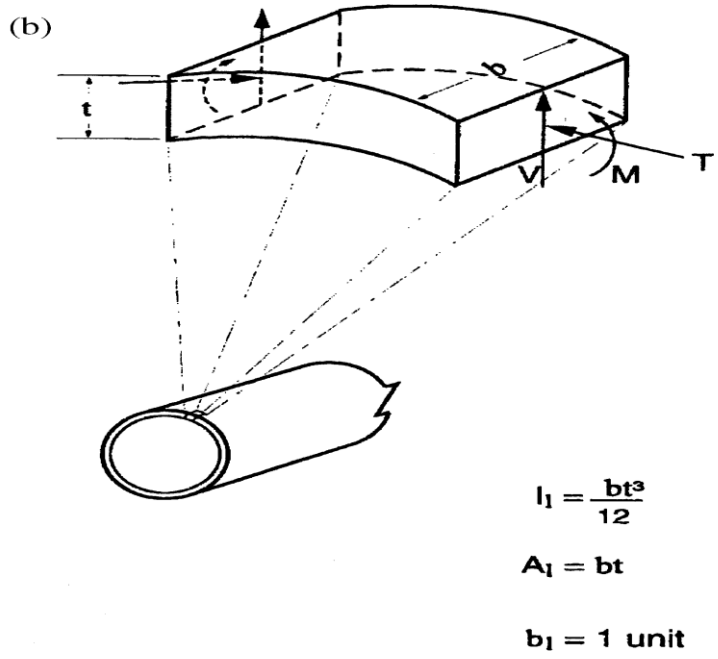

(b) Induced circumferential forces and moments caused by waves propagating perpendicular to tunnel axis

Figure 2. 2: Induced forces and moments caused by seismic waves (Pescara et al., 2011)

2.6. Seismic design loading criteria

Bearing capacity analysis of lining is dependent on loadings. Design loading criteria for underground structures has to incorporate the additional loading imposed by ground shaking and deformation. Once the ground motion parameters for the maximum and operational design earthquakes have been determined, load criteria (Hashasha et al., 2001) are developed for the underground structure using the load factor design method.

2.6.1. Loading criteria for maximum design earthquake, MDE

For circular tunnel lining, the recommended seismic loading using load factor design method is given as (Hashasha et al., 2001):

$$U_{req} = D + LL + EX + H + EQ \tag{2.1}$$

Where U_{req} - Required structural strength capacity,

D- Effects due to dead loads of structural components,

LL- Effects due to live loads,

EQ- Effects due to design earthquake motion,

EX- Effects of static loads due to excavation,

H- Effects due to hydrostatic water pressure.

2.6.2. Loading criteria for operating design earthquake, ODE

For circular tunnel lining, the recommended seismic loading using load factor design method is given as (Hashasha et al., 2001):

$$U_{req} = 1.05D + 1.3LL + \beta_2(EX + H) + 1.3EQ \tag{2.3}$$

Where D, LL, EX, H, EQ and U_{req} are as defined above,

β_2=1.05 if extreme loads are assumed for EX and H with little uncertainty. Otherwise, use β_2=1.3 for EX only, as H is usually well defined.

2.7. Tunnel Lining

As FHWA (2009:317) notes:"*Tunnel linings are structural systems installed after excavation to provide ground support, to maintain the tunnel opening, to limit the inflow of ground water, to support appurtenances and to provide a base for the final finished exposed surface of the tunnel. They can be used for initial stabilization of the excavation, permanent ground support or a combination of both.*"

Tunnels are expected to deform when loads act on it. However, the deformation is dependent on the relative stiffness of the lining and the ground (Wang and Munfakh 2001). Compressibility ratio, C, and flexibility ratio, F, are the two ratios used to assess relative stiffness, the most important being flexibility ratio as it is related to the resistance of lining to distortions.

The compressibility ratio is the ratio of the ground extensional stiffness to that of liner extensional stiffness. It is the ratio between the pressure required to cause a unit diametric strain of the free-field ground and that of the liner. It can be expressed as:

$$C = \frac{E_m\left(1-\nu_l^2\right)r}{E_l t\left(1+\nu_m\right)\left(1-2\nu_m\right)} \tag{2.4}$$

Where E_m- Young's modulus of the ground;

ν_m - Poisson's ratio of the ground;

ν_l - Poisson's ratio of the lining;

r - Radius of the tunnel; and

t - Thickness of the tunnel lining.

Likewise, the flexibility ratio is the ratio of the ground flexural stiffness to that of the liner. It is the ratio between the shear stress required to cause a unit diametric strain of the free-field ground and that of the liner. An infinite, elastic, homogeneous and isotropic ground

subjected to a pure shear loading is considered for the calculation. The flexibility ratio is given by:

$$F = \frac{E_m\left(1-\nu_l^2\right)r^3}{6E_l I_c\left(1+\nu_m\right)} \tag{2.5}$$

Where I_c - Moment of inertia of the tunnel lining per unit width.

Ground structure interaction effect can be neglected for most circular tunnels since their flexibility ratio is beyond 20 (FHWA, 2009).

The load developed and the carrying capacity of lining depends on relative stiffness of the lining with respect to the soil (Bakker, 2003; Norman, 1981; FHWA, 2009). The deformation of the medium with which the tunnel is located result in the deformation of lining as the relative flexibility of lining is higher than that of the medium. The deformation created in the medium results in mobilization of shear strength of the medium while the deformation created on the lining results in moment redistribution within the lining.

Due to the occurrence of moment redistribution, the major loading on the lining will be axial load or thrust. This ductility is provided in concrete by the formation of cracks. Under reinforcing or no reinforcing promotes the initiation of cracks (FHWA, 2009).

2.8. Model for analysis

It is better to use models if interaction needs to be accounted (The British Tunneling Society and The Institution of Civil Engineer, 2004; Pack, 2014; Moldovan and Popa, 2012). Most simplifying assumptions can be discarded and taken in their natural form by using models other than analytical methods. For example, geometrical shapes, soil layering, staged construction effects, volume loss...can be considered by using numerical analysis such as finite element models.

2.9. Seismic Protection of Tunnel

Seismic protections for tunnels will be more important where structural or ground stiffness changes. Abrupt stiffness changes result in differential settlement and stress concentrations. Such changes in stiffness occur for (Lanzano, 2008):

- Connections of tunnels with structures such as building and stations;
- Joining points of different structural material;
- Ground media with varying stiffness.

Seismic isolations, flexible joint and soft layer provision (Kawashima, 2000; Lanzano, 2008) will be provided to reduce the seismic force imposed on the tunnel. Seismic isolation helps in reducing stiffness of the structure so that the seismic force will decrease. Figure 2.3 shows seismic isolation used for underground structures.

Bended steel plates and rubbers are used as flexible joint. Stoppers will be provided with the joints to prevent pull out. Such joints will allow differential longitudinal, transversal and relative rotational movement; resist static and dynamic earth and water loads and provide water tightness.

If the stiffness changes abruptly in the medium, the seismic force can be reduced by inserting soft layer between the structure and the ground medium. This helps in avoiding direct transmission of seismic deformation to the lining. After several tests to identify appropriate material for such purpose, silicone, urethane resin and asphalt were proposed (Kawashima, 2000).

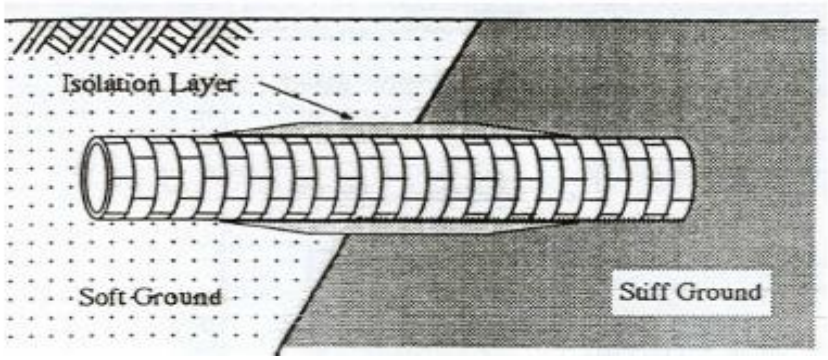

Figure 2. 3: Seismic isolation of underground structures

(Kawashima, 2000)

Ground stabilization, drainage, soil reinforcement, grouting or earth retaining structures can be used as a strategy to protect tunnel from ground failure or large permanent deformations. Cut-off walls can be used when the structure is located in liquefiable soil to protect from floatation.

CHAPTER 3 SEISMIC HAZARD ANALYSIS

Mamo, 2005, cited in Kinde et.al., 2011 stated the existence of three seismic zones in Ethiopian proper. These seismic zones are the Afar triangle seismic zone, the escarpment seismic zone and Ethiopian rift system seismic zone. The railway alignment considered in this thesis is located in an area identified by Ethiopian geological survey as Were-Ilu area, located between 10°-11°N and 39°-40°30' E. This area is located in the escarpment seismic zone which leads to the consideration of seismic analysis for the railway track. The recommended value of the reference peak ground acceleration for the tunnel, T-04, as given by Yapi Merkezi (2014) is a_g = 0.2 g. The map in Figure 3.1 illustrates where 10% probability of exceedence of peak ground acceleration could exist in the next 50 years (Humanitarian information unit, cited in Yapi Merkezi, 2014).

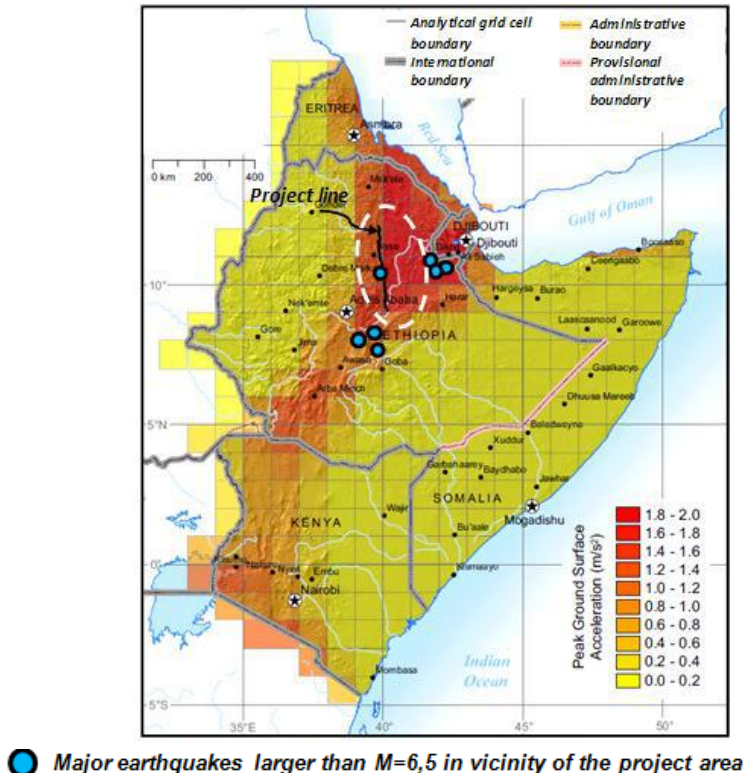

Figure 3. 1: PGA values with 10% probability of exceedance in 50 years

(Humanitarian information unit, cited in Yapi Merkezi, 2014)

Since the analysis in this thesis is full dynamic analysis, acceleration time history records are required. In Ethiopia, such records are not available. Therefore, using the property of the site under consideration, records from earthquake database need to be filtered. Besides the site fault mechanism and shear wave velocity of the top 30m layer, the input parameters for selecting appropriate acceleration time records require results of deaggregation process. The deaggregation by itself requires results from probabilistic seismic hazard analysis.

3.1. Probabilistic seismic hazard analysis

In order to assess risk to a structure from earthquake shaking, annual probability (rate) of exceeding some level of earthquake ground shaking at a site, for a range of intensity levels should be determined first. Reliable estimation of the seismic hazard in a region requires the prediction of the size, location and magnitude of future earthquake events (Green et al., 1994). These estimations are presented below.

3.1.1. Earthquake source identification

Sources which are expected to cause damaging ground motions are identified based on interpretation of geological, geophysical and seismological data and can be represented as point, line (fault) or area source.

Seismic sources that are modeled as point source refers to the epicenter of past earthquakes clustered in a relatively small area. For this thesis 74 point sources identified by the Institute of Geophysics, space science and Astronomy (IGSSA) are used.

3.1.2. Earthquake magnitude identification

Energy is related to earthquake magnitude in such a way that one unit magnitude results in 32 fold increase in energy and 10 fold in ground displacement (Wiemer, 2015). Magnitudes for this thesis are identified from contemporary earthquake data collected by the Institute of Geophyiscs, Space Science and Astronomy in the region defined by 9.40°-11.48° latitude and 38.93°-41.10° longitude.

Recurrence relations are used to describe distribution of earthquake magnitudes. Guttenberg-Richter recurrence law is the well known recurrence relation (Anagnos and Kiremidjian, 1988; Baker, 2008; Green, 1994; Htwe and WenBin, 2009; Morales-Esteban et al.,2012; Stewart et al., 2001; Kijko, 2003; Boore and Atkinson, 2008; Lewis et al., 2006).

The basic assumption of Probabilistic seismic hazard analysis (PSHA) is that the recurrence relation obtained from past seismicity is appropriate for prediction of future seismicity (Kijko, 2003; Theodorakatou, 2007).Based on this assumption; Guttenberg-Richter recurrence law which is given below is used.

$$\log \lambda_m = a - bm \quad \text{Or} \tag{3.1}$$

$$\ln \lambda_m = \alpha - \beta m \tag{3.2}$$

$$\alpha = a \ln 10 \ \text{And} \ \beta = b \ln 10 \tag{3.2a}$$

Where λ_m is the rate of earthquakes with magnitudes greater than *m*, and *a* and *b* are constants.

Large ‘a’ implies higher seismic activity and overall rate of earthquake (10^a is the mean yearly number of earthquakes of magnitude greater than or equal to 0) while ‘b’ defines the ratio of small to large magnitude (Baker, 2008; Theodorakatou, 2007).

Earthquake magnitudes are sorted in ascending order. The number of exceedance of each earthquake magnitude identified is divided by the period of exceedance so as to get the mean annual rate of exceedance of an earthquake magnitude. Fitting linear equation for a plot of logarithm of mean annual rate of exceedance versus earthquake magnitude of the contemporary earthquake data obtained from the Institute of Geophysics, Space Science and Astronomy gives a linear relationship as was expected for Guttenberg-Richter recurrence law. This linear equation provides a slope, the ‘b’ value of the Guttenberg-Richter recurrence law, of 1.012.

Earthquakes with magnitudes greater than approximately 4.5 or 5 need to be considered since lower values aren't expected to have engineering importance (Bell, 2002; Morales-Esteban et al., 2012; Baker, 2008; Stewart et al., 2001; Green et al., 1994). Therefore magnitudes greater than five are used for this probabilistic seismic hazard analysis.

Upper bound of earthquake, m_{max} is used to truncate recurrence relationships so that physically possible earthquakes will be predicted. The largest historical earthquake (m_{max}^{obs}) is almost always the lower limit for $m_{max.}$ In practice, m_{max} is usually defined by adding an increment, Δm to the largest known magnitude (m_{max}^{obs}) in the source (Green et al., 1994; Kijko, 2003).This value is taken from study made by Ayele (2017) and its value is 6.86.

On the same study made by Ayele (2017), the constant b is given as 0.93. This value differs from the one obtained by fitting curve. So as to be consistent with the upper bound earthquake magnitude, 6.86, Ayele's (2017) b value is taken.

For Guttenberg-Richter recurrence law, magnitude distribution is expressed by exponential distribution with probability density function (PDF) and cumulative distribution function (CDF) given as follows (Baker, 2008).

$$f_M(m) = b\ln(10)10^{-b(m-m_{\min})} \tag{3.3}$$
$$= \beta 10^{-b(m-m_{\min})}$$

And

$$F_M(m) = 1-10^{-b(m-m_{\min})} \tag{3.4}$$

Where $f_M(m)$ and $F_M(m)$ denotes probability density function and cumulative distribution function for M respectively and m_{min} represents the smallest magnitude of earthquake used on the recurrence law calculation.

Using upper and lower limits of earthquake, the recurrence law is termed as bounded Guttenberg-Richter recurrence law with the following expressions for PDF and CDF (Baker, 2008).

$$f_M(m) = \frac{b\ln(10)10^{-b(m-m_{\min})}}{1-10^{-b(m_{\max}-m_{\min})}} \tag{3.5}$$

$$= \frac{\beta 10^{-b(m-m_{\min})}}{1-10^{-b(m_{\max}-m_{\min})}}$$

And

$$F_M(m) = \frac{1-10^{-b(m-m_{\min})}}{1-10^{-b(m_{\max}-m_{\min})}} \tag{3.6}$$

This probabilistic distribution will be used in the next section which demands the discretization of magnitudes. The probabilities of occurrence of discrete magnitude are given by (Baker, 2008):

$$P(M = m_j) = F_M(m_{j+1}) - F_M(m_j) \tag{3.7}$$

Where, m_j is discretized magnitude in the order of $m_j < m_{j+1}$.

Magnitudes in this thesis are spaced at 0.1. The closer the spacing, the better the approximation will be. The calculation is tabulated in Table 3.1. The first column shows the earthquake magnitudes spaced in 0.1 intervals the second column places the cumulative distribution of the corresponding magnitude while the third column shows the probability of occurrence of the discrete sets of magnitudes.

Table 3. 1: Probability of occurrence of discrete magnitudes

Eq	$F_M(m_j)$	$p(M=m_j)$
5	0	0.196
5.1	0.196	0.158
5.2	0.355	0.128
5.3	0.483	0.103
5.4	0.586	0.083
5.5	0.669	0.067
5.6	0.737	0.054
5.7	0.791	0.044
5.8	0.835	0.035
5.9	0.870	0.029
6	0.899	0.023
6.1	0.922	0.019
6.2	0.941	0.015
6.3	0.956	0.012
6.4	0.968	0.010
6.5	0.978	0.008
6.6	0.986	0.006
6.7	0.992	0.005
6.8	0.997	0.003
6.86	1	0.002

3.1.3. Earthquake distance identification

Source-to-site distance is used to characterize the decrease in ground motion as it propagates away from the earthquake source. The distribution of distance between earthquake source and site of interest should be modeled. This is also done on the contemporary data collected by the Institute of Geophysics, Space Science and Astronomy as it includes the location of the source. From the different types of distances used in PSHA, epicentral and hypocentral data need only the location of rupture initiation. The data obtained for this thesis provides a point as a location for the source indicating that it is rupture initiation point. Due to this reason and the input requirement for ground motion prediction equation described hereafter, epicentral distance will be used.

Using the points along the tunnel alignment where survey data were taken in combination with seismic source coordinates, the hypocentral distance is calculated by the following formula, which is derived from Pythagorean Theorem.

$$R_{hyp} = \sqrt{\left((X_s - X_t)^2 + (Y_s - Y_t)^2 + (Z_s - Z_t)^2\right)} \tag{3.8}$$

Where X, Y, Z are easting, northing and elevation while the subscripts s and t refers to source and tunnel respectively. Each survey point along the tunnel alignment is taken into account for each source in the distance determination and the point which gives the shortest distance is taken as the hypocentral distance for that specified source.

Then the epicentral distance, R_{ep}, is calculated using the Pythagorean Theorem as shown in Figure 3.2. This is calculated at the depth of the tunnel as it gives similar value when it is projected on surface.

$$R_{ep} = \sqrt{\left(R_{hyp}{}^{2} - \left(Z_s - Z_t\right)^2\right)} \tag{3.9}$$

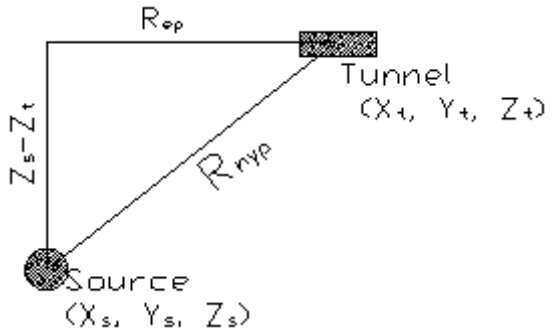

Figure 3. 2: Hypocentral and epicentral distance

3.1.4. Ground motion intensity

The theme of probabilistic seismic hazard analysis is prediction of ground motion. Ground motion prediction models which are developed through statistical regression from observations are used to predict probability distribution of ground motion intensity.

Many ground motion prediction equations (GMPEs) are compiled in a report document by Douglas.J (2011) which is studied as part of a research activity. Stewart et al., (2015) recommended ground motion prediction equations for global earthquake model separately for active shallow crustal region, stable continental regions and subduction zones.

The site which is considered under this thesis is located in Escarpment seismic zone so that the ground motion prediction equation should be appropriate for active shallow crustal regions. For global earthquake, a total of three prediction equations are recommended by Stewart et al., (2015) and one is mentioned as a simplest version of one of them. Therefore, this prediction equation developed by Boore and Atkinson (2008) is selected since the input parameters agree with the available data.

This GMPE is developed empirically by regression of recorded strong motion data for average horizontal component ground motions as a function of earthquake magnitude, distance from site, shear wave velocity of the top 30m and fault type and is applicable for moment magnitude (M) =5-8, closest horizontal distance to the surface projection of the fault plane (R_{JB}) < 200km and the time averaged shear wave velocity from the surface to 30m (V_{s30}) = 180-1300m/s.

R_{JB}, the closest distance to the surface projection of the fault, is approximately equal to the epicentral distance for events of M< 6 as described by Boore and Atkinson (2008). Therefore for simplicity this epicentral distance is used for this thesis even though the magnitudes used for this thesis exceed 6. Excluding this discrepancy, the epicentral distance which is taken to be equal to R_{JB}, ranges from 3.31-139.79km. This range is in the limit of R_{JB} values stated for the applicability of Boore and Atkinson (2008) GMPEs.

Fig 3.3 (b): Section 178+807 to 178+804 (modified after Yapi Merkezi, 2014)

Soil properties can be used in deriving wave velocities in soil overburdens. Young's modulus, E, Poisson's ratio, ν and density, ρ given in Table 3.2 are used for the derivation. The terrain which is traversed by the railway alignment is shown in Figure 3.3(a) with a magnified image for the section considered, 178+807 to 178+864, shown in Figure 3.3(b). The shear wave velocity of the top 30m layer calculation results in 119.7m/s which doesn't fail in the allowable range. However, Yapi Merkezi (2016) provides an assumed weathered homogeneous layer with its property(shear modulus, G and density, ρ) which result in 202.18m/s of shear wave velocity of the top 30m layer. This value is in the allowable range unlike the previous one. Therefore, this assumed homogeneous layer is used for the analysis afterwards.

Fig 3.3 (a): Terrain traversed by the railway alignment (Yapi Merkezi, 2014)

Table 3.2: Mechanical behaviour of intact rock and rockmass (Yapi Merkezi, 2014; Yapi Merkezi, 2016)

	Layer	A	B	C
Mechanical behavior of intact rock	unit weight [kN/m^3]	26	24	20
	static elastic modulus[GPa]	25	6	4
	poisson ratio	0.2	0.25	0.31
Rock mass design parametres	unit weight [kN/m^3]	26	24	20
	static elastic modulus[MPa]	3200	250	70
	poisson ratio	0.2	0.25	0.31

The earthquake magnitudes used in this thesis range from 5-6.86 which is still in the allowable range. Therefore, taking the equalization of R_{JB} with epicentral distance for magnitudes larger than 6 as drawbacks, the rest of the requirements to use the above mentioned GMPE (Boore and Atkinson, 2008) is fulfilled. The GMPE provided by Boore and Atkinson (2008) is given by:

$$\ln Y = F_M(M) + F_D(R_{JB}, M) + F_S(V_{s30}.R_{JB}, M) + \varepsilon\sigma_T \tag{3.10}$$

$$\sigma_T = \sqrt{(\sigma^2 + T^2)} \tag{3.11}$$

F_M - magnitude scaling

The magnitude scaling is given by:

a) $M \le M_h$

$$F_M(M) = e_1 U + e_2 SS + e_3 NS + e_4 RS + e_5(M - M_h) + e_6(M - M_h)^2 \tag{3.12a}$$

b) $M > M_h$

$$F_M(M) = e_1 U + e_2 SS + e_3 NS + e_4 RS + e_7(M - M_h) \tag{3.12b}$$

F_D - distance function

$$F_D(R_{JB}, M) = [c_1 + c_2(M - M_{ref})]\ln\left(R/R_{ref}\right) + c_3(R - R_{ref}) \tag{3.13}$$

$$R = \sqrt{(R_{JB}^2 + h^2)} \tag{3.14}$$

F_S - Site amplification

$$F_s = F_{LIN} + F_{NL} \tag{3.15}$$

$$F_{LIN} = b_{lin} \ln\left(V_{s30}/V_{ref}\right) \tag{3.16}$$

The nonlinear term is given by:

a) $pga4nl \le a_1$:

$$F_{NL} = b_{nl} \ln\left(pga\_low / 0.1 \right) \tag{3.17}$$

b) $a_1 < pga4nl \le a_2$:

$$F_{NL} = b_{nl} \ln\left(pga\_low / 0.1 \right) + c\left[\ln\left(pga4nl / a_1 \right) \right]^2 + d\left[\ln\left(pga4nl / a_1 \right) \right]^3 \tag{3.18a}$$

$$c = \frac{\left(3\Delta y - b_{nl}\Delta x\right)}{\Delta x^2} \tag{3.18b}$$

$$d = \frac{-\left(2\Delta y - b_{nl}\Delta x\right)}{\Delta x^3} \tag{3.18c}$$

$$\Delta x = \ln\left(a_2 / a_1 \right) \tag{3.18d}$$

$$\Delta y = b_{nl} \ln\left(a_2 / pga\_low \right) \tag{3.18e}$$

c) $a_2 < pga4nl$:

$$F_{NL} = b_{nl} \ln\left(pga4nl / 0.1 \right) \tag{3.19}$$

The nonlinear slope b_{nl} is a function of both period and V_{S30} as given by:

a) $V_{s30} \le V_1$:

$$b_{nl} = b_1 \tag{3.20a}$$

b) $V_1 < V_{s30} \le V_2$:

$$b_{nl} = \left(b_1 - b_2\right) \ln\left(V_{s30}/V_2\right) \ln V_1 / V_2 + b_2 \tag{3.20b}$$

c) $V_2 < V_{s30} < V_{ref}$:

$$b_{nl} = \frac{b_2 \ln\left(V_{s30} / V_{ref} \right)}{\ln\left(V_2 / V_{ref} \right)} \tag{3.20c}$$

d) $V_{ref} \leq V_{s30}$:

$$b_{nl} = 0.0 \tag{3.20d}$$

Where V_1=180 m/ s, V_2=300 m/ s, and b_1 and b_2 are period-dependent coefficients

e - Fractional number of standard deviations of single predicted values of ln Y

e_1-e_7 - Magnitude scaling coefficients

Y- Peak ground acceleration, PGA in g

σ - Intra-event aleatory uncertainty

T- Inter-event aleatory uncertainty

c_1, c_2, c_3, M_{ref}, R_{ref} and h are coefficients

h - near-source effective depth coefficient

R_{ref} - Reference distance at which near source predictions are pegged

Mref - Reference magnitude to which the magnitude dependence of the geometric spreading is referenced

U, SS, NS, RS - Dummy variables used to denote unspecified, strike-slip, normal slip and reverse slip fault

M_h - Hinge magnitude

F_{LIN} and F_{NL} - linear and nonlinear terms, respectively

b_{lin} - period dependent coefficient

V_{ref} - specified reference velocity= 760m/s

a_1, a_2 - Assigned threshold levels for linear & nonlinear amplifications with 0.03g and 0.09g values respectively

pga _ low - Variable assigned to transition between linear and nonlinear behaviors and with value of 0.06g

pga4nl - Predicted peak ground acceleration in g for V_{ref} = 760m/s with F_s=0 and ε=0

The assigned values for reference values are arbitrary and are largely a matter of convenience. All the coefficients given in Boore and Atkinson (2008) GMPE are tabulated in Table 3.3.

Table 3. 3: Coefficients used by Boore and Atkinson (2008) GMPE for estimating peak ground acceleration

1. Magnitude scaling							
		Fault mechanism					
			Normal	Strike slip	Reverse slip	Unspecified	Hinge moment, M_h
e_1	-0.53804	U	0	0	0	1	6.75
e_2	-0.5035	SS	0	1	0	0	
e_3	-0.75472	NS	1	0	0	0	
e_4	-0.5097	RS	0	0	1	0	
e_5	0.28805						
e_6	-0.10164						
e_7	0						
2. Distance function							
c_1	-0.6605						
c_2	0.1197						
c_3	-0.01151						
h	1.35						
R_{ref}	1km						
M_{ref}	4.5						
3.Site amplification							
inear terms		Nonlinear terms					
b_{lin}	-0.36	a_1	0.03g				
V_{ref}	760m/s	a_2	0.09g				
		pga_low	0.06g				
		V_1	180m/s				
		V_2	300m/s				
		b_1	-0.64				
		b_2	-0.14				
		V_{ref}	760m/s				
4. Aleatory uncertainities							
	For specified fault type	For unspecified fault type					
σ	0.502	0.502					
τ	0.26	0.265					
σ_τ	0.564	0.566					

Magnitude scaling is calculated in Table 3.4. The first two columns show the symbols and values of coefficients of the magnitude scaling. 3rd to 6th columns show the dummy variables assigned to the fault mechanism. 7th column is set for hinge magnitude, magnitude by which magnitude scaling change from quadratic form to linear form (Boore and Atkinson, 2008). 8th column contains magnitudes at 0.1 spacing ranging from a minimum value of 5 to a maximum value of 6.86. Starting from the 9th column to the end column, the magnitude scaling is calculated using Equations 3.12a and 3.12b for each faulting mechanism.

Table 3. 4: Magnitude scaling

		Faulting mechanism								
		strike slip						Strike slip	Normal	unspecified
		SS	U	NS	RS	M_h=6.75	M	F_M(M)	F_M(M)	F_M(M)
e_1	-0.53804	1	0	0	0	6.75	5	-1.31886	-1.57008	-1.3534
e_2	-0.5035	Normal				6.75	5.1	-1.2554974	-1.50672	-1.2900374
e_3	-0.75472	SS	U	NS	RS	6.75	5.2	-1.1941676	-1.44539	-1.2287076
e_4	-0.5097	0	0	1	0	6.75	5.3	-1.1348706	-1.38609	-1.1694106
e_5	0.28805	Unspecified				6.75	5.4	-1.0776064	-1.32883	-1.1121464
e_6	-0.10164	SS	U	NS	RS	6.75	5.5	-1.022375	-1.2736	-1.056915
e_7	0	0	1	0	0	6.75	5.6	-0.9691764	-1.2204	-1.0037164
						6.75	5.7	-0.9180106	-1.16923	-0.9525506
						6.75	5.8	-0.8688776	-1.1201	-0.9034176
						6.75	5.9	-0.8217774	-1.073	-0.8563174
						6.75	6	-0.77671	-1.02793	-0.81125
						6.75	6.1	-0.7336754	-0.9849	-0.7682154
						6.75	6.2	-0.6926736	-0.94389	-0.7272136
						6.75	6.3	-0.6537046	-0.90492	-0.6882446
						6.75	6.4	-0.6167684	-0.86799	-0.6513084
						6.75	6.5	-0.581865	-0.83309	-0.616405
						6.75	6.6	-0.5489944	-0.80021	-0.5835344
						6.75	6.7	-0.5181566	-0.76938	-0.5526966
						6.75	6.8	-0.5035	-0.75472	-0.53804
						6.75	6.86	-0.5035	-0.75472	-0.53804

Distance function is calculated in Table 3.5. The first two columns show the coefficients used to describe decay of amplitude with magnitude. As Boore and Atkinson (2008) noted:" c_1 is the effective geometric spreading rate (slope) for an event of M=M_{ref}, while the c_2 provides a means to describe magnitude-dependent distance decay (it changes the slope for

events that are greater or smaller than M_{ref}). c_3 *is* a coefficient required to match the more rapid decay of the data used to derive it at greater distances."

In the 3rd column, the 74 sources used in this analysis are placed. 4th column is assigned for M_{ref} (a reference magnitude to which magnitude dependence of geometric spreading is referenced (Boore and Atkinson, 2008)).

The first row shows the discrete sets of magnitude. The 8th column shows the calculated values of R as given by Equation 3.14. All the cells bounded by the 8th column and 4th rows are the calculations done for distance function as given by Equation 3.13.

Table 3. 5: Distance function calculation

								Magnitude																		
								5	5.1	5.2	5.3	5.4	5.5	5.6	5.7	5.8	5.9	6	6.1	6.2	6.3	6.4	6.5	6.6	6.7	6.8	6.86
		Source	M_{ref}	R_{ref} (km)	h	$R_{ep}=R_{JB}$ (km)	$R=\sqrt{(R_{JB}^2+h^2)}$	$F_D(R_{JB},M)$																			
c_1	-0.6605	1	4.5	1	1.35	111.18	111.19	-4.10	-4.04	-3.99	-3.93	-3.87	-3.82	-3.76	-3.70	-3.65	-3.59	-3.53	-3.48	-3.42	-3.36	-3.31	-3.25	-3.20	-3.14	-3.08	-3.05
c_2	0.1197	2	4.5	1	1.35	57.20	57.21	-3.08	-3.03	-2.98	-2.93	-2.88	-2.84	-2.79	-2.74	-2.69	-2.64	-2.59	-2.54	-2.50	-2.45	-2.40	-2.35	-2.30	-2.25	-2.21	-2.18
c_3	-0.01151	3	4.5	1	1.35	26.02	26.05	-2.25	-2.21	-2.17	-2.13	-2.09	-2.05	-2.01	-1.97	-1.93	-1.90	-1.86	-1.82	-1.78	-1.74	-1.70	-1.66	-1.62	-1.58	-1.54	-1.52
		4	4.5	1	1.35	47.03	47.05	-2.84	-2.80	-2.75	-2.70	-2.66	-2.61	-2.57	-2.52	-2.47	-2.43	-2.38	-2.34	-2.29	-2.24	-2.20	-2.15	-2.11	-2.06	-2.01	-1.99
		5	4.5	1	1.35	5.12	5.29	-1.05	-1.03	-1.01	-0.99	-0.97	-0.95	-0.93	-0.91	-0.89	-0.87	-0.85	-0.83	-0.81	-0.79	-0.77	-0.75	-0.73	-0.71	-0.69	-0.68
		6	4.5	1	1.35	8.82	8.92	-1.41	-1.38	-1.35	-1.33	-1.30	-1.27	-1.25	-1.22	-1.20	-1.17	-1.14	-1.12	-1.09	-1.07	-1.04	-1.01	-0.99	-0.96	-0.93	-0.92
		7	4.5	1	1.35	18.40	18.45	-1.95	-1.92	-1.88	-1.85	-1.81	-1.78	-1.74	-1.71	-1.67	-1.64	-1.60	-1.57	-1.53	-1.50	-1.46	-1.43	-1.39	-1.36	-1.32	-1.30
		8	4.5	1	1.35	6.90	7.03	-1.24	-1.22	-1.19	-1.17	-1.15	-1.12	-1.10	-1.08	-1.05	-1.03	-1.01	-0.98	-0.96	-0.94	-0.91	-0.89	-0.87	-0.84	-0.82	-0.81
		9	4.5	1	1.35	15.54	15.60	-1.82	-1.79	-1.75	-1.72	-1.69	-1.65	-1.62	-1.59	-1.55	-1.52	-1.49	-1.46	-1.42	-1.39	-1.36	-1.32	-1.29	-1.26	-1.23	-1.21
		10	4.5	1	1.35	42.76	42.78	-2.74	-2.69	-2.65	-2.60	-2.56	-2.51	-2.47	-2.42	-2.38	-2.33	-2.29	-2.24	-2.20	-2.15	-2.11	-2.06	-2.02	-1.97	-1.93	-1.90
		11	4.5	1	1.35	3.31	3.57	-0.79	-0.78	-0.76	-0.75	-0.73	-0.72	-0.70	-0.69	-0.67	-0.66	-0.64	-0.63	-0.61	-0.60	-0.58	-0.57	-0.55	-0.54	-0.52	-0.51
		12	4.5	1	1.35	40.93	40.95	-2.69	-2.65	-2.60	-2.56	-2.51	-2.47	-2.42	-2.38	-2.33	-2.29	-2.25	-2.20	-2.16	-2.11	-2.07	-2.02	-1.98	-1.93	-1.89	-1.86
		13	4.5	1	1.35	28.77	28.80	-2.34	-2.30	-2.26	-2.22	-2.18	-2.14	-2.10	-2.06	-2.02	-1.98	-1.94	-1.90	-1.86	-1.82	-1.78	-1.74	-1.69	-1.65	-1.61	-1.59
		14	4.5	1	1.35	6.95	7.08	-1.25	-1.22	-1.20	-1.18	-1.15	-1.13	-1.10	-1.08	-1.06	-1.03	-1.01	-0.99	-0.96	-0.94	-0.92	-0.89	-0.87	-0.85	-0.82	-0.81
		15	4.5	1	1.35	73.36	73.37	-3.41	-3.36	-3.31	-3.26	-3.21	-3.16	-3.10	-3.05	-3.00	-2.95	-2.90	-2.85	-2.80	-2.74	-2.69	-2.64	-2.59	-2.54	-2.49	-2.46
		16	4.5	1	1.35	64.54	64.55	-3.23	-3.18	-3.13	-3.09	-3.04	-2.99	-2.94	-2.89	-2.84	-2.79	-2.74	-2.69	-2.64	-2.59	-2.54	-2.49	-2.44	-2.39	-2.34	-2.31
		17	4.5	1	1.35	88.30	88.31	-3.70	-3.64	-3.59	-3.54	-3.48	-3.43	-3.37	-3.32	-3.27	-3.21	-3.16	-3.11	-3.05	-3.00	-2.95	-2.89	-2.84	-2.78	-2.73	-2.70
		18	4.5	1	1.35	116.77	116.77	-4.19	-4.13	-4.08	-4.02	-3.96	-3.91	-3.85	-3.79	-3.74	-3.68	-3.62	-3.57	-3.51	-3.45	-3.39	-3.34	-3.28	-3.22	-3.17	-3.13
		19	4.5	1	1.35	93.35	93.36	-3.79	-3.73	-3.68	-3.62	-3.57	-3.52	-3.46	-3.41	-3.35	-3.30	-3.24	-3.19	-3.14	-3.08	-3.03	-2.97	-2.92	-2.86	-2.81	-2.78
		20	4.5	1	1.35	65.79	65.80	-3.26	-3.21	-3.16	-3.11	-3.06	-3.01	-2.96	-2.91	-2.86	-2.81	-2.76	-2.71	-2.66	-2.61	-2.56	-2.51	-2.46	-2.41	-2.36	-2.33
		21	4.5	1	1.35	81.50	81.51	-3.57	-3.52	-3.46	-3.41	-3.36	-3.31	-3.25	-3.20	-3.15	-3.10	-3.04	-2.99	-2.94	-2.89	-2.83	-2.78	-2.73	-2.67	-2.62	-2.59
		22	4.5	1	1.35	18.87	18.92	-1.97	-1.94	-1.90	-1.87	-1.83	-1.80	-1.76	-1.73	-1.69	-1.66	-1.62	-1.58	-1.55	-1.51	-1.48	-1.44	-1.41	-1.37	-1.34	-1.32
		23	4.5	1	1.35	33.71	33.73	-2.49	-2.45	-2.41	-2.36	-2.32	-2.28	-2.24	-2.20	-2.15	-2.11	-2.07	-2.03	-1.98	-1.94	-1.90	-1.86	-1.82	-1.77	-1.73	-1.71
		24	4.5	1	1.35	22.16	22.20	-2.11	-2.07	-2.03	-1.99	-1.96	-1.92	-1.88	-1.85	-1.81	-1.77	-1.74	-1.70	-1.66	-1.62	-1.59	-1.55	-1.51	-1.48	-1.44	-1.42
		25	4.5	1	1.35	26.54	26.57	-2.26	-2.23	-2.19	-2.15	-2.11	-2.07	-2.03	-1.99	-1.95	-1.91	-1.87	-1.83	-1.79	-1.75	-1.71	-1.68	-1.64	-1.60	-1.56	-1.53
		26	4.5	1	1.35	30.11	30.14	-2.38	-2.34	-2.30	-2.26	-2.22	-2.18	-2.14	-2.10	-2.05	-2.01	-1.97	-1.93	-1.89	-1.85	-1.81	-1.77	-1.73	-1.69	-1.65	-1.62
		27	4.5	1	1.35	33.78	33.81	-2.49	-2.45	-2.41	-2.37	-2.32	-2.28	-2.24	-2.20	-2.16	-2.11	-2.07	-2.03	-1.99	-1.94	-1.90	-1.86	-1.82	-1.78	-1.73	-1.71
		28	4.5	1	1.35	7.75	7.87	-1.32	-1.29	-1.27	-1.24	-1.22	-1.19	-1.17	-1.15	-1.12	-1.10	-1.07	-1.05	-1.02	-1.00	-0.97	-0.95	-0.92	-0.90	-0.87	-0.86
		29	4.5	1	1.35	11.02	11.11	-1.56	-1.53	-1.50	-1.48	-1.45	-1.42	-1.39	-1.36	-1.33	-1.30	-1.27	-1.25	-1.22	-1.19	-1.16	-1.13	-1.10	-1.07	-1.04	-1.03
		30	4.5	1	1.35	23.42	23.46	-2.15	-2.12	-2.08	-2.04	-2.00	-1.96	-1.93	-1.89	-1.85	-1.81	-1.78	-1.74	-1.70	-1.66	-1.63	-1.59	-1.55	-1.51	-1.47	-1.45
		31	4.5	1	1.35	8.14	8.25	-1.35	-1.33	-1.30	-1.27	-1.25	-1.22	-1.20	-1.17	-1.15	-1.12	-1.10	-1.07	-1.05	-1.02	-1.00	-0.97	-0.95	-0.92	-0.90	-0.88
		32	4.5	1	1.35	77.03	77.05	-3.48	-3.43	-3.38	-3.33	-3.28	-3.22	-3.17	-3.12	-3.07	-3.02	-2.96	-2.91	-2.86	-2.81	-2.76	-2.70	-2.65	-2.60	-2.55	-2.52
		33	4.5	1	1.35	15.55	15.61	-1.82	-1.79	-1.75	-1.72	-1.69	-1.65	-1.62	-1.59	-1.56	-1.52	-1.49	-1.46	-1.42	-1.39	-1.36	-1.33	-1.29	-1.26	-1.23	-1.21
		34	4.5	1	1.35	26.41	26.45	-2.26	-2.22	-2.18	-2.14	-2.10	-2.06	-2.02	-1.99	-1.95	-1.91	-1.87	-1.83	-1.79	-1.75	-1.71	-1.67	-1.63	-1.59	-1.55	-1.53
		35	4.5	1	1.35	59.14	59.16	-3.12	-3.07	-3.02	-2.97	-2.92	-2.88	-2.83	-2.78	-2.73	-2.68	-2.63	-2.58	-2.53	-2.49	-2.44	-2.39	-2.34	-2.29	-2.24	-2.21
		36	4.5	1	1.35	23.32	23.36	-2.15	-2.11	-2.07	-2.04	-2.00	-1.96	-1.92	-1.89	-1.85	-1.81	-1.77	-1.73	-1.70	-1.66	-1.62	-1.58	-1.55	-1.51	-1.47	-1.45
		37	4.5	1	1.35	47.26	47.28	-2.85	-2.80	-2.76	-2.71	-2.66	-2.62	-2.57	-2.53	-2.48	-2.43	-2.39	-2.34	-2.30	-2.25	-2.20	-2.16	-2.11	-2.06	-2.02	-1.99
		38	4.5	1	1.35	3.61	3.86	-0.84	-0.83	-0.81	-0.80	-0.78	-0.76	-0.75	-0.73	-0.71	-0.70	-0.68	-0.67	-0.65	-0.63	-0.62	-0.60	-0.59	-0.57	-0.55	-0.54
		39	4.5	1	1.35	33.42	33.44	-2.48	-2.44	-2.40	-2.36	-2.31	-2.27	-2.23	-2.19	-2.15	-2.10	-2.06	-2.02	-1.98	-1.94	-1.89	-1.85	-1.81	-1.77	-1.73	-1.70
		40	4.5	1	1.35	72.28	72.29	-3.39	-3.34	-3.29	-3.24	-3.19	-3.14	-3.08	-3.03	-2.98	-2.93	-2.88	-2.83	-2.78	-2.73	-2.67	-2.62	-2.57	-2.52	-2.47	-2.44
		41	4.5	1	1.35	30.81	30.84	-2.40	-2.36	-2.32	-2.28	-2.24	-2.20	-2.16	-2.12	-2.07	-2.03	-1.99	-1.95	-1.91	-1.87	-1.83	-1.79	-1.75	-1.71	-1.66	-1.64
		42	4.5	1	1.35	30.81	30.84	-2.40	-2.36	-2.32	-2.28	-2.24	-2.20	-2.16	-2.12	-2.07	-2.03	-1.99	-1.95	-1.91	-1.87	-1.83	-1.79	-1.75	-1.71	-1.66	-1.64
		43	4.5	1	1.35	101.99	102.00	-3.94	-3.89	-3.83	-3.77	-3.72	-3.66	-3.61	-3.55	-3.50	-3.44	-3.39	-3.33	-3.28	-3.22	-3.17	-3.11	-3.05	-3.00	-2.94	-2.91
		44	4.5	1	1.35	97.23	97.23	-3.86	-3.80	-3.75	-3.69	-3.64	-3.58	-3.53	-3.47	-3.42	-3.36	-3.31	-3.25	-3.20	-3.14	-3.09	-3.04	-2.98	-2.93	-2.87	-2.84
		45	4.5	1	1.35	48.37	48.39	-2.88	-2.83	-2.78	-2.74	-2.69	-2.64	-2.60	-2.55	-2.50	-2.46	-2.41	-2.36	-2.32	-2.27	-2.23	-2.18	-2.13	-2.09	-2.04	-2.01
		46	4.5	1	1.35	69.83	69.84	-3.34	-3.29	-3.24	-3.19	-3.14	-3.09	-3.04	-2.99	-2.94	-2.89	-2.83	-2.78	-2.73	-2.68	-2.63	-2.58	-2.53	-2.48	-2.43	-2.40
		47	4.5	1	1.35	58.36	58.37	-3.10	-3.05	-3.01	-2.96	-2.91	-2.86	-2.81	-2.76	-2.71	-2.67	-2.62	-2.57	-2.52	-2.47	-2.42	-2.37	-2.32	-2.28	-2.23	-2.20
		48	4.5	1	1.35	27.80	27.83	-2.31	-2.27	-2.23	-2.19	-2.15	-2.11	-2.07	-2.03	-1.99	-1.95	-1.91	-1.87	-1.83	-1.79	-1.75	-1.71	-1.67	-1.63	-1.59	-1.57
		49	4.5	1	1.35	88.05	88.06	-3.69	-3.64	-3.58	-3.53	-3.48	-3.42	-3.37	-3.32	-3.26	-3.21	-3.16	-3.10	-3.05	-3.00	-2.94	-2.89	-2.83	-2.78	-2.73	-2.69
		50	4.5	1	1.35	21.82	21.86	-2.09	-2.06	-2.02	-1.98	-1.95	-1.91	-1.87	-1.83	-1.80	-1.76	-1.72	-1.69	-1.65	-1.61	-1.58	-1.54	-1.50	-1.47	-1.43	-1.41
		51	4.5	1	1.35	19.97	20.01	-2.02	-1.98	-1.95	-1.91	-1.88	-1.84	-1.80	-1.77	-1.73	-1.70	-1.66	-1.62	-1.59	-1.55	-1.52	-1.48	-1.44	-1.41	-1.37	-1.35
		52	4.5	1	1.35	108.78	108.79	-4.06	-4.00	-3.95	-3.89	-3.83	-3.78	-3.72	-3.66	-3.61	-3.55	-3.50	-3.44	-3.38	-3.33	-3.27	-3.22	-3.16	-3.10	-3.05	-3.01
		53	4.5	1	1.35	78.69	78.70	-3.52	-3.46	-3.41	-3.36	-3.31	-3.26	-3.20	-3.15	-3.10	-3.05	-2.99	-2.94	-2.89	-2.84	-2.79	-2.73	-2.68	-2.63	-2.58	-2.54
		54	4.5	1	1.35	87.27	87.28	-3.68	-3.62	-3.57	-3.52	-3.46	-3.41	-3.36	-3.30	-3.25	-3.20	-3.14	-3.09	-3.04	-2.98	-2.93	-2.87	-2.82	-2.77	-2.71	-2.68
		55	4.5	1	1.35	131.88	131.89	-4.44	-4.38	-4.32	-4.26	-4.21	-4.15	-4.09	-4.03	-3.97	-3.91	-3.85	-3.80	-3.74	-3.68	-3.62	-3.56	-3.50	-3.45	-3.39	-3.35
		56	4.5	1	1.35	117.90	117.91	-4.21	-4.15	-4.10	-4.04	-3.98	-3.93	-3.87	-3.81	-3.75	-3.70	-3.64	-3.58	-3.53	-3.47	-3.41	-3.35	-3.30	-3.24	-3.18	-3.15
		57	4.5	1	1.35	119.06	119.07	-4.23	-4.17	-4.12	-4.06	-4.00	-3.94	-3.89	-3.83	-3.77	-3.72	-3.66	-3.60	-3.54	-3.49	-3.43	-3.37	-3.31	-3.26	-3.20	-3.17
		58	4.5	1	1.35	98.35	98.36	-3.88	-3.82	-3.77	-3.71	-3.66	-3.60	-3.55	-3.49	-3.44	-3.38	-3.33	-3.27	-3.22	-3.16	-3.11	-3.05	-3.00	-2.94	-2.89	-2.86
		59	4.5	1	1.35	101.12	101.13	-3.93	-3.87	-3.81	-3.76	-3.70	-3.65	-3.59	-3.54	-3.48	-3.43	-3.37	-3.32	-3.26	-3.21	-3.15	-3.10	-3.04	-2.99	-2.93	-2.90
		60	4.5	1	1.35	97.08	97.09	-3.85	-3.80	-3.74	-3.69	-3.64	-3.58	-3.53	-3.47	-3.42	-3.36	-3.31	-3.25	-3.20	-3.14	-3.09	-3.03	-2.98	-2.92	-2.87	-2.84
		61	4.5	1	1.35	104.74	104.75	-3.99	-3.93	-3.88	-3.82	-3.77	-3.71	-3.65	-3.60	-3.54	-3.49	-3.43	-3.38	-3.32	-3.26	-3.21	-3.15	-3.10	-3.04	-2.99	-2.95
		62	4.5	1	1.35	19.97	20.01	-2.02	-1.98	-1.95	-1.91	-1.88	-1.84	-1.80	-1.77	-1.73	-1.70	-1.66	-1.62	-1.59	-1.55	-1.52	-1.48	-1.44	-1.41	-1.37	-1.35
		63	4.5	1	1.35	110.84	110.84	-4.09	-4.04	-3.98	-3.92	-3.87	-3.81	-3.75	-3.70	-3.64	-3.59	-3.53	-3.47	-3.42	-3.36	-3.30	-3.25	-3.19	-3.13	-3.08	-3.04
		64	4.5	1	1.35	119.63	119.64	-4.24	-4.18	-4.12	-4.07	-4.01	-3.95	-3.90	-3.84	-3.78	-3.72	-3.67	-3.61	-3.55	-3.49	-3.44	-3.38	-3.32	-3.27	-3.21	-3.17
		65	4.5	1	1.35	139.79	139.79	-4.56	-4.51	-4.45	-4.39	-4.33	-4.27	-4.21	-4.15	-4.09	-4.03	-3.97	-3.91	-3.86	-3.80	-3.74	-3.68	-3.62	-3.56	-3.50	-3.46
		66	4.5	1	1.35	137.55	137.56	-4.53	-4.47	-4.41	-4.35	-4.29	-4.23	-4.18	-4.12	-4.06	-4.00	-3.94	-3.88	-3.82	-3.76	-3.70	-3.65	-3.59	-3.53	-3.47	-3.43
		67	4.5	1	1.35	133.96	133.97	-4.47	-4.41	-4.35	-4.30	-4.24	-4.18	-4.12	-4.06	-4.00	-3.94	-3.89	-3.83	-3.77	-3.71	-3.65	-3.59	-3.53	-3.48	-3.42	-3.38
		68	4.5	1	1.35	135.87	135.88	-4.50	-4.44	-4.39	-4.33	-4.27	-4.21	-4.15	-4.09	-4.03	-3.97	-3.91	-3.86	-3.80	-3.74	-3.68	-3.62	-3.56	-3.50	-3.44	-3.41
		69	4.5	1	1.35	32.91	32.93	-2.47	-2.42	-2.38	-2.34	-2.30	-2.26	-2.22	-2.17	-2.13	-2.09	-2.05	-2.01	-1.96	-1.92	-1.88	-1.84	-1.80	-1.76	-1.71	-1.69
		70	4.5	1	1.35	108.00	108.01	-4.04	-3.99	-3.93	-3.88	-3.82	-3.76	-3.71	-3.65	-3.60	-3.54	-3.48	-3.43	-3.37	-3.32	-3.26	-3.20	-3.15	-3.09	-3.04	-3.00
		71	4.5	1	1.35	33.27	33.30	-2.48	-2.44	-2.39	-2.35	-2.31	-2.27	-2.23	-2.18	-2.14	-2.10	-2.06	-2.02	-1.97	-1.93	-1.89	-1.85	-1.81	-1.76	-1.72	-1.70
		72	4.5	1	1.35	41.34	41.36	-2.70	-2.66	-2.61	-2.57	-2.52	-2.48	-2.43	-2.39	-2.34	-2.30	-2.25	-2.21	-2.17	-2.12	-2.08	-2.03	-1.99	-1.94	-1.90	-1.87
		73	4.5	1	1.35	101.56	101.57	-3.93	-3.88	-3.82	-3.77	-3.71	-3.66	-3.60	-3.55	-3.49	-3.44	-3.38	-3.32	-3.27	-3.21	-3.16	-3.10	-3.05	-2.99	-2.94	-2.90
		74	4.5	1	1.35	96.53	96.54	-3.84	-3.79	-3.74	-3.68	-3.63	-3.57	-3.52	-3.46	-3.41	-3.35	-3.30	-3.24	-3.19	-3.13	-3.08	-3.02	-2.97	-2.91	-2.86	-2.83

The site amplification is a function of R_{JB}, the closest distance to surface projection of fault, V_{s30}, shear wave velocity of the top 30m layer and M, magnitude. As stated above R_{JB} is taken to be equal to epicentral distance and the magnitude is clearly defined. Yapi Merkezi's report (2014) classifies the medium into five soil groups labeled from A-E increasing in degree of weathering (It is not based on ground type classification). Though the section dealt in this thesis is composed of the soil classes labeled from A-C, representative geotechnical parameter has been assigned for an assumed single profile by Yapi Merkezi (2016) and this single layer is used for subsequent analysis. Accordingly, shear wave velocity is calculated using wave equation:

$$V_s = \sqrt{\frac{G}{\rho}} \tag{3.21}$$

Where G- Shear modulus

ρ– Density of the soil

Finally the shear wave velocity of the top 30m is calculated as:

$$V_{s30} = \frac{\sum H_i}{\sum \frac{H_i}{V_{si}}} \tag{3.22}$$

Where H_i- Depth of a single soil class

V_{si} – Shear wave velocity of single soil class

V_{s30} value for a section between 178+807-178+864 is 202.18m/s.

The site amplification calculations vary for each source so that there are a number of site amplification sheets. The site amplification calculation for source 1 is given in Table 3.6. Site amplification has two components: linear and nonlinear. As can be seen in table 3.6 a single column is assigned for the linear site amplification, as it is constant while three

columns are assigned for the nonlinear term. This is because of the dependency of nonlinear term on pga4nl which intern depends on the faulting mechanism.

Table 3. 6: Sample calculation for site amplification at source 1 (178+807 - 178+864)

Site amplification															
						pga4nl			F_{NL}			F_{LIN}	$F_S = F_{NL}+F_{LIN}$		
		Section	V_{s30} (m/s)	b_{nl}	M	Strike slip	Normal	unspecified	Strike slip	Normal	unspecified		Strike slip	Normal	unspecified
b_{lin}	-0.36	178+807-178+864	202.18	-0.526	5	0.0044	0.003	0.004	0.269	0.269	0.269	0.477	0.746	0.746	0.746
V_{ref}	760		202.18	-0.526	5.1	0.005	0.004	0.005	0.269	0.269	0.269	0.477	0.746	0.746	0.746
a_1	0.03		202.18	-0.526	5.2	0.0056	0.004	0.005	0.269	0.269	0.269	0.477	0.746	0.746	0.746
a_2	0.09		202.18	-0.526	5.3	0.0063	0.005	0.006	0.269	0.269	0.269	0.477	0.746	0.746	0.746
ga_lov	0.06		202.18	-0.526	5.4	0.0071	0.006	0.007	0.269	0.269	0.269	0.477	0.746	0.746	0.746
V_1	180		202.18	-0.526	5.5	0.0079	0.006	0.008	0.269	0.269	0.269	0.477	0.746	0.746	0.746
V_2	300		202.18	-0.526	5.6	0.0088	0.007	0.009	0.269	0.269	0.269	0.477	0.746	0.746	0.746
b_1	-0.64		202.18	-0.526	5.7	0.0098	0.008	0.010	0.269	0.269	0.269	0.477	0.746	0.746	0.746
b_2	-0.14		202.18	-0.526	5.8	0.0109	0.009	0.011	0.269	0.269	0.269	0.477	0.746	0.746	0.746
Δx	1.099		202.18	-0.526	5.9	0.0121	0.009	0.012	0.269	0.269	0.269	0.477	0.746	0.746	0.746
			202.18	-0.526	6	0.0134	0.010	0.013	0.269	0.269	0.269	0.477	0.746	0.746	0.746
			202.18	-0.526	6.1	0.0148	0.012	0.014	0.269	0.269	0.269	0.477	0.746	0.746	0.746
			202.18	-0.526	6.2	0.0163	0.013	0.016	0.269	0.269	0.269	0.477	0.746	0.746	0.746
			202.18	-0.526	6.3	0.018	0.014	0.017	0.269	0.269	0.269	0.477	0.746	0.746	0.746
			202.18	-0.526	6.4	0.0197	0.015	0.019	0.269	0.269	0.269	0.477	0.746	0.746	0.746
			202.18	-0.526	6.5	0.0216	0.017	0.021	0.269	0.269	0.269	0.477	0.746	0.746	0.746
			202.18	-0.526	6.6	0.0236	0.018	0.023	0.269	0.269	0.269	0.477	0.746	0.746	0.746
			202.18	-0.526	6.7	0.0258	0.020	0.025	0.269	0.269	0.269	0.477	0.746	0.746	0.746
			202.18	-0.526	6.8	0.0277	0.022	0.027	0.269	0.269	0.269	0.477	0.746	0.746	0.746
			202.18	-0.526	6.86	0.0286	0.022	0.028	0.269	0.269	0.269	0.477	0.746	0.746	0.746
			202.18	-0.526	6.9	0	0	0	0.269	0.269	0.269	0.477	0.746	0.746	0.746
			202.18	-0.526					0.269	0.269	0.269	0.477	0.746	0.746	0.746
			202.18	-0.526					0.269	0.269	0.269	0.477	0.746	0.746	0.746
			202.18	-0.526					0.269	0.269	0.269	0.477	0.746	0.746	0.746
			202.18	-0.526					0.269	0.269	0.269	0.477	0.746	0.746	0.746

The PGA calculation for source 1 is given in Table 3.7. The 2nd, 3rd and 4th columns are assigned for magnitude scaling according to faulting mechanism. The 6th column is filled with distance function while the next three columns show the site amplification values according to faulting mechanism. The error term comes in 17th and 18th column after calculating the standard deviations for the sum of magnitude scaling, distance function and site amplification. The last two columns show the PGA values for strike slip and normal faulting mechanism successively.

Table 3.7: PGA for source 1 at 178+807 - 178+864

PGA																						
	$F_M(M)$			Distance function		$F_S(V_{s30},R_{JB},M)$			$\ln Y' = F_M(M) + F_D(R_{JB},M) + F_S(V_{s30},R_{JB},M)$			$(\ln Y'-\ln \ddot{y})^2$			For specified fault type			$\ln Y = F_M(M)+F_D(R_{JB},M)+F_S(V_{s30},R_{JB},M)+\varepsilon\sigma_T$		**Y in g**	
	Strike slip	Normal	unspecified	$F_D(R_{JB},M)$	Section	Strike slip	Normal	unspecified	Strike slip	Normal	unspecified	Strike slip	Normal	unspecified	$\varepsilon=(\ln Y'-\ln \ddot{y})/s$			Strike slip	Normal	Strike slip	Normal
M															σ_T	Strike slip	Normal				
5	-1.32	-1.57	-1.353	-4.098		0.746	0.746	0.746	-4.671	-4.923	-4.706	1.036	1.036	1.036	0.565	-1.710	-1.710	-5.638	-5.890	0.004	0.003
5.1	-1.26	-1.507	-1.290	-4.042		0.746	0.746	0.746	-4.552	-4.803	-4.586	0.807	0.807	0.807	0.565	-1.509	-1.509	-5.405	-5.656	0.004	0.003
5.2	-1.19	-1.445	-1.229	-3.985		0.746	0.746	0.746	-4.434	-4.685	-4.468	0.609	0.609	0.609	0.565	-1.311	-1.311	-5.175	-5.427	0.006	0.004
5.3	-1.13	-1.386	-1.169	-3.929		0.746	0.746	0.746	-4.318	-4.569	-4.353	0.442	0.442	0.442	0.565	-1.117	-1.117	-4.950	-5.201	0.007	0.006
5.4	-1.08	-1.329	-1.112	-3.872		0.746	0.746	0.746	-4.205	-4.456	-4.239	0.304	0.304	0.304	0.565	-0.926	-0.926	-4.728	-4.979	0.009	0.007
5.5	-1.02	-1.274	-1.057	-3.816		0.746	0.746	0.746	-4.093	-4.344	-4.127	0.193	0.193	0.193	0.565	-0.738	-0.738	-4.510	-4.762	0.011	0.009
5.6	-0.97	-1.22	-1.004	-3.760		0.746	0.746	0.746	-3.983	-4.235	-4.018	0.109	0.109	0.109	0.565	-0.554	-0.554	-4.297	-4.548	0.014	0.011
5.7	-0.92	-1.169	-0.953	-3.703		0.746	0.746	0.746	-3.876	-4.127	-3.910	0.049	0.049	0.049	0.565	-0.374	-0.374	-4.087	-4.338	0.017	0.013
5.8	-0.87	-1.12	-0.903	-3.647		0.746	0.746	0.746	-3.77	-4.021	-3.805	0.014	0.014	0.014	0.565	-0.196	-0.196	-3.881	-4.132	0.021	0.016
5.9	-0.82	-1.073	-0.856	-3.591		0.746	0.746	0.746	-3.667	-3.918	-3.701	0.000	0.000	0.000	0.565	-0.022	-0.022	-3.679	-3.931	0.025	0.020
6	-0.78	-1.028	-0.811	-3.534		0.746	0.746	0.746	-3.565	-3.817	-3.600	0.008	0.008	0.008	0.565	0.148	0.148	-3.482	-3.733	0.031	0.024
6.1	-0.73	-0.985	-0.768	-3.478		0.746	0.746	0.746	-3.466	-3.717	-3.500	0.035	0.035	0.035	0.565	0.315	0.315	-3.288	-3.539	0.037	0.029
6.2	-0.69	-0.944	-0.727	-3.421		0.746	0.746	0.746	-3.368	-3.620	-3.403	0.081	0.081	0.081	0.565	0.479	0.479	-3.098	-3.349	0.045	0.035
6.3	-0.65	-0.905	-0.688	-3.365		0.746	0.746	0.746	-3.273	-3.524	-3.308	0.145	0.145	0.145	0.565	0.639	0.639	-2.912	-3.163	0.054	0.042
6.4	-0.62	-0.868	-0.651	-3.309		0.746	0.746	0.746	-3.18	-3.431	-3.214	0.224	0.224	0.224	0.565	0.796	0.796	-2.730	-2.981	0.065	0.051
6.5	-0.58	-0.833	-0.616	-3.252		0.746	0.746	0.746	-3.088	-3.340	-3.123	0.319	0.319	0.319	0.565	0.949	0.949	-2.552	-2.803	0.078	0.061
6.6	-0.55	-0.8	-0.584	-3.196		0.746	0.746	0.746	-2.999	-3.250	-3.034	0.428	0.428	0.428	0.565	1.099	1.099	-2.378	-2.629	0.093	0.072
6.7	-0.52	-0.769	-0.553	-3.139		0.746	0.746	0.746	-2.912	-3.163	-2.947	0.550	0.550	0.550	0.565	1.246	1.246	-2.208	-2.459	0.110	0.086
6.8	-0.5	-0.755	-0.538	-3.083		0.746	0.746	0.746	-2.841	-3.092	-2.875	0.660	0.660	0.660	0.565	1.365	1.365	-2.069	-2.320	0.126	0.098
6.86	-0.5	-0.755	-0.538	-3.049	178+807-178+864	0.746	0.746	0.746	-2.807	-3.058	-2.842	0.716	0.716	0.716	0.565	1.422	1.422	-2.003	-2.254	0.135	0.105
								Sum	-73.07	-78.094	-73.760	6.729									
								mean,	-3.653	-3.905	-3.688										
								standard deviation, s				0.595									

According to Yapi Merkezi's basic design report (2014) and supplemented by the Ethiopian Geological survey report (Belay et al., 2009), the structure of the area is composed of normal and strike slip faults. Boore and Atkinson (2008) states that amplitudes of event terms of normal fault earthquakes are lower than strike-slip and reverse earthquakes for most periods. This is also the case seen while calculating PGA. Besides strike slip can produce larger movement (Kramer, 1996) which leads to larger ground acceleration. Therefore, PGA values of strike slip fault type are considered. The PGA values for strike slip and for all sources are summarized in Table 3.8. As can be seen from Table 3.8, the maximum estimated PGA for the site under consideration at section 178+807-178+864 is 0.63g. As FHWA (2009) summarizes from Power et al. (1998) work, ground shaking from;

- PGA $\leq$ 0.2g caused no damage in tunnels.
- PGA between 0.2g - 0.5g caused damage ranging slight to heavy.
- PGA > 0.5g caused damage ranging slight to heavy.

Table 3. 8: Summary of PGA for all sources considering strike slip (178+807 - 178+864)

Summary of PGA for strike slip																					
Source	Distance	Magnitude																			
		5	5.1	5.2	5.3	5.4	5.5	5.6	5.7	5.8	5.9	6	6.1	6.2	6.3	6.4	6.5	6.6	6.7	6.8	6.86
1	111.2	0.004	0.004	0.006	0.007	0.009	0.011	0.014	0.017	0.021	0.025	0.031	0.037	0.045	0.054	0.065	0.078	0.093	0.110	0.126	0.135
2	57.2	0.010	0.012	0.015	0.019	0.024	0.029	0.036	0.045	0.055	0.067	0.081	0.097	0.116	0.137	0.161	0.186	0.213	0.242	0.266	0.277
3	26.02	0.020	0.025	0.033	0.042	0.053	0.066	0.082	0.099	0.119	0.140	0.162	0.185	0.207	0.229	0.252	0.275	0.301	0.328	0.350	0.360
4	47.03	0.012	0.015	0.019	0.024	0.030	0.037	0.046	0.056	0.069	0.084	0.101	0.120	0.142	0.165	0.190	0.217	0.244	0.271	0.293	0.302
5	5.117	0.058	0.068	0.079	0.093	0.108	0.125	0.144	0.166	0.190	0.216	0.246	0.278	0.313	0.351	0.393	0.437	0.485	0.536	0.573	0.587
6	8.82	0.044	0.055	0.068	0.081	0.095	0.109	0.126	0.145	0.166	0.189	0.214	0.243	0.273	0.307	0.344	0.384	0.426	0.472	0.508	0.522
7	18.4	0.025	0.033	0.043	0.055	0.069	0.085	0.103	0.122	0.142	0.163	0.183	0.204	0.227	0.251	0.278	0.306	0.337	0.369	0.396	0.408
8	6.895	0.051	0.062	0.073	0.086	0.100	0.115	0.133	0.153	0.176	0.200	0.228	0.258	0.291	0.327	0.366	0.409	0.454	0.503	0.540	0.554
9	15.54	0.029	0.038	0.049	0.062	0.077	0.094	0.112	0.130	0.149	0.168	0.189	0.212	0.236	0.263	0.292	0.323	0.357	0.392	0.421	0.434
10	42.76	0.013	0.016	0.021	0.026	0.033	0.041	0.051	0.063	0.077	0.093	0.111	0.132	0.154	0.178	0.204	0.230	0.256	0.282	0.302	0.311
11	3.308	0.065	0.076	0.089	0.104	0.121	0.140	0.161	0.185	0.211	0.240	0.272	0.307	0.345	0.386	0.431	0.478	0.528	0.581	0.618	0.630
12	40.93	0.014	0.017	0.022	0.027	0.034	0.043	0.054	0.066	0.080	0.097	0.116	0.137	0.160	0.184	0.210	0.236	0.261	0.286	0.305	0.314
13	28.77	0.018	0.023	0.030	0.039	0.049	0.061	0.075	0.092	0.110	0.131	0.153	0.176	0.199	0.223	0.245	0.268	0.292	0.317	0.339	0.348
14	6.947	0.051	0.062	0.073	0.086	0.099	0.115	0.133	0.153	0.175	0.200	0.227	0.258	0.291	0.327	0.366	0.408	0.453	0.502	0.539	0.553
15	73.36	0.007	0.009	0.011	0.014	0.017	0.021	0.026	0.032	0.040	0.048	0.059	0.071	0.085	0.102	0.121	0.143	0.168	0.195	0.219	0.231
16	64.54	0.008	0.010	0.013	0.016	0.020	0.025	0.031	0.038	0.047	0.057	0.069	0.084	0.101	0.120	0.142	0.166	0.192	0.220	0.245	0.256
17	88.3	0.005	0.007	0.008	0.010	0.013	0.016	0.020	0.025	0.030	0.037	0.045	0.054	0.065	0.079	0.094	0.112	0.133	0.156	0.178	0.189
18	116.8	0.003	0.004	0.005	0.006	0.008	0.010	0.012	0.015	0.019	0.023	0.028	0.034	0.041	0.050	0.060	0.072	0.085	0.101	0.116	0.124
19	93.35	0.005	0.006	0.008	0.010	0.012	0.015	0.018	0.023	0.028	0.034	0.041	0.050	0.060	0.072	0.086	0.103	0.122	0.145	0.165	0.176
20	65.79	0.008	0.010	0.013	0.016	0.020	0.025	0.030	0.037	0.046	0.056	0.068	0.082	0.098	0.117	0.138	0.162	0.188	0.216	0.241	0.253
21	81.5	0.006	0.008	0.009	0.012	0.015	0.018	0.023	0.028	0.034	0.042	0.050	0.061	0.074	0.088	0.106	0.125	0.148	0.173	0.196	0.207
22	18.87	0.025	0.033	0.043	0.054	0.068	0.084	0.102	0.121	0.141	0.162	0.182	0.203	0.225	0.250	0.276	0.304	0.334	0.366	0.392	0.404
23	33.71	0.016	0.020	0.026	0.033	0.042	0.053	0.065	0.080	0.097	0.116	0.137	0.160	0.183	0.208	0.232	0.256	0.279	0.302	0.322	0.332
24	22.16	0.022	0.029	0.038	0.048	0.061	0.075	0.092	0.111	0.131	0.152	0.174	0.195	0.216	0.239	0.263	0.289	0.317	0.346	0.370	0.381
25	26.54	0.019	0.025	0.032	0.041	0.052	0.065	0.081	0.098	0.117	0.138	0.160	0.183	0.206	0.228	0.250	0.274	0.299	0.326	0.348	0.358
26	30.11	0.017	0.023	0.029	0.037	0.047	0.059	0.072	0.088	0.107	0.127	0.148	0.172	0.195	0.219	0.242	0.264	0.288	0.313	0.334	0.343
27	33.78	0.016	0.020	0.026	0.033	0.042	0.052	0.065	0.080	0.097	0.116	0.137	0.159	0.183	0.208	0.232	0.256	0.278	0.302	0.322	0.331
28	7.754	0.048	0.059	0.071	0.083	0.097	0.112	0.130	0.149	0.171	0.195	0.221	0.251	0.283	0.318	0.356	0.397	0.441	0.489	0.525	0.540
29	11.02	0.037	0.048	0.061	0.075	0.090	0.105	0.121	0.139	0.158	0.180	0.203	0.230	0.258	0.289	0.323	0.360	0.399	0.441	0.475	0.489
30	23.42	0.021	0.028	0.036	0.046	0.058	0.072	0.089	0.107	0.127	0.148	0.170	0.192	0.214	0.236	0.259	0.284	0.311	0.339	0.363	0.374
31	8.135	0.046	0.058	0.070	0.083	0.096	0.111	0.128	0.147	0.169	0.192	0.219	0.248	0.279	0.314	0.351	0.392	0.436	0.483	0.519	0.533
32	77.03	0.007	0.008	0.010	0.013	0.016	0.020	0.025	0.030	0.037	0.045	0.055	0.066	0.080	0.096	0.114	0.135	0.159	0.185	0.208	0.220
33	15.55	0.029	0.038	0.049	0.062	0.077	0.094	0.112	0.130	0.149	0.168	0.189	0.212	0.236	0.263	0.292	0.323	0.356	0.392	0.421	0.434
34	26.41	0.019	0.025	0.032	0.042	0.053	0.066	0.081	0.098	0.118	0.139	0.161	0.184	0.206	0.228	0.251	0.274	0.299	0.326	0.348	0.358
35	59.14	0.009	0.012	0.015	0.018	0.023	0.028	0.035	0.043	0.053	0.064	0.078	0.094	0.112	0.132	0.155	0.180	0.207	0.236	0.260	0.272
36	23.32	0.021	0.028	0.036	0.046	0.058	0.072	0.089	0.107	0.127	0.149	0.171	0.193	0.214	0.236	0.259	0.285	0.311	0.340	0.364	0.374
37	47.26	0.012	0.015	0.019	0.024	0.030	0.037	0.046	0.056	0.069	0.084	0.100	0.120	0.141	0.164	0.190	0.216	0.243	0.270	0.292	0.302
38	3.613	0.063	0.074	0.087	0.102	0.118	0.137	0.158	0.181	0.207	0.236	0.267	0.301	0.339	0.379	0.423	0.470	0.519	0.572	0.609	0.621
39	33.42	0.016	0.021	0.026	0.034	0.042	0.053	0.066	0.081	0.098	0.117	0.138	0.161	0.184	0.209	0.233	0.257	0.279	0.303	0.323	0.332
40	72.28	0.007	0.009	0.011	0.014	0.018	0.022	0.027	0.033	0.040	0.049	0.060	0.072	0.087	0.104	0.124	0.146	0.171	0.198	0.222	0.234
41	30.81	0.017	0.022	0.028	0.036	0.046	0.057	0.071	0.087	0.105	0.125	0.146	0.169	0.193	0.217	0.240	0.262	0.286	0.311	0.331	0.341
42	30.81	0.017	0.022	0.028	0.036	0.046	0.057	0.071	0.087	0.105	0.125	0.146	0.169	0.193	0.217	0.240	0.262	0.286	0.311	0.331	0.341
43	102	0.004	0.005	0.007	0.008	0.010	0.013	0.016	0.020	0.024	0.029	0.036	0.043	0.052	0.063	0.075	0.090	0.107	0.126	0.145	0.155
44	97.23	0.005	0.006	0.007	0.009	0.011	0.014	0.017	0.021	0.026	0.032	0.039	0.047	0.056	0.068	0.081	0.097	0.115	0.136	0.156	0.166
45	48.37	0.012	0.015	0.018	0.023	0.029	0.036	0.044	0.055	0.067	0.081	0.098	0.117	0.138	0.161	0.186	0.212	0.240	0.267	0.289	0.299
46	69.83	0.007	0.009	0.012	0.015	0.018	0.023	0.028	0.035	0.042	0.052	0.063	0.076	0.091	0.109	0.129	0.152	0.177	0.205	0.229	0.241
47	58.36	0.009	0.012	0.015	0.019	0.023	0.029	0.035	0.044	0.053	0.065	0.079	0.095	0.113	0.134	0.157	0.183	0.210	0.238	0.262	0.274
48	27.8	0.019	0.024	0.031	0.040	0.050	0.063	0.078	0.094	0.113	0.134	0.156	0.179	0.202	0.225	0.247	0.270	0.295	0.321	0.342	0.352
49	88.05	0.005	0.007	0.008	0.011	0.013	0.016	0.020	0.025	0.030	0.037	0.045	0.054	0.066	0.079	0.094	0.112	0.133	0.157	0.178	0.189
50	21.82	0.022	0.029	0.038	0.049	0.061	0.076	0.093	0.112	0.132	0.153	0.175	0.196	0.217	0.240	0.264	0.290	0.318	0.348	0.372	0.383
51	19.97	0.024	0.031	0.041	0.052	0.065	0.081	0.098	0.118	0.138	0.159	0.180	0.200	0.222	0.246	0.271	0.299	0.328	0.359	0.384	0.396
52	108.8	0.004	0.005	0.006	0.007	0.009	0.011	0.014	0.017	0.021	0.026	0.032	0.039	0.047	0.056	0.068	0.081	0.096	0.114	0.131	0.140
53	78.69	0.006	0.008	0.010	0.012	0.016	0.019	0.024	0.029	0.036	0.044	0.053	0.064	0.077	0.093	0.111	0.131	0.154	0.180	0.204	0.215
54	87.27	0.005	0.007	0.009	0.011	0.013	0.017	0.020	0.025	0.031	0.038	0.046	0.055	0.067	0.080	0.096	0.114	0.135	0.159	0.180	0.191
55	131.9	0.003	0.003	0.004	0.005	0.006	0.008	0.010	0.012	0.015	0.018	0.022	0.027	0.033	0.040	0.048	0.057	0.068	0.081	0.093	0.100
56	117.9	0.003	0.004	0.005	0.006	0.008	0.010	0.012	0.015	0.019	0.023	0.028	0.034	0.041	0.049	0.059	0.070	0.084	0.099	0.114	0.122
57	119.1	0.003	0.004	0.005	0.006	0.008	0.010	0.012	0.015	0.018	0.022	0.027	0.033	0.040	0.048	0.058	0.069	0.082	0.098	0.112	0.120
58	98.35	0.004	0.006	0.007	0.009	0.011	0.014	0.017	0.021	0.025	0.031	0.038	0.046	0.055	0.067	0.080	0.095	0.113	0.134	0.153	0.163
59	101.1	0.004	0.005	0.007	0.008	0.010	0.013	0.016	0.020	0.024	0.030	0.036	0.044	0.053	0.064	0.076	0.091	0.108	0.128	0.147	0.157
60	97.08	0.005	0.006	0.007	0.009	0.011	0.014	0.017	0.021	0.026	0.032	0.039	0.047	0.057	0.068	0.081	0.097	0.115	0.136	0.156	0.166
61	104.7	0.004	0.005	0.006	0.008	0.010	0.012	0.015	0.019	0.023	0.028	0.034	0.041	0.050	0.060	0.072	0.086	0.102	0.121	0.139	0.148
62	19.97	0.024	0.031	0.041	0.052	0.065	0.081	0.098	0.118	0.138	0.159	0.180	0.200	0.222	0.246	0.271	0.299	0.328	0.359	0.384	0.396
63	110.8	0.004	0.005	0.006	0.007	0.009	0.011	0.014	0.017	0.021	0.025	0.031	0.038	0.045	0.055	0.066	0.078	0.093	0.111	0.127	0.136
64	119.6	0.003	0.004	0.005	0.006	0.008	0.010	0.012	0.015	0.018	0.022	0.027	0.033	0.040	0.048	0.057	0.069	0.082	0.097	0.111	0.119
65	139.8	0.002	0.003	0.004	0.004	0.006	0.007	0.009	0.011	0.013	0.016	0.020	0.024	0.029	0.035	0.042	0.051	0.061	0.072	0.083	0.089
66	137.5	0.002	0.003	0.004	0.005	0.006	0.007	0.009	0.011	0.014	0.017	0.020	0.025	0.030	0.036	0.044	0.053	0.063	0.075	0.086	0.092
67	134	0.002	0.003	0.004	0.005	0.006	0.008	0.009	0.012	0.014	0.018	0.022	0.026	0.032	0.038	0.046	0.055	0.066	0.079	0.091	0.097
68	135.9	0.002	0.003	0.004	0.005	0.006	0.007	0.009	0.011	0.014	0.017	0.021	0.026	0.031	0.037	0.045	0.054	0.064	0.076	0.088	0.094
69	32.91	0.016	0.021	0.027	0.034	0.043	0.054	0.067	0.082	0.099	0.118	0.139	0.162	0.186	0.210	0.234	0.258	0.281	0.305	0.325	0.334
70	108	0.004	0.005	0.006	0.007	0.009	0.012	0.014	0.018	0.022	0.027	0.032	0.039	0.047	0.057	0.069	0.082	0.097	0.115	0.132	0.141
71	33.27	0.016	0.021	0.026	0.034	0.043	0.053	0.066	0.081	0.098	0.117	0.138	0.161	0.185	0.209	0.233	0.257	0.280	0.304	0.324	0.333
72	41.34	0.013	0.017	0.022	0.027	0.034	0.043	0.053	0.065	0.080	0.096	0.115	0.136	0.159	0.183	0.208	0.234	0.260	0.285	0.305	0.313
73	101.6	0.004	0.005	0.007	0.008	0.010	0.013	0.016	0.020	0.024	0.029	0.036	0.044	0.053	0.063	0.076	0.090	0.108	0.127	0.146	0.156
74	96.53	0.010	0.013	0.016	0.020	0.025	0.030	0.038	0.046	0.057	0.069	0.085	0.102	0.124	0.149	0.178	0.212	0.252	0.298	0.341	0.363

The probability of peak ground acceleration exceeding a certain value of interest, for a given occurrence of earthquake should be determined for every combination of discretized magnitude and distance of each identified source. From the concept of probability, the probability that a particular ground motion parameter Y or for this case PGA exceeds a certain value x for an earthquake of a given magnitude m, occurring at a given distance r is given by:

$$(PGA > x \mid m, r) = 1 - F_x(x) \tag{3.23}$$

Where $F_X(x)$ is the cumulative distribution function of the ground motion parameter. Lognormal distribution is used to model many engineering data (Martin and Perez, 2009). As stated by Huyse et al. (2003) peak ground acceleration distribution is characterized by lognormal distribution provided that the annual probability of exceedance is not less than 10^{-6}. Therefore, lognormal distribution is used in this thesis. The calculation is done for PGA values ranging from 0.05g to 0.8g with an increment of 0.05g. Sample calculation is tabulated in Table 3.9 for 0.05g for the tunnel section between 178+807-178+864.

Table 3. 9: Probability of PGA exceeding 0.05g for a given occurrence of earthquake (178+807 - 178+864

Distance	P[PGA>0.05|m,r]																			
	Magnitude																			
	5	5.1	5.2	5.3	5.4	5.5	5.6	5.7	5.8	5.9	6	6.1	6.2	6.3	6.4	6.5	6.6	6.7	6.8	6.86
3.308	0.581	0.630	0.677	0.719	0.758	0.793	0.823	0.850	0.874	0.894	0.911	0.925	0.937	0.948	0.956	0.963	0.969	0.974	0.977	0.978
3.613	0.574	0.624	0.670	0.713	0.753	0.788	0.819	0.846	0.870	0.891	0.908	0.923	0.936	0.946	0.955	0.962	0.968	0.973	0.976	0.977
5.117	0.545	0.595	0.643	0.688	0.729	0.766	0.800	0.829	0.855	0.877	0.897	0.913	0.927	0.939	0.949	0.957	0.964	0.970	0.974	0.975
6.895	0.508	0.569	0.620	0.665	0.708	0.747	0.782	0.813	0.841	0.865	0.886	0.904	0.919	0.932	0.943	0.952	0.960	0.966	0.970	0.972
6.947	0.507	0.568	0.619	0.665	0.707	0.746	0.781	0.813	0.840	0.864	0.885	0.903	0.919	0.932	0.943	0.952	0.960	0.966	0.970	0.972
7.754	0.486	0.553	0.610	0.658	0.700	0.740	0.775	0.807	0.835	0.860	0.881	0.900	0.915	0.929	0.940	0.950	0.958	0.965	0.969	0.970
8.135	0.476	0.546	0.605	0.655	0.698	0.737	0.773	0.804	0.833	0.857	0.879	0.898	0.914	0.927	0.939	0.949	0.957	0.964	0.968	0.970
8.820	0.459	0.532	0.596	0.649	0.693	0.733	0.768	0.800	0.829	0.854	0.876	0.895	0.911	0.925	0.937	0.947	0.955	0.963	0.967	0.969
11.024	0.409	0.488	0.561	0.625	0.679	0.723	0.759	0.791	0.819	0.845	0.867	0.887	0.904	0.918	0.931	0.941	0.950	0.958	0.963	0.965
15.538	0.332	0.413	0.493	0.567	0.634	0.691	0.738	0.777	0.807	0.832	0.854	0.874	0.891	0.906	0.919	0.931	0.940	0.949	0.955	0.957
15.551	0.331	0.413	0.493	0.567	0.633	0.690	0.738	0.776	0.807	0.832	0.854	0.874	0.891	0.906	0.919	0.931	0.940	0.949	0.955	0.957
18.405	0.296	0.375	0.455	0.531	0.602	0.664	0.717	0.761	0.797	0.825	0.848	0.867	0.885	0.900	0.913	0.925	0.935	0.944	0.950	0.952
18.867	0.291	0.369	0.449	0.526	0.597	0.660	0.713	0.758	0.795	0.824	0.847	0.867	0.884	0.899	0.912	0.924	0.934	0.943	0.949	0.951
19.966	0.279	0.356	0.435	0.513	0.585	0.649	0.704	0.751	0.789	0.820	0.845	0.864	0.882	0.897	0.910	0.922	0.932	0.941	0.947	0.950
19.966	0.279	0.356	0.435	0.513	0.585	0.649	0.704	0.751	0.789	0.820	0.845	0.864	0.882	0.897	0.910	0.922	0.932	0.941	0.947	0.950
21.820	0.262	0.336	0.414	0.491	0.564	0.631	0.689	0.738	0.779	0.813	0.840	0.861	0.878	0.893	0.907	0.919	0.929	0.938	0.944	0.947
22.161	0.259	0.333	0.410	0.487	0.561	0.627	0.686	0.736	0.778	0.812	0.839	0.860	0.878	0.893	0.906	0.918	0.928	0.938	0.944	0.946
23.316	0.249	0.321	0.398	0.474	0.548	0.616	0.676	0.727	0.771	0.806	0.835	0.858	0.876	0.891	0.904	0.916	0.927	0.936	0.942	0.945
23.422	0.248	0.320	0.396	0.473	0.547	0.615	0.675	0.727	0.770	0.806	0.835	0.857	0.875	0.891	0.904	0.916	0.927	0.936	0.942	0.945
26.016	0.228	0.296	0.370	0.446	0.520	0.589	0.652	0.707	0.754	0.793	0.825	0.850	0.871	0.887	0.900	0.912	0.923	0.932	0.939	0.941
26.411	0.225	0.293	0.366	0.442	0.516	0.585	0.648	0.704	0.751	0.791	0.823	0.849	0.870	0.886	0.900	0.912	0.922	0.932	0.938	0.941
26.538	0.224	0.292	0.365	0.440	0.514	0.584	0.647	0.703	0.750	0.790	0.822	0.849	0.869	0.886	0.899	0.911	0.922	0.931	0.938	0.941
27.798	0.216	0.281	0.353	0.428	0.502	0.572	0.636	0.693	0.742	0.783	0.817	0.844	0.866	0.884	0.898	0.910	0.920	0.930	0.937	0.939
28.772	0.210	0.274	0.344	0.418	0.492	0.562	0.627	0.685	0.735	0.777	0.812	0.841	0.864	0.882	0.896	0.908	0.919	0.929	0.935	0.938
30.106	0.202	0.264	0.333	0.405	0.479	0.550	0.615	0.675	0.726	0.770	0.806	0.836	0.860	0.879	0.894	0.907	0.918	0.927	0.934	0.937
30.807	0.198	0.259	0.327	0.399	0.472	0.543	0.609	0.669	0.721	0.766	0.803	0.833	0.858	0.878	0.893	0.906	0.917	0.926	0.933	0.936
30.807	0.198	0.259	0.327	0.399	0.472	0.543	0.609	0.669	0.721	0.766	0.803	0.833	0.858	0.878	0.893	0.906	0.917	0.926	0.933	0.936
32.906	0.186	0.245	0.310	0.380	0.452	0.523	0.591	0.652	0.706	0.753	0.792	0.825	0.851	0.873	0.890	0.903	0.914	0.924	0.931	0.934
33.268	0.185	0.242	0.307	0.377	0.449	0.520	0.587	0.649	0.703	0.750	0.790	0.823	0.850	0.872	0.889	0.903	0.914	0.924	0.931	0.934
33.416	0.184	0.241	0.306	0.376	0.448	0.519	0.586	0.648	0.702	0.750	0.790	0.823	0.850	0.872	0.889	0.903	0.914	0.924	0.931	0.934
33.707	0.182	0.239	0.304	0.373	0.445	0.516	0.584	0.645	0.700	0.748	0.788	0.821	0.849	0.871	0.888	0.902	0.914	0.923	0.930	0.933
33.782	0.182	0.239	0.303	0.373	0.444	0.515	0.583	0.645	0.700	0.747	0.788	0.821	0.848	0.871	0.888	0.902	0.913	0.923	0.930	0.933
40.927	0.150	0.198	0.255	0.317	0.384	0.453	0.521	0.587	0.647	0.701	0.748	0.788	0.822	0.850	0.872	0.891	0.905	0.917	0.924	0.928
41.343	0.148	0.196	0.252	0.314	0.381	0.450	0.518	0.583	0.644	0.698	0.745	0.786	0.820	0.848	0.871	0.890	0.905	0.917	0.924	0.927
42.758	0.142	0.189	0.244	0.305	0.370	0.438	0.506	0.572	0.633	0.689	0.737	0.779	0.814	0.844	0.868	0.887	0.903	0.915	0.923	0.926
47.029	0.126	0.170	0.220	0.277	0.340	0.405	0.472	0.539	0.602	0.660	0.712	0.757	0.796	0.828	0.856	0.878	0.896	0.910	0.920	0.923
47.264	0.126	0.169	0.219	0.276	0.338	0.404	0.471	0.537	0.600	0.658	0.710	0.756	0.795	0.828	0.855	0.877	0.895	0.910	0.919	0.923
48.372	0.122	0.164	0.213	0.269	0.331	0.396	0.462	0.528	0.592	0.651	0.703	0.750	0.790	0.824	0.852	0.874	0.893	0.908	0.918	0.922
57.196	0.095	0.130	0.172	0.222	0.277	0.337	0.400	0.465	0.529	0.591	0.649	0.701	0.748	0.788	0.823	0.851	0.875	0.894	0.908	0.913
58.358	0.092	0.126	0.168	0.216	0.270	0.330	0.392	0.457	0.521	0.583	0.642	0.695	0.742	0.783	0.819	0.848	0.872	0.892	0.906	0.911
59.142	0.090	0.124	0.164	0.212	0.266	0.325	0.387	0.451	0.516	0.578	0.637	0.690	0.738	0.780	0.816	0.846	0.871	0.891	0.905	0.910
64.538	0.077	0.107	0.144	0.188	0.238	0.294	0.354	0.417	0.480	0.543	0.603	0.660	0.711	0.756	0.795	0.829	0.857	0.880	0.896	0.903
65.789	0.074	0.103	0.140	0.183	0.232	0.287	0.347	0.409	0.472	0.535	0.595	0.652	0.704	0.750	0.791	0.825	0.854	0.878	0.894	0.901
69.826	0.066	0.093	0.126	0.167	0.214	0.266	0.324	0.385	0.447	0.510	0.571	0.629	0.683	0.731	0.774	0.811	0.842	0.868	0.886	0.894
72.277	0.061	0.087	0.119	0.157	0.203	0.254	0.311	0.371	0.433	0.495	0.556	0.615	0.670	0.720	0.764	0.802	0.835	0.862	0.881	0.889
73.361	0.059	0.084	0.115	0.154	0.198	0.249	0.305	0.364	0.426	0.488	0.550	0.609	0.664	0.714	0.759	0.798	0.832	0.860	0.879	0.887
77.034	0.053	0.076	0.105	0.141	0.183	0.232	0.286	0.344	0.405	0.467	0.528	0.588	0.644	0.696	0.743	0.785	0.820	0.850	0.871	0.880
78.693	0.050	0.073	0.101	0.136	0.177	0.225	0.278	0.335	0.396	0.457	0.519	0.579	0.635	0.688	0.736	0.778	0.815	0.846	0.867	0.877
81.496	0.046	0.067	0.094	0.127	0.167	0.213	0.264	0.321	0.380	0.441	0.503	0.563	0.620	0.674	0.723	0.767	0.805	0.838	0.861	0.870
87.265	0.039	0.057	0.081	0.110	0.147	0.190	0.238	0.292	0.350	0.410	0.471	0.531	0.590	0.645	0.697	0.743	0.784	0.820	0.846	0.857
88.053	0.038	0.056	0.079	0.108	0.144	0.187	0.235	0.288	0.346	0.406	0.467	0.527	0.586	0.641	0.693	0.740	0.782	0.818	0.843	0.855
88.297	0.038	0.055	0.078	0.108	0.144	0.186	0.234	0.287	0.345	0.404	0.465	0.526	0.584	0.640	0.692	0.739	0.781	0.817	0.843	0.854
93.351	0.032	0.048	0.068	0.095	0.128	0.168	0.213	0.264	0.320	0.378	0.438	0.499	0.558	0.615	0.668	0.717	0.761	0.800	0.828	0.840
96.532	0.100	0.136	0.179	0.230	0.286	0.347	0.411	0.476	0.541	0.603	0.661	0.715	0.764	0.806	0.843	0.874	0.900	0.922	0.936	0.942
97.078	0.028	0.043	0.062	0.087	0.118	0.155	0.199	0.248	0.302	0.359	0.419	0.479	0.539	0.596	0.651	0.701	0.746	0.787	0.817	0.830
97.225	0.028	0.043	0.062	0.086	0.117	0.155	0.198	0.247	0.301	0.359	0.418	0.479	0.538	0.596	0.650	0.700	0.746	0.787	0.816	0.829
98.351	0.027	0.041	0.060	0.084	0.114	0.151	0.194	0.243	0.296	0.353	0.413	0.473	0.532	0.590	0.645	0.695	0.741	0.783	0.813	0.826
101.123	0.025	0.038	0.055	0.078	0.107	0.142	0.184	0.231	0.284	0.340	0.399	0.459	0.518	0.576	0.631	0.683	0.730	0.772	0.804	0.818
101.560	0.025	0.037	0.055	0.078	0.106	0.141	0.182	0.229	0.282	0.338	0.396	0.456	0.516	0.574	0.629	0.681	0.728	0.771	0.802	0.816
101.991	0.024	0.037	0.054	0.077	0.105	0.140	0.181	0.228	0.280	0.336	0.394	0.454	0.514	0.572	0.627	0.679	0.727	0.769	0.801	0.815
104.743	0.022	0.034	0.050	0.071	0.099	0.132	0.171	0.217	0.268	0.323	0.381	0.440	0.500	0.558	0.614	0.667	0.715	0.759	0.792	0.806
108.004	0.020	0.031	0.046	0.066	0.091	0.123	0.161	0.205	0.254	0.308	0.365	0.424	0.483	0.542	0.599	0.652	0.702	0.746	0.780	0.795
108.782	0.019	0.030	0.045	0.064	0.090	0.121	0.158	0.202	0.251	0.304	0.361	0.420	0.480	0.538	0.595	0.649	0.698	0.743	0.777	0.793
110.835	0.018	0.028	0.042	0.061	0.085	0.116	0.152	0.195	0.243	0.295	0.352	0.410	0.469	0.528	0.585	0.639	0.690	0.735	0.770	0.786
111.180	0.018	0.028	0.042	0.061	0.085	0.115	0.151	0.193	0.241	0.294	0.350	0.408	0.468	0.527	0.584	0.638	0.688	0.734	0.769	0.785
116.766	0.015	0.024	0.036	0.052	0.074	0.101	0.135	0.174	0.220	0.270	0.324	0.382	0.440	0.499	0.557	0.612	0.664	0.712	0.748	0.765
117.899	0.014	0.023	0.035	0.051	0.072	0.099	0.132	0.171	0.215	0.265	0.319	0.376	0.435	0.494	0.551	0.607	0.659	0.707	0.744	0.761
119.063	0.014	0.022	0.033	0.049	0.070	0.096	0.129	0.167	0.211	0.261	0.314	0.371	0.429	0.488	0.546	0.602	0.654	0.703	0.740	0.757
119.635	0.014	0.022	0.033	0.048	0.069	0.095	0.127	0.165	0.209	0.258	0.312	0.368	0.427	0.485	0.543	0.599	0.652	0.700	0.738	0.755
131.879	0.009	0.015	0.023	0.035	0.051	0.072	0.098	0.130	0.168	0.212	0.261	0.314	0.370	0.427	0.485	0.542	0.597	0.649	0.690	0.708
133.962	0.008	0.014	0.022	0.033	0.048	0.068	0.094	0.125	0.162	0.205	0.253	0.305	0.361	0.418	0.476	0.533	0.588	0.640	0.681	0.700
135.873	0.008	0.013	0.020	0.031	0.046	0.065	0.090	0.120	0.156	0.198	0.246	0.297	0.352	0.409	0.467	0.524	0.579	0.632	0.673	0.693
137.550	0.007	0.012	0.019	0.030	0.044	0.062	0.086	0.116	0.152	0.193	0.239	0.290	0.345	0.401	0.459	0.516	0.572	0.625	0.667	0.686
139.788	0.007	0.011	0.018	0.028	0.041	0.059	0.082	0.111	0.145	0.186	0.231	0.281	0.335	0.391	0.449	0.506	0.562	0.615	0.657	0.677

3.1.5. Construction of the hazard curve

The GMPE model discussed above gives the probability of exceeding a given level of PGA for a given magnitude and distance. The distance and magnitude distributions and probability expression of ground motion for a given source are combined to produce a statement of the probability that given the occurrence of a seismic event with a magnitude of interest anywhere on the source, the site PGA will exceed an acceleration of interest (Green et al., 1994). A hazard curve combines all of the above information into one plot. This is computed in probability computations as:

$$P(PGA > x) = \iint P(PPGA > x(\mathrm{PGA} > \mathrm{x} \mid m, r) f_M(m) f_R(r) dmdr \qquad (3.24)$$

This can be expressed in a summation form for discretized distribution (range of possible M_j and R_k will be discretized into ΔM and ΔR intervals with a total of n_M and n_R increments, respectively) as:

$$P(PGA > x) = \sum_{j=1}^{n_M} \sum_{k=1}^{n_R} P(PGA > x \mid \mathrm{m_j}, r_k) P(M = m_j) P(R = r_k) \qquad (3.25)$$

Where ΔM- is interval range for discretized earthquake magnitude

ΔR- is interval range for discretized distance

P (PGA> x|m_j, r_k) - from GMPE model

f_M(m) - PDF for earthquake magnitude

f_R(r) - PDF for distance

This calculation, for P (PGA>0.05g) for the tunnel section between 178+807-178+864, is given in Table 3.10.

Table 3. 10: Probability of PGA greater than 0.05, given the occurrence of earthquake (178+807 - 178+864)

Distance	P(PGA> x)																			
	Magnitude																			
	5	5.1	5.2	5.3	5.4	5.5	5.6	5.7	5.8	5.9	6	6.1	6.2	6.3	6.4	6.5	6.6	6.7	6.8	6.86
3.308	0.00154	0.00135	0.00117	0.001004	0.000854	0.000721	0.000605	0.000504	0.000418	0.000346	0.000284	0.000233	0.000191	0.000156	0.000127	0.000103	8.39E-05	6.81E-05	3.45E-05	2.07E-05
3.613	0.001521	0.001335	0.001159	0.000996	0.000848	0.000717	0.000602	0.000502	0.000417	0.000344	0.000284	0.000233	0.00019	0.000156	0.000127	0.000103	8.38E-05	6.8E-05	3.44E-05	2.06E-05
5.117	0.001444	0.001275	0.001112	0.000961	0.000822	0.000698	0.000588	0.000492	0.00041	0.000339	0.00028	0.00023	0.000189	0.000154	0.000126	0.000103	8.34E-05	6.78E-05	3.43E-05	2.06E-05
6.895	0.001347	0.001218	0.001071	0.000929	0.000798	0.00068	0.000574	0.000482	0.000403	0.000334	0.000277	0.000228	0.000187	0.000153	0.000125	0.000102	8.31E-05	6.75E-05	3.42E-05	2.05E-05
6.947	0.001344	0.001216	0.00107	0.000928	0.000797	0.000679	0.000574	0.000482	0.000403	0.000334	0.000276	0.000228	0.000187	0.000153	0.000125	0.000102	8.31E-05	6.75E-05	3.42E-05	2.05E-05
7.754	0.001289	0.001184	0.001055	0.000918	0.00079	0.000673	0.00057	0.000479	0.0004	0.000332	0.000275	0.000227	0.000186	0.000153	0.000125	0.000102	8.29E-05	6.74E-05	3.42E-05	2.05E-05
8.135	0.001264	0.001168	0.001047	0.000914	0.000786	0.000671	0.000568	0.000477	0.000399	0.000332	0.000275	0.000226	0.000186	0.000152	0.000125	0.000102	8.28E-05	6.74E-05	3.42E-05	2.05E-05
8.820	0.001218	0.001139	0.00103	0.000907	0.000782	0.000667	0.000565	0.000475	0.000397	0.00033	0.000274	0.000226	0.000186	0.000152	0.000124	0.000101	8.27E-05	6.73E-05	3.41E-05	2.05E-05
11.024	0.001084	0.001046	0.000971	0.000873	0.000765	0.000658	0.000558	0.000469	0.000393	0.000327	0.000271	0.000224	0.000184	0.000151	0.000124	0.000101	8.22E-05	6.69E-05	3.4E-05	2.04E-05
15.538	0.000879	0.000885	0.000852	0.000792	0.000714	0.000628	0.000542	0.000461	0.000387	0.000322	0.000267	0.00022	0.000181	0.000149	0.000122	9.97E-05	8.14E-05	6.63E-05	3.37E-05	2.02E-05
15.551	0.000879	0.000884	0.000852	0.000792	0.000714	0.000628	0.000542	0.000461	0.000387	0.000322	0.000267	0.00022	0.000181	0.000149	0.000122	9.97E-05	8.14E-05	6.63E-05	3.37E-05	2.02E-05
18.405	0.000784	0.000802	0.000786	0.000742	0.000678	0.000604	0.000527	0.000452	0.000382	0.000319	0.000265	0.000219	0.00018	0.000148	0.000121	9.91E-05	8.09E-05	6.59E-05	3.35E-05	2.01E-05
18.867	0.000771	0.00079	0.000776	0.000734	0.000673	0.0006	0.000524	0.00045	0.000381	0.000319	0.000265	0.000219	0.00018	0.000148	0.000121	9.9E-05	8.08E-05	6.59E-05	3.35E-05	2.01E-05
19.966	0.00074	0.000763	0.000753	0.000716	0.000659	0.00059	0.000518	0.000446	0.000378	0.000317	0.000264	0.000218	0.000179	0.000147	0.000121	9.88E-05	8.07E-05	6.57E-05	3.34E-05	2.01E-05
19.966	0.00074	0.000763	0.000753	0.000716	0.000659	0.00059	0.000518	0.000446	0.000378	0.000317	0.000264	0.000218	0.000179	0.000147	0.000121	9.88E-05	8.07E-05	6.57E-05	3.34E-05	2.01E-05
21.820	0.000694	0.00072	0.000716	0.000686	0.000636	0.000574	0.000506	0.000438	0.000373	0.000314	0.000262	0.000217	0.000179	0.000147	0.00012	9.85E-05	8.04E-05	6.55E-05	3.33E-05	2E-05
22.161	0.000686	0.000712	0.000709	0.00068	0.000632	0.000571	0.000504	0.000437	0.000372	0.000314	0.000262	0.000217	0.000179	0.000147	0.00012	9.84E-05	8.03E-05	6.55E-05	3.33E-05	2E-05
23.316	0.00066	0.000687	0.000687	0.000662	0.000618	0.00056	0.000497	0.000432	0.000369	0.000312	0.000261	0.000216	0.000178	0.000146	0.00012	9.82E-05	8.02E-05	6.54E-05	3.32E-05	2E-05
23.422	0.000657	0.000685	0.000685	0.000661	0.000617	0.000559	0.000496	0.000431	0.000369	0.000312	0.000261	0.000216	0.000178	0.000146	0.00012	9.82E-05	8.02E-05	6.54E-05	3.32E-05	2E-05
26.016	0.000605	0.000634	0.00064	0.000622	0.000586	0.000536	0.000479	0.000419	0.000361	0.000307	0.000258	0.000214	0.000177	0.000146	0.000119	9.78E-05	7.98E-05	6.51E-05	3.31E-05	1.99E-05
26.411	0.000597	0.000627	0.000633	0.000617	0.000581	0.000533	0.000477	0.000418	0.00036	0.000306	0.000257	0.000214	0.000177	0.000146	0.000119	9.77E-05	7.98E-05	6.51E-05	3.31E-05	1.99E-05
26.538	0.000595	0.000625	0.000631	0.000615	0.00058	0.000532	0.000476	0.000417	0.000359	0.000306	0.000257	0.000214	0.000177	0.000146	0.000119	9.77E-05	7.98E-05	6.51E-05	3.31E-05	1.99E-05
27.798	0.000573	0.000602	0.000611	0.000597	0.000565	0.00052	0.000467	0.000411	0.000355	0.000303	0.000255	0.000213	0.000176	0.000145	0.000119	9.75E-05	7.96E-05	6.5E-05	3.3E-05	1.98E-05
28.772	0.000557	0.000586	0.000595	0.000584	0.000554	0.000512	0.000461	0.000407	0.000352	0.000301	0.000254	0.000212	0.000176	0.000145	0.000119	9.74E-05	7.95E-05	6.49E-05	3.3E-05	1.98E-05
30.106	0.000535	0.000565	0.000575	0.000566	0.00054	0.0005	0.000452	0.0004	0.000348	0.000298	0.000252	0.000211	0.000175	0.000145	0.000119	9.72E-05	7.94E-05	6.48E-05	3.3E-05	1.98E-05
30.807	0.000525	0.000554	0.000565	0.000557	0.000532	0.000494	0.000448	0.000397	0.000345	0.000296	0.000251	0.00021	0.000175	0.000144	0.000119	9.71E-05	7.93E-05	6.47E-05	3.29E-05	1.98E-05
30.807	0.000525	0.000554	0.000565	0.000557	0.000532	0.000494	0.000448	0.000397	0.000345	0.000296	0.000251	0.00021	0.000175	0.000144	0.000119	9.71E-05	7.93E-05	6.47E-05	3.29E-05	1.98E-05
32.906	0.000494	0.000524	0.000536	0.000531	0.00051	0.000476	0.000434	0.000387	0.000338	0.000291	0.000247	0.000208	0.000173	0.000143	0.000118	9.68E-05	7.91E-05	6.46E-05	3.29E-05	1.97E-05
33.268	0.00049	0.000519	0.000531	0.000526	0.000506	0.000473	0.000432	0.000385	0.000337	0.00029	0.000247	0.000208	0.000173	0.000143	0.000118	9.68E-05	7.91E-05	6.45E-05	3.28E-05	1.97E-05
33.416	0.000487	0.000517	0.000529	0.000524	0.000505	0.000472	0.000431	0.000384	0.000336	0.00029	0.000247	0.000207	0.000173	0.000143	0.000118	9.68E-05	7.91E-05	6.45E-05	3.28E-05	1.97E-05
33.707	0.000484	0.000513	0.000525	0.000521	0.000502	0.00047	0.000429	0.000383	0.000335	0.000289	0.000246	0.000207	0.000173	0.000143	0.000118	9.67E-05	7.91E-05	6.45E-05	3.28E-05	1.97E-05
33.782	0.000483	0.000512	0.000524	0.00052	0.000501	0.000469	0.000428	0.000382	0.000335	0.000289	0.000246	0.000207	0.000173	0.000143	0.000118	9.67E-05	7.9E-05	6.45E-05	3.28E-05	1.97E-05
40.927	0.000396	0.000425	0.000441	0.000443	0.000433	0.000412	0.000383	0.000348	0.00031	0.000271	0.000234	0.000199	0.000167	0.00014	0.000116	9.54E-05	7.83E-05	6.41E-05	3.26E-05	1.96E-05
41.343	0.000392	0.00042	0.000436	0.000439	0.000429	0.000409	0.000381	0.000346	0.000308	0.00027	0.000233	0.000198	0.000167	0.000139	0.000116	9.54E-05	7.83E-05	6.4E-05	3.26E-05	1.96E-05
42.758	0.000377	0.000405	0.000422	0.000425	0.000417	0.000399	0.000372	0.000339	0.000303	0.000266	0.00023	0.000196	0.000166	0.000139	0.000115	9.51E-05	7.81E-05	6.39E-05	3.26E-05	1.96E-05
47.029	0.000335	0.000363	0.000381	0.000387	0.000383	0.000369	0.000347	0.00032	0.000288	0.000255	0.000222	0.000191	0.000162	0.000136	0.000114	9.41E-05	7.75E-05	6.36E-05	3.24E-05	1.95E-05
47.264	0.000333	0.000361	0.000379	0.000385	0.000381	0.000367	0.000346	0.000318	0.000287	0.000255	0.000222	0.000191	0.000162	0.000136	0.000113	9.4E-05	7.75E-05	6.36E-05	3.24E-05	1.95E-05
48.372	0.000323	0.000351	0.000369	0.000376	0.000373	0.00036	0.00034	0.000313	0.000283	0.000252	0.00022	0.000189	0.000161	0.000135	0.000113	9.37E-05	7.73E-05	6.35E-05	3.24E-05	1.95E-05
57.196	0.000252	0.000279	0.000298	0.000309	0.000312	0.000307	0.000294	0.000276	0.000253	0.000229	0.000203	0.000177	0.000152	0.00013	0.000109	9.12E-05	7.57E-05	6.25E-05	3.2E-05	1.93E-05
58.358	0.000244	0.00027	0.00029	0.000301	0.000305	0.0003	0.000288	0.000271	0.00025	0.000226	0.0002	0.000175	0.000151	0.000129	0.000109	9.09E-05	7.55E-05	6.23E-05	3.2E-05	1.93E-05
59.142	0.000238	0.000265	0.000284	0.000296	0.0003	0.000296	0.000285	0.000268	0.000247	0.000224	0.000199	0.000174	0.00015	0.000128	0.000108	9.06E-05	7.53E-05	6.22E-05	3.19E-05	1.92E-05
64.538	0.000204	0.000229	0.000249	0.000262	0.000269	0.000268	0.00026	0.000247	0.00023	0.00021	0.000188	0.000166	0.000145	0.000124	0.000106	8.88E-05	7.42E-05	6.15E-05	3.16E-05	1.91E-05
65.789	0.000197	0.000222	0.000241	0.000255	0.000262	0.000262	0.000255	0.000243	0.000226	0.000207	0.000186	0.000164	0.000143	0.000123	0.000105	8.84E-05	7.39E-05	6.13E-05	3.15E-05	1.9E-05
69.826	0.000175	0.000198	0.000218	0.000233	0.000241	0.000242	0.000238	0.000228	0.000214	0.000197	0.000178	0.000159	0.000139	0.00012	0.000103	8.69E-05	7.29E-05	6.07E-05	3.13E-05	1.89E-05
72.277	0.000162	0.000186	0.000205	0.00022	0.000229	0.000231	0.000228	0.00022	0.000207	0.000191	0.000174	0.000155	0.000136	0.000118	0.000101	8.6E-05	7.23E-05	6.03E-05	3.11E-05	1.88E-05
73.361	0.000157	0.00018	0.0002	0.000214	0.000224	0.000227	0.000224	0.000216	0.000204	0.000189	0.000172	0.000153	0.000135	0.000117	0.000101	8.56E-05	7.2E-05	6.01E-05	3.1E-05	1.87E-05
77.034	0.000141	0.000163	0.000182	0.000197	0.000207	0.000211	0.00021	0.000204	0.000194	0.000181	0.000165	0.000148	0.000131	0.000114	9.87E-05	8.41E-05	7.1E-05	5.94E-05	3.07E-05	1.86E-05
78.693	0.000134	0.000155	0.000174	0.000189	0.0002	0.000204	0.000204	0.000199	0.00019	0.000177	0.000162	0.000146	0.000129	0.000113	9.77E-05	8.34E-05	7.05E-05	5.91E-05	3.06E-05	1.85E-05
81.496	0.000123	0.000143	0.000162	0.000177	0.000188	0.000194	0.000194	0.00019	0.000182	0.000171	0.000157	0.000142	0.000126	0.000111	9.6E-05	8.22E-05	6.97E-05	5.85E-05	3.04E-05	1.84E-05
87.265	0.000103	0.000122	0.000139	0.000154	0.000166	0.000173	0.000175	0.000173	0.000168	0.000159	0.000147	0.000134	0.00012	0.000106	9.25E-05	7.97E-05	6.79E-05	5.73E-05	2.98E-05	1.81E-05
88.053	0.0001	0.000119	0.000136	0.000151	0.000163	0.00017	0.000173	0.000171	0.000166	0.000157	0.000146	0.000133	0.000119	0.000105	9.2E-05	7.93E-05	6.76E-05	5.71E-05	2.98E-05	1.81E-05
88.297	9.95E-05	0.000118	0.000136	0.00015	0.000162	0.000169	0.000172	0.00017	0.000165	0.000156	0.000145	0.000133	0.000119	0.000105	9.18E-05	7.92E-05	6.75E-05	5.71E-05	2.97E-05	1.8E-05
93.351	8.49E-05	0.000102	0.000118	0.000133	0.000144	0.000153	0.000157	0.000157	0.000153	0.000146	0.000137	0.000126	0.000114	0.000101	8.87E-05	7.69E-05	6.59E-05	5.59E-05	2.92E-05	1.78E-05
96.532	0.000265	0.000291	0.00031	0.000321	0.000322	0.000316	0.000302	0.000282	0.000259	0.000233	0.000207	0.00018	0.000155	0.000133	0.000112	9.37E-05	7.79E-05	6.44E-05	3.3E-05	1.99E-05
97.078	7.54E-05	9.15E-05	0.000107	0.000121	0.000133	0.000141	0.000146	0.000147	0.000145	0.000139	0.000131	0.000121	0.00011	9.8E-05	8.64E-05	7.51E-05	6.46E-05	5.5E-05	2.88E-05	1.75E-05
97.225	7.51E-05	9.11E-05	0.000107	0.000121	0.000132	0.000141	0.000146	0.000147	0.000144	0.000139	0.000131	0.000121	0.00011	9.79E-05	8.63E-05	7.5E-05	6.45E-05	5.5E-05	2.88E-05	1.75E-05
98.351	7.24E-05	8.81E-05	0.000103	0.000117	0.000129	0.000137	0.000143	0.000144	0.000142	0.000137	0.000129	0.000119	0.000108	9.7E-05	8.56E-05	7.45E-05	6.41E-05	5.47E-05	2.87E-05	1.75E-05
101.123	6.62E-05	8.11E-05	9.58E-05	0.000109	0.000121	0.00013	0.000135	0.000137	0.000136	0.000131	0.000124	0.000116	0.000106	9.47E-05	8.38E-05	7.32E-05	6.32E-05	5.4E-05	2.84E-05	1.73E-05
101.560	6.53E-05	8.01E-05	9.47E-05	0.000108	0.00012	0.000128	0.000134	0.000136	0.000135	0.000131	0.000124	0.000115	0.000105	9.44E-05	8.35E-05	7.3E-05	6.3E-05	5.39E-05	2.83E-05	1.72E-05
101.991	6.44E-05	7.9E-05	9.36E-05	0.000107	0.000119	0.000127	0.000133	0.000135	0.000134	0.00013	0.000123	0.000115	0.000105	9.4E-05	8.33E-05	7.28E-05	6.29E-05	5.37E-05	2.83E-05	1.72E-05
104.743	5.89E-05	7.28E-05	8.67E-05	9.98E-05	0.000111	0.00012	0.000126	0.000129	0.000128	0.000125	0.000119	0.000111	0.000102	9.18E-05	8.15E-05	7.15E-05	6.19E-05	5.3E-05	2.79E-05	1.7E-05
108.004	5.3E-05	6.6E-05	7.92E-05	9.17E-05	0.000103	0.000112	0.000118	0.000121	0.000122	0.000119	0.000114	0.000107	9.84E-05	8.91E-05	7.95E-05	6.99E-05	6.07E-05	5.22E-05	2.75E-05	1.68E-05
108.782	5.17E-05	6.44E-05	7.74E-05	8.99E-05	0.000101	0.00011	0.000116	0.00012	0.00012	0.000118	0.000113	0.000106	9.77E-05	8.85E-05	7.9E-05	6.95E-05	6.04E-05	5.19E-05	2.74E-05	1.67E-05
110.835	4.83E-05	6.05E-05	7.31E-05	8.53E-05	9.62E-05	0.000105	0.000112	0.000115	0.000116	0.000114	0.00011	0.000103	9.56E-05	8.68E-05	7.77E-05	6.85E-05	5.97E-05	5.14E-05	2.72E-05	1.66E-05
111.180	4.77E-05	5.99E-05	7.24E-05	8.45E-05	9.54E-05	0.000104	0.000111	0.000115	0.000116	0.000114	0.000109	0.000103	9.52E-05	8.66E-05	7.75E-05	6.83E-05	5.95E-05	5.13E-05	2.71E-05	1.66E-05
116.766	3.97E-05	5.04E-05	6.17E-05	7.3E-05	8.33E-05	9.22E-05	9.91E-05	0.000103	0.000105	0.000104	0.000101	9.62E-05	8.97E-05	8.21E-05	7.39E-05	6.56E-05	5.75E-05	4.97E-05	2.64E-05	1.62E-05
117.899	3.82E-05	4.87E-05	5.98E-05	7.08E-05	8.11E-05	8.99E-05	9.68E-05	0.000101	0.000103	0.000103	9.97E-05	9.49E-05	8.86E-05	8.12E-05	7.32E-05	6.5E-05	5.7E-05	4.94E-05	2.63E-05	1.61E-05
119.063	3.68E-05	4.7E-05	5.78E-05	6.86E-05	7.88E-05	8.76E-05	9.45E-05	9.91E-05	0.000101	0.000101	9.81E-05	9.35E-05	8.74E-05	8.02E-05	7.25E-05	6.45E-05	5.66E-05	4.91E-05	2.61E-05	1.6E-05
119.635	3.61E-05	4.61E-05	5.69E-05	6.76E-05	7.77E-05	8.65E-05	9.34E-05	9.8E-05	0.0001	9.99E-05	9.74E-05	9.29E-05	8.69E-05	7.98E-05	7.21E-05	6.42E-05	5.64E-05	4.89E-05	2.6E-05	1.59E-05
131.879	2.38E-05	3.13E-05	3.97E-05	4.84E-05	5.71E-05	6.51E-05	7.2E-05	7.73E-05	8.07E-05	8.21E-05	8.15E-05	7.92E-05	7.53E-05	7.03E-05	6.44E-05	5.81E-05	5.17E-05	4.53E-05	2.43E-05	1.5E-05
133.962	2.22E-05	2.93E-05	3.73E-05	4.57E-05	5.41E-05	6.2E-05	6.88E-05	7.41E-05	7.77E-05	7.93E-05	7.9E-05	7.7E-05	7.34E-05	6.87E-05	6.31E-05	5.71E-05	5.09E-05	4.47E-05	2.4E-05	1.48E-05
135.873	2.08E-05	2.76E-05	3.52E-05	4.33E-05	5.15E-05	5.92E-05	6.59E-05	7.13E-05	7.5E-05	7.68E-05	7.67E-05	7.5E-05	7.17E-05	6.72E-05	6.19E-05	5.61E-05	5.01E-05	4.42E-05	2.38E-05	1.46E-05
137.550	1.96E-05	2.61E-05	3.35E-05	4.13E-05	4.93E-05	5.69E-05	6.35E-05	6.89E-05	7.27E-05	7.46E-05	7.48E-05	7.32E-05	7.02E-05	6.6E-05	6.09E-05	5.53E-05	4.95E-05	4.36E-05	2.35E-05	1.45E-05
139.788	1.81E-05	2.43E-05	3.13E-05	3.88E-05	4.65E-05	5.39E-05	6.04E-05	6.58E-05	6.97E-05	7.18E-05	7.22E-05	7.1E-05	6.82E-05	6.43E-05	5.95E-05	5.42E-05	4.86E-05	4.3E-05	2.32E-05	1.43E-05
Sum	**0.339**																			

This total probability is probability of exceedance given an earthquake which doesn't account the probability for the occurrence of the earthquake. It can be converted to annual rate of exceedance by multiplying the probability with annual rate of occurrence of earthquakes. Therefore, to account for the probability of earthquake occurrence, rate of PGA > x will be computed using total probability theorem through the following formula.

$$\lambda(\mathrm{PGA} > \mathrm{x}) = \lambda(M_j > m_{\min}) \sum_{j=1}^{n_M} \sum_{k=1}^{n_R} P(PGA > x \mid \mathrm{m_j}, r_k) P(M = m_j) P(R = r_k) \qquad (3.26)$$

Where λ (M > m_{min}) is the rate of occurrence of earthquakes greater than m_{min} from the source, and

λ (PGA > x) is the rate of PGA > x.

For site with the anticipation of shaking from many sources (n_s sources), the annual rate of exceedance will be modified as:

$$\lambda(\mathrm{PGA} > \mathrm{x}) = \sum_{i=1}^{n_s} \lambda(M_j > m_{\min}) \sum_{j=1}^{n_M} \sum_{k=1}^{n_R} P(PGA > x \mid \mathrm{m_j}, r_k) P(M = m_j) P(R = r_k) \qquad (3.27)$$

λ(PGA > x) for the tunnel section between 178+807-178+864 and for discretized PGA values are tabulated in Table 3.11.

Table 3. 11: Annual rate of exceedance

x	P(PGA>X)	$\lambda(M_j > m_{min})$	$\lambda(PGA > x)$
0.05	0.3393	0.0347	0.0118
0.1	0.2094	0.0347	0.0073
0.15	0.1488	0.0347	0.0052
0.2	0.1135	0.0347	0.0039
0.25	0.0903	0.0347	0.0031
0.3	0.0741	0.0347	0.0026
0.35	0.0622	0.0347	0.0022
0.4	0.0530	0.0347	0.0018
0.45	0.0459	0.0347	0.0016
0.5	0.0401	0.0347	0.0014
0.55	0.0354	0.0347	0.0012
0.6	0.0315	0.0347	0.0011
0.65	0.0282	0.0347	0.0010
0.7	0.0255	0.0347	0.0009
0.75	0.0231	0.0347	0.0008
0.8	0.0210	0.0347	0.0007

Hazard curve is a plot of annual exceedance rate of PGA versus PGA and is done by incorporating all the information compiled in formulating the equation for rate of exceedance of PGA. The hazard curve as a plot of the result in Table 3.11 is shown in Figure 3.4.

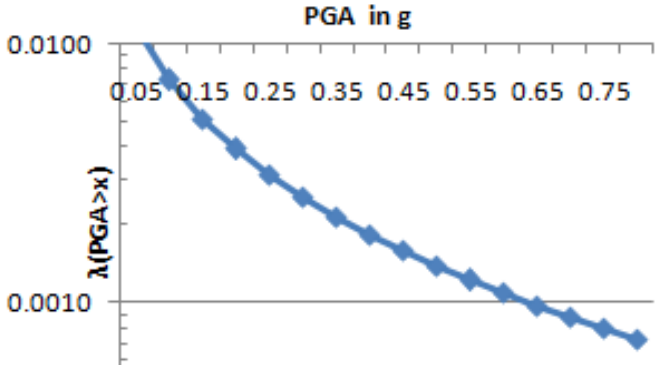

Figure 3. 4: Hazard curve for the site considered at section 178+807-178+864

3.2. Deaggregation

In the preceding calculations, seismic hazard analysis is used to find PGA which has certain percent probability of exceedance based on aggregation of contributions from potential earthquake magnitudes and source to site distances. For this calculation, combinations of magnitudes and distances have been used so that this effect can't be dedicated to single or few pairs of magnitude and distance. As stated by McGuire (1995) analysis often requires single design earthquake where the earthquake threat is characterized by single magnitude and distance.

Both ground motion intensity measure and intensity level of interest will determine the earthquake of interest or design earthquake. PGA is taken as ground motion intensity measure while the PGA with a certain probability of exceedance in years of a specific level of seismic action is taken as intensity level of interest.

FHWA (2009) provides two design ground motion levels with two performance requirements as discussed in Chapter 1, for structures in seismic regions: MDE for no collapse requirement and ODE for damage limitation requirement. 10% and 2% probability of exceedance in 50 years are the reference seismic actions which are used to describe design seismic action for damage limitation and no collapse requirement respectively.

10% and 2% probability of exceedance in 50 years are equivalent to a return period of 475 and 2475 years respectively. The rate of exceedance is obtained by reciprocating the return periods which result in 0.0021 and 0.0004 for ODE and MDE respectively. Therefore, the ground motion intensities which specify the design earthquakes are PGA with probability of exceedance of 0.0021 and 0.0004 for ODE and MDE respectively.

Through interpolation, PGA value for ODE is obtained as 0.36g. Similar calculation has been done by varying the top 30m shear wave velocity. 0.36g results from assumed weathered homogeneous layer provided by Yapi Merkezi (2016) with property(shear modulus, G and density, ρ) given in Table 3.12. PGA which specifies ODE has been calculated using intact rock property for calculating the top 30m shear wave velocity and resulted in a value of 0.22g. In addition, shear wave velocity for thickness of 30m below the tunnel level has been used and resulted in PGA value of 0.24g, again for ODE.

As shown in Table 3.12, while considering multi layered weathered rock, PGA value is not calculated. This is due to a lower value of V_{s30} which deviates from the threshold values of V_{s30} to be used in GMPE of Boor and Atkinson.

PGA for MDE has been calculated for the case which uses intact rock property during shear wave velocity calculation and resulted in 0.87g.

Table 3. 12: Summary of assumed layer with calculated PGA

	Assumed layer							
Layer name	Homogeneous weathered layer		Multi layered intact rock		Multi layered weathered rock		Layer below tunnel	
	property							
	G, kPa	ρ_{sat}, kg/m^3	G, kPa	ρ_{sat}, kg/m^3	G, kPa	ρ_{sat}, kg/m^3	G, kPa	ρ_{sat}, kg/m^3
C			1.53E+06	2038.74	2.60E+04	2038.74		
B	100000	2446.48	2.40E+06	2446.48	1.00E+05	2446.48		
A			1.04E+07	2650.36	1.33E+06	2650.36	1.33E+06	2650.36
v_{s30}, m/s		202.176		876.496		119.698		708.392
PGA(ODE)		0.36g		0.22g		N.A		0.24g

N.B. For the layer below the tunnel, the calculated shear wave velocity isnot for the top 30m layer rather for 30m thick layer at a depth

N.A - Not applicable

Using deaggregation process, the earthquake scenario which most likely causes peak ground acceleration with the specified probability of exceedance will be identified. Deaggregation (Bazzurro and Cornell, 1999) is obtained by dividing the total contribution accumulated in each discretized range for the rate of earthquake by rate of all earthquakes.

The parameters involved in distribution of magnitudes and distance are discretized so that it will be described in terms of percentage contribution to PGA>x as (Baker, 2008):

$$P(M = m, R = r \mid PGA > x) = \frac{\lambda(PGA > x, M = m, R = r)}{\lambda(PGA > x)} \tag{3.28}$$

The numerator of the above equation is computed using PSHA by omitting the summation over both magnitude and distance. Therefore,

$$\lambda(PGA > x, M = m, R = r) = P(M_i = m)P(R_i = r)\sum_{k=1}^{n_s}\lambda(M_i > m_{\min})P(PGA > x \mid m_j, r_k) \tag{3.29}$$

Deaggregation calculation is given in Table 3.13 for the PGA value of 0.36g. The second column is assigned for $P(R=r_k)$ which is constant throughout as point source has equal probability. The second row gives values for $P(M=m_j)$ as given in Table 3.1.

As per Bazzuro(1999), the most likely event to exceed a specified level of PGA is the one described by modal values of the joint M-R-ε distribution. Similarly, Thenhaus et al. (2003) state that the discretized interval with the largest relative contributions, the modes, identifies those earthquakes that contribute the most to the total hazard. When joint M-R-ε distribution is used, the deaggregation process is termed as 3D hazard deaggregation.

For this thesis, 2D hazard deaggregation is used by using the M-R distribution and excluding the number of standard deviation from the median. For this step also, the discretization range for magnitude which is equal to 0.1 is maintained.

The modes from Table 3.13 result in two pairs of values: one with magnitude of 5.6 and radius around 20km and the other with magnitude of 5.8 and radius around 33km. Therefore, this pair of values is the most likely scenario which corresponds to 10% probability of exceedance in 50years for the site specified. Existing ground motion records for the following response analysis is selected using the first design earthquake (magnitude of 5.6 and radius of 20km).

Table 3. 13: Deaggregation

Distance	m	5	5.1	5.2	5.3	5.4	5.5	5.6	5.7	5.8	5.9	6	6.1	6.2	6.3	6.4	6.5	6.6	6.7	6.8	6.86
	$P(M=m_j)$	0.1963	0.1585	0.1279	0.1033	0.0834	0.0673	0.0544	0.0439	0.0354	0.0286	0.0231	0.0187	0.0151	0.0122	0.0098	0.0079	0.0064	0.0052	0.0026	0.0016
	$P(R=r_k)$	$P(M=m_j, R=r_k \mid x>0.358) = [\lambda(M_j>m_{min})P(x>0.358 \mid m_j,r_k)P(M=m_j)P(R=r_k)]/\lambda(x>0.358)$																			
3.308	0.014	0.00382	0.00387	0.00385	0.00376	0.00362	0.00342	0.00319	0.00294	0.00267	0.00240	0.00214	0.00188	0.00164	0.00142	0.00122	0.00105	0.00089	0.00075	0.00039	0.00023
3.613	0.014	0.00370	0.00376	0.00374	0.00367	0.00353	0.00335	0.00313	0.00288	0.00263	0.00236	0.00210	0.00186	0.00162	0.00141	0.00121	0.00104	0.00088	0.00074	0.00039	0.00023
5.117	0.014	0.00322	0.00330	0.00332	0.00327	0.00318	0.00304	0.00286	0.00265	0.00243	0.00220	0.00197	0.00175	0.00154	0.00134	0.00116	0.00100	0.00085	0.00072	0.00038	0.00023
6.895	0.014	0.00270	0.00291	0.00298	0.00296	0.00289	0.00278	0.00263	0.00245	0.00226	0.00206	0.00186	0.00166	0.00146	0.00128	0.00111	0.00096	0.00082	0.00070	0.00037	0.00022
6.947	0.014	0.00268	0.00290	0.00297	0.00295	0.00288	0.00277	0.00262	0.00245	0.00226	0.00206	0.00185	0.00165	0.00146	0.00128	0.00111	0.00096	0.00082	0.00070	0.00037	0.00022
7.754	0.014	0.00242	0.00271	0.00285	0.00286	0.00279	0.00269	0.00255	0.00238	0.00220	0.00201	0.00181	0.00162	0.00143	0.00126	0.00109	0.00094	0.00081	0.00069	0.00036	0.00022
8.135	0.014	0.00230	0.00261	0.00279	0.00282	0.00276	0.00266	0.00252	0.00236	0.00218	0.00199	0.00179	0.00160	0.00142	0.00124	0.00108	0.00094	0.00080	0.00069	0.00036	0.00022
8.820	0.014	0.00210	0.00245	0.00267	0.00275	0.00271	0.00261	0.00247	0.00231	0.00214	0.00195	0.00176	0.00158	0.00140	0.00123	0.00107	0.00092	0.00079	0.00068	0.00036	0.00022
11.024	0.014	0.00160	0.00197	0.00227	0.00247	0.00254	0.00250	0.00237	0.00221	0.00204	0.00187	0.00169	0.00151	0.00134	0.00118	0.00103	0.00089	0.00076	0.00065	0.00034	0.00021
15.538	0.014	0.00100	0.00132	0.00163	0.00189	0.00207	0.00216	0.00215	0.00207	0.00193	0.00175	0.00158	0.00141	0.00125	0.00110	0.00096	0.00083	0.00071	0.00061	0.00032	0.00020
15.551	0.014	0.00100	0.00132	0.00163	0.00189	0.00207	0.00216	0.00215	0.00207	0.00193	0.00175	0.00158	0.00141	0.00125	0.00110	0.00096	0.00083	0.00071	0.00061	0.00032	0.00020
18.405	0.014	0.00079	0.00106	0.00134	0.00159	0.00179	0.00192	0.00196	0.00193	0.00184	0.00170	0.00153	0.00136	0.00120	0.00106	0.00092	0.00080	0.00069	0.00059	0.00031	0.00019
18.867	0.014	0.00076	0.00102	0.00130	0.00155	0.00175	0.00188	0.00193	0.00191	0.00182	0.00169	0.00152	0.00136	0.00120	0.00105	0.00092	0.00079	0.00068	0.00059	0.00031	0.00019
19.966	0.014	0.00070	0.00095	0.00121	0.00145	0.00165	0.00179	0.00185	0.00185	0.00178	0.00166	0.00151	0.00134	0.00118	0.00104	0.00091	0.00078	0.00067	0.00058	0.00030	0.00019
21.820	0.014	0.00070	0.00095	0.00121	0.00145	0.00165	0.00179	0.00185	0.00185	0.00178	0.00166	0.00151	0.00134	0.00118	0.00104	0.00091	0.00078	0.00067	0.00058	0.00030	0.00019
22.161	0.014	0.00061	0.00083	0.00107	0.00130	0.00150	0.00165	0.00173	0.00174	0.00170	0.00160	0.00147	0.00132	0.00116	0.00102	0.00089	0.00077	0.00066	0.00057	0.00030	0.00018
23.316	0.014	0.00059	0.00081	0.00105	0.00128	0.00148	0.00162	0.00171	0.00172	0.00168	0.00159	0.00146	0.00131	0.00116	0.00102	0.00088	0.00077	0.00066	0.00056	0.00030	0.00018
23.422	0.014	0.00055	0.00075	0.00098	0.00120	0.00139	0.00154	0.00163	0.00166	0.00163	0.00155	0.00144	0.00130	0.00115	0.00101	0.00088	0.00076	0.00065	0.00056	0.00029	0.00018
26.016	0.014	0.00054	0.00075	0.00097	0.00119	0.00138	0.00153	0.00162	0.00165	0.00162	0.00155	0.00143	0.00130	0.00115	0.00100	0.00087	0.00076	0.00065	0.00056	0.00029	0.00018
26.411	0.014	0.00046	0.00064	0.00083	0.00103	0.00121	0.00136	0.00147	0.00151	0.00151	0.00146	0.00137	0.00125	0.00112	0.00098	0.00085	0.00074	0.00064	0.00054	0.00029	0.00018
26.538	0.014	0.00045	0.00062	0.00081	0.00101	0.00119	0.00134	0.00144	0.00149	0.00149	0.00144	0.00135	0.00124	0.00111	0.00098	0.00085	0.00074	0.00063	0.00054	0.00029	0.00017
27.798	0.014	0.00045	0.00062	0.00081	0.00100	0.00118	0.00133	0.00144	0.00149	0.00148	0.00144	0.00135	0.00124	0.00111	0.00098	0.00085	0.00074	0.00063	0.00054	0.00029	0.00017
28.772	0.014	0.00041	0.00057	0.00075	0.00094	0.00111	0.00126	0.00136	0.00142	0.00143	0.00139	0.00132	0.00121	0.00109	0.00097	0.00084	0.00073	0.00063	0.00054	0.00028	0.00017
30.106	0.014	0.00039	0.00054	0.00071	0.00089	0.00106	0.00120	0.00131	0.00137	0.00139	0.00136	0.00129	0.00119	0.00108	0.00096	0.00084	0.00072	0.00062	0.00053	0.00028	0.00017
30.807	0.014	0.00036	0.00050	0.00066	0.00083	0.00099	0.00113	0.00124	0.00131	0.00133	0.00131	0.00125	0.00116	0.00106	0.00095	0.00083	0.00072	0.00062	0.00053	0.00028	0.00017
32.906	0.014	0.00035	0.00048	0.00063	0.00080	0.00096	0.00110	0.00121	0.00128	0.00130	0.00128	0.00123	0.00115	0.00105	0.00094	0.00082	0.00071	0.00061	0.00053	0.00028	0.00017
33.268	0.014	0.00035	0.00048	0.00063	0.00080	0.00096	0.00110	0.00121	0.00128	0.00130	0.00128	0.00123	0.00115	0.00105	0.00094	0.00082	0.00071	0.00061	0.00053	0.00028	0.00017
33.416	0.014	0.00031	0.00043	0.00056	0.00071	0.00086	0.00100	0.00111	0.00118	0.00122	0.00121	0.00117	0.00110	0.00101	0.00091	0.00081	0.00070	0.00060	0.00052	0.00027	0.00017
33.707	0.014	0.00030	0.00042	0.00055	0.00070	0.00085	0.00098	0.00109	0.00117	0.00120	0.00120	0.00116	0.00110	0.00101	0.00091	0.00081	0.00070	0.00060	0.00052	0.00027	0.00017
33.782	0.014	0.00030	0.00042	0.00055	0.00069	0.00084	0.00098	0.00108	0.00116	0.00120	0.00120	0.00116	0.00109	0.00101	0.00091	0.00080	0.00070	0.00060	0.00052	0.00027	0.00017
40.927	0.014	0.00030	0.00041	0.00054	0.00068	0.00083	0.00096	0.00107	0.00115	0.00119	0.00119	0.00115	0.00109	0.00100	0.00090	0.00080	0.00070	0.00060	0.00052	0.00027	0.00017
41.343	0.014	0.00030	0.00041	0.00054	0.00068	0.00083	0.00096	0.00107	0.00115	0.00118	0.00118	0.00115	0.00108	0.00100	0.00090	0.00080	0.00070	0.00060	0.00052	0.00027	0.00017
42.758	0.014	0.00020	0.00028	0.00038	0.00048	0.00059	0.00070	0.00080	0.00088	0.00093	0.00096	0.00096	0.00093	0.00088	0.00081	0.00074	0.00065	0.00057	0.00050	0.00026	0.00016
47.029	0.014	0.00020	0.00028	0.00037	0.00047	0.00058	0.00069	0.00078	0.00087	0.00092	0.00095	0.00095	0.00092	0.00087	0.00081	0.00073	0.00065	0.00057	0.00049	0.00026	0.00016
47.264	0.014	0.00019	0.00026	0.00034	0.00044	0.00054	0.00065	0.00074	0.00082	0.00088	0.00091	0.00091	0.00089	0.00085	0.00079	0.00072	0.00064	0.00057	0.00049	0.00026	0.00016
48.372	0.014	0.00015	0.00021	0.00028	0.00036	0.00045	0.00054	0.00062	0.00070	0.00076	0.00080	0.00081	0.00081	0.00078	0.00073	0.00068	0.00061	0.00054	0.00048	0.00025	0.00016
57.196	0.014	0.00015	0.00021	0.00028	0.00036	0.00044	0.00053	0.00062	0.00069	0.00075	0.00079	0.00081	0.00080	0.00077	0.00073	0.00067	0.00061	0.00054	0.00048	0.00025	0.00016
58.358	0.014	0.00014	0.00020	0.00026	0.00034	0.00042	0.00051	0.00059	0.00067	0.00073	0.00077	0.00078	0.00078	0.00076	0.00072	0.00066	0.00060	0.00054	0.00047	0.00025	0.00015
59.142	0.014	0.00009	0.00013	0.00017	0.00023	0.00029	0.00036	0.00042	0.00048	0.00054	0.00058	0.00061	0.00063	0.00062	0.00061	0.00057	0.00053	0.00049	0.00044	0.00024	0.00015
64.538	0.014	0.00008	0.00012	0.00016	0.00022	0.00028	0.00034	0.00040	0.00046	0.00052	0.00056	0.00059	0.00061	0.00061	0.00059	0.00056	0.00053	0.00048	0.00043	0.00023	0.00015
65.789	0.014	0.00008	0.00012	0.00016	0.00021	0.00027	0.00033	0.00039	0.00045	0.00051	0.00055	0.00058	0.00060	0.00060	0.00058	0.00056	0.00052	0.00048	0.00043	0.00023	0.00014
69.826	0.014	0.00006	0.00009	0.00012	0.00017	0.00021	0.00027	0.00032	0.00037	0.00042	0.00047	0.00050	0.00052	0.00053	0.00052	0.00051	0.00048	0.00044	0.00040	0.00022	0.00014
72.277	0.014	0.00006	0.00008	0.00012	0.00016	0.00020	0.00025	0.00031	0.00036	0.00041	0.00045	0.00048	0.00050	0.00051	0.00051	0.00049	0.00047	0.00044	0.00040	0.00022	0.00014
73.361	0.014	0.00005	0.00007	0.00010	0.00013	0.00017	0.00022	0.00026	0.00031	0.00036	0.00040	0.00043	0.00045	0.00047	0.00047	0.00046	0.00044	0.00041	0.00038	0.00021	0.00013
77.034	0.014	0.00004	0.00006	0.00009	0.00012	0.00016	0.00020	0.00024	0.00029	0.00033	0.00037	0.00040	0.00043	0.00044	0.00044	0.00044	0.00042	0.00040	0.00037	0.00021	0.00013
78.693	0.014	0.00004	0.00006	0.00008	0.00011	0.00015	0.00019	0.00023	0.00028	0.00032	0.00036	0.00039	0.00041	0.00043	0.00043	0.00043	0.00041	0.00039	0.00036	0.00020	0.00013
81.496	0.014	0.00003	0.00005	0.00007	0.00010	0.00013	0.00016	0.00020	0.00024	0.00028	0.00032	0.00035	0.00038	0.00039	0.00040	0.00040	0.00039	0.00037	0.00035	0.00019	0.00012
87.265	0.014	0.00003	0.00004	0.00006	0.00009	0.00012	0.00015	0.00019	0.00023	0.00027	0.00030	0.00033	0.00036	0.00038	0.00039	0.00039	0.00038	0.00036	0.00034	0.00019	0.00012
88.053	0.014	0.00003	0.00004	0.00006	0.00008	0.00011	0.00014	0.00017	0.00021	0.00025	0.00028	0.00031	0.00033	0.00035	0.00036	0.00036	0.00036	0.00034	0.00033	0.00018	0.00012
88.297	0.014	0.00002	0.00003	0.00004	0.00006	0.00008	0.00011	0.00014	0.00017	0.00020	0.00023	0.00026	0.00029	0.00031	0.00032	0.00032	0.00032	0.00031	0.00030	0.00017	0.00011
93.351	0.014	0.00002	0.00003	0.00004	0.00006	0.00008	0.00011	0.00014	0.00017	0.00020	0.00023	0.00026	0.00028	0.00030	0.00031	0.00032	0.00032	0.00031	0.00030	0.00017	0.00011
96.532	0.014	0.00002	0.00003	0.00004	0.00006	0.00008	0.00011	0.00013	0.00017	0.00020	0.00023	0.00026	0.00028	0.00030	0.00031	0.00032	0.00032	0.00031	0.00029	0.00017	0.00011
97.078	0.014	0.00001	0.00002	0.00003	0.00005	0.00007	0.00009	0.00011	0.00014	0.00017	0.00020	0.00022	0.00024	0.00026	0.00028	0.00028	0.00029	0.00028	0.00027	0.00016	0.00010
97.225	0.014	0.00010	0.00014	0.00019	0.00025	0.00031	0.00038	0.00045	0.00051	0.00057	0.00062	0.00065	0.00067	0.00067	0.00066	0.00064	0.00060	0.00056	0.00051	0.00028	0.00018
98.351	0.014	0.00001	0.00002	0.00003	0.00004	0.00006	0.00007	0.00010	0.00012	0.00015	0.00017	0.00020	0.00022	0.00024	0.00025	0.00026	0.00027	0.00026	0.00026	0.00015	0.00009
101.123	0.014	0.00001	0.00002	0.00003	0.00004	0.00006	0.00007	0.00010	0.00012	0.00015	0.00017	0.00020	0.00022	0.00024	0.00025	0.00026	0.00027	0.00026	0.00026	0.00015	0.00009
101.560	0.014	0.00001	0.00002	0.00003	0.00004	0.00005	0.00007	0.00009	0.00012	0.00014	0.00017	0.00019	0.00021	0.00023	0.00025	0.00026	0.00026	0.00026	0.00025	0.00015	0.00009
101.991	0.014	0.00001	0.00001	0.00002	0.00003	0.00005	0.00006	0.00008	0.00011	0.00013	0.00015	0.00018	0.00020	0.00022	0.00023	0.00024	0.00025	0.00024	0.00024	0.00014	0.00009
104.743	0.014	0.00001	0.00001	0.00002	0.00003	0.00005	0.00006	0.00008	0.00010	0.00013	0.00015	0.00018	0.00020	0.00022	0.00023	0.00024	0.00024	0.00024	0.00024	0.00014	0.00009
108.004	0.014	0.00001	0.00001	0.00002	0.00003	0.00005	0.00006	0.00008	0.00010	0.00013	0.00015	0.00017	0.00019	0.00021	0.00023	0.00024	0.00024	0.00024	0.00024	0.00014	0.00009
108.782	0.014	0.00001	0.00001	0.00002	0.00003	0.00004	0.00006	0.00007	0.00009	0.00012	0.00014	0.00016	0.00018	0.00020	0.00021	0.00022	0.00023	0.00023	0.00023	0.00013	0.00008
110.835	0.014	0.00001	0.00001	0.00002	0.00002	0.00004	0.00005	0.00006	0.00008	0.00010	0.00012	0.00015	0.00017	0.00018	0.00020	0.00021	0.00021	0.00022	0.00021	0.00013	0.00008
111.180	0.014	0.00001	0.00001	0.00002	0.00002	0.00003	0.00005	0.00006	0.00008	0.00010	0.00012	0.00014	0.00016	0.00018	0.00019	0.00020	0.00021	0.00021	0.00021	0.00012	0.00008
116.766	0.014	0.00001	0.00001	0.00001	0.00002	0.00003	0.00004	0.00006	0.00008	0.00009	0.00011	0.00013	0.00015	0.00017	0.00018	0.00020	0.00020	0.00020	0.00020	0.00012	0.00008
117.899	0.014	0.00001	0.00001	0.00001	0.00002	0.00003	0.00004	0.00006	0.00007	0.00009	0.00011	0.00013	0.00015	0.00017	0.00018	0.00019	0.00020	0.00020	0.00020	0.00012	0.00008
119.063	0.014	0.00000	0.00001	0.00001	0.00002	0.00002	0.00003	0.00005	0.00006	0.00008	0.00009	0.00011	0.00013	0.00015	0.00016	0.00017	0.00018	0.00018	0.00018	0.00011	0.00007
119.635	0.014	0.00000	0.00001	0.00001	0.00002	0.00002	0.00003	0.00004	0.00006	0.00007	0.00009	0.00011	0.00013	0.00014	0.00016	0.00017	0.00017	0.00018	0.00018	0.00011	0.00007
131.879	0.014	0.00000	0.00001	0.00001	0.00002	0.00002	0.00003	0.00004	0.00006	0.00007	0.00009	0.00011	0.00012	0.00014	0.00015	0.00016	0.00017	0.00017	0.00017	0.00010	0.00007
133.962	0.014	0.00000	0.00001	0.00001	0.00001	0.00002	0.00003	0.00004	0.00006	0.00007	0.00009	0.00010	0.00012	0.00014	0.00015	0.00016	0.00017	0.00017	0.00017	0.00010	0.00007
135.873	0.014	0.00000	0.00000	0.00001	0.00001	0.00001	0.00002	0.00003	0.00004	0.00005	0.00006	0.00007	0.00008	0.00010	0.00011	0.00012	0.00013	0.00013	0.00014	0.00008	0.00005
137.550	0.014	0.00000	0.00000	0.00000	0.00001	0.00001	0.00002	0.00002	0.00003	0.00004	0.00005	0.00007	0.00008	0.00009	0.00010	0.00011	0.00012	0.00013	0.00013	0.00008	0.00005
139.788	0.014	0.00000	0.00000	0.00000	0.00001	0.00001	0.00002	0.00002	0.00003	0.00004	0.00005	0.00006	0.00008	0.00009	0.00010	0.00011	0.00012	0.00012	0.00013	0.00008	0.00005

3.3. Ground motion selection

PSHA is commonly used to compute the ground motion hazard for which geotechnical and structural systems are analyzed and designed. To define seismic load for dynamic analysis of structure, an appropriate ground motion need to be selected. Since there are no records of accelerograms for Ethiopian earthquakes, other records should be adapted so that ground motion selection is required. Ground motion selection utilizes deaggregation results of magnitude and distance to identify causal events for an interest value associated with an annual rate of exceedance (Lin and Baker, 2011).

Ground motions are selected to represent design ground motions of the specified site. These could be natural time history or artificial time history. A set of natural time histories that have ground motion characteristics similar to those estimated for the design ground motions are preferred for use as natural time histories. Typical practice in structural design is to select seven ground motions (Haselton et al., 2012).

For this thesis natural time histories from the database of Pacific Earthquake Engineering Research Center (PEER) are used by taking the first pair of most likely magnitude and radius from the deaggregation calculation, shear wave velocity range and fault mechanism. The interface is as shown in Figure 3.5.

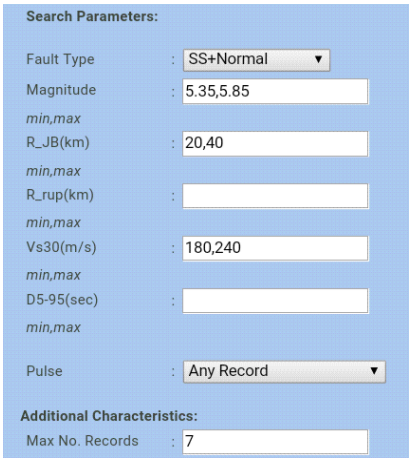

Figure 3. 5: Search parameters to be feed in PEER ground motion database

With this input parameters, PEER ground motion database provides three ground motions even though it is required to have 7 motions for nonlinear analysis. In order to obtain seven motions, the range of the parameters needs to be widened. However, this will lead to discrepancy from the most likely scenario of earthquake causing the specified level of intensity of ground motion dealt with previously. The increase in number is required to widen the probability of inclusion of ranges of probabilities. After all, the average will be taken. Therefore, to maintain the site specific values, these motions are taken.

Among the three ground motions, the fault mechanism of the two ground motions is strike slip while one ground motion has been obtained for Normal oblique faulting mechanism. Even though the PGA calculation has been done using strike slip to maximize its effect and the site has been reported for the existence of both strike and normal slip, the dominant faulting mechanism is normal fault. Therefore, the ground motion with the normal oblique faulting mechanism is selected. Description of this selected ground motion is provided in Table 3.14.

Table 3. 14: Description of selected ground motion

PEER Ground Motion Database Time Series Search Report -- NGA-West2 -- 2017-09-08						
Earthquake Name	Year	Station Name	Magnitude	Mechanism	R_{jb} (km)	V_{s30} (m/sec)
"L'Aquila Italy"	2009	"Avezzano"	5.6	Normal Oblique	27.38	199

The selected ground motion is applied at the bottom of the model and its effect is required on the structure which is located 320m below the surface. Therefore, attenuation of ground motion parameter with depth should be taken into consideration. As given by FHWA (2009) for depths greater than 30m, the reduction factor is 0.7.

The PGA of the selected ground motion is 0.03g. This PGA is scaled to the PGA defined by the PSHA in the previous section which is 0.36g. Therefore, scaling factor with respect to PGA becomes:

$$\frac{0.36g}{0.03g} = 11.9$$

Combining the depth attenuation factor, the unit conversion factor, PGA scaling and a factor to maximize the load effect, as discussed in section 2.6.2, result in a total factor, K, calculated as:

$$K = 0.7 * 9.81 \ {}^{m}\!/_{s^2}\!/_{g} * 11.9 * 1.3$$

$$K = 106.23$$

All the data points of the selected motion are subjected to this factor so that the record is proportioned according to the expected PGA at the site. The original and scaled time acceleration histories are shown in Figure 3.6.

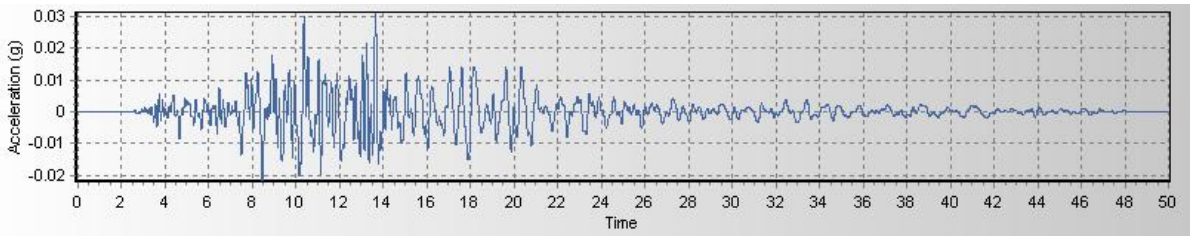

a) Time acceleration history of selected ground motion

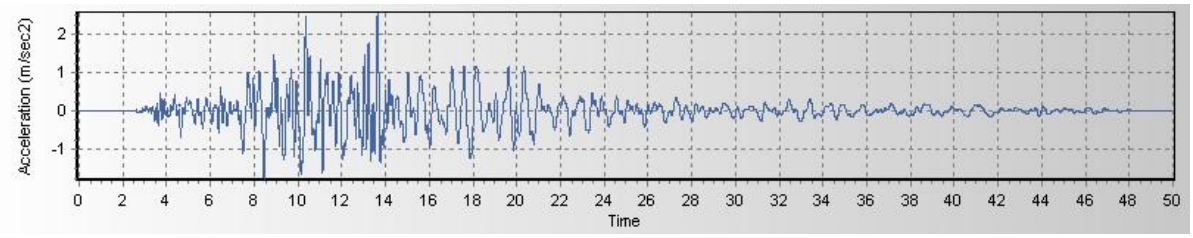

b) Scaled time acceleration history

Figure 3. 6: Original and scaled time acceleration histories

CHAPTER 4 NUMERICAL MODELING

The finite element code PLAXIS is used to analyze the tunnel under consideration assuming a plane strain condition holds due to the geometry of the tunnel. As far as seismicity is considered, of the three types of 2D continuum method of numerical analysis given by FHWA (2009), dynamic time history analysis is used.

Dynamic time history analysis uses ground motion time histories applied at the base of a model. It can be used to refine analysis. Here, the soil and tunnel responses are mechanically coupled unlike the other two methods (Bilotta et al., 2007).

The analysis of response of the tunnel for the specified earthquake event defined by magnitude and distance is referred to scenario based assessment (Haselton et al., 2012).

4.1. Model geometry

Geometry lines are used to define the layers of soil, invert and ballast while tunnel designer is used to draw the tunnel as shown in Figure 4.1. NATM tunnel type with the provision of lining and interface is selected so as to simulate the noncircular tunnel by providing different radius for different sections of the tunnel. NATM tunnel is mostly applicable in mountainous area (Kevvadas 2005).

4.2. Fixity

Standard earthquake boundary is used as fixity since the analysis carried out is dynamic analysis due to the application of the earthquake.

In using standard earthquake boundaries, absorbent boundaries are made at right and left of vertical boundaries with prescribed displacement of 1m in horizontal direction and 0m in the vertical direction at the bottom boundary. These can be seen in Figure 4.1.

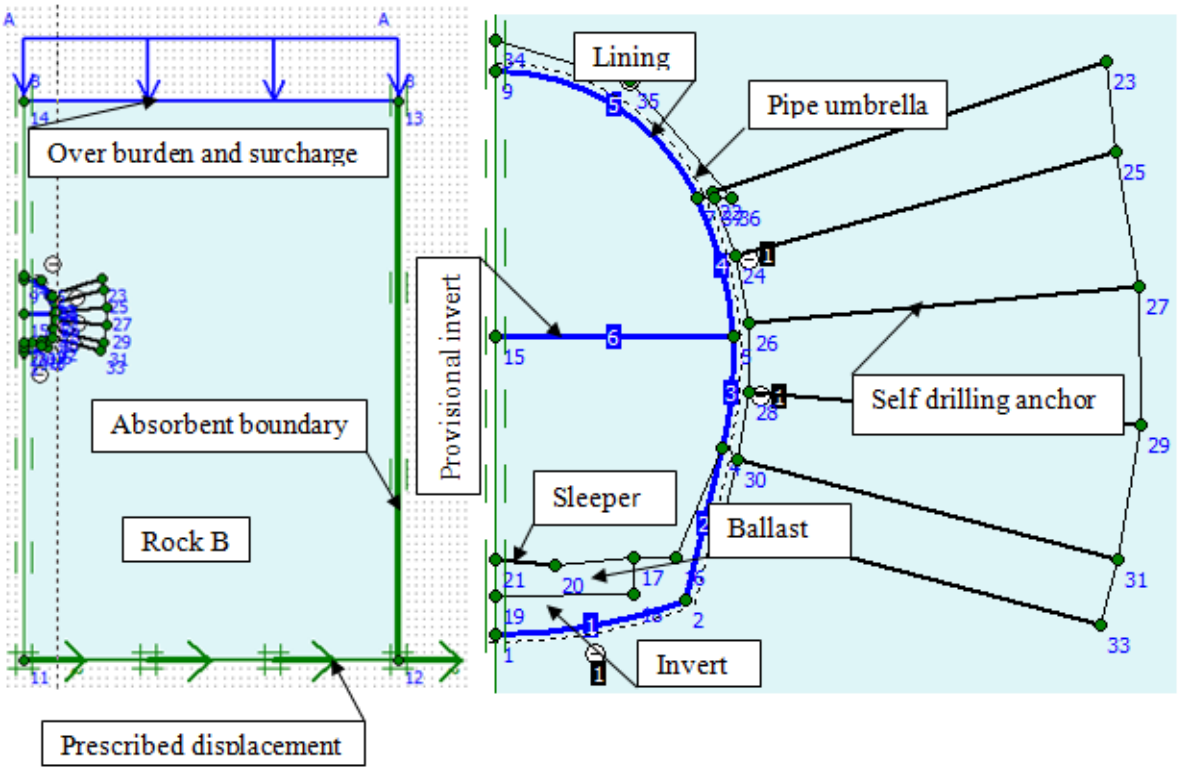

Figure 4. 1: Model geometry for section 178+807-178+864

4.3. Material Properties

Material properties are assigned for each material used in the model according to the element and the section under consideration. The ground medium, ballast and invert are modeled as soil. Continuous elements, such as lining is modeled as plate while discontinuous element like sleeper is modeled as anchor. Geotechnical parameters are obtained from drawings provided by the contractor (Yapi Merkezi).

4.3.1. Supports

Five support types are identified for the whole length of tunnel ranging from A1-A5. Support types A1, A2 and A3 refer to the massive self-supporting rock mass with different degree of fracturing, while section A4 and A5 refer to poor to very poor rock mass conditions (Yapi Merkezi, 2016). The A5 standard support type is used for the section stretching from 178+807 to 178+864.

Shotcrete is used as the main lining material for the tunnel under consideration which is capable of being used as a permanent or initial support. Besides rock reinforcement, Lattice girders (Figure 4.2(b)) and pipe umbrella (Figure 4.2(a)) are used for different sections in addition to the shotcrete. Installed lattice girders and pipe umbrella with shotcrete is shown in Figure 4.3.

a)Pipe umbrella b) Lattice girders

Figure 4. 2: Pipe umbrella and lattice girder used on site

Figure 4. 3: Primary lining installation

Rock bolts have a friction or grout anchor in the rock and are tensioned as soon as that anchorage is attained to actively introduce a compressive force into the surrounding ground (Hung et al, 2009; Singh et al., 2016). This axial force increase shear capacity of the rock.

Yapi Merkezi specifies the use of self drilling anchor for the tunnel section between 178+807 to 178+864.

4.3.2. Interfaces

Frictional interface is assumed to occur between the lining and the ground with two extreme cases: full slip and no slip. Full slip assumes no shear to develop at the interface while no slip condition ensures the full attachment of the tunnel with the ground. Most tunnels lie between these two extremes.

Full slippage occurs for very strong earthquakes (Maximum Design Earthquakes) and soft soils while for frequent seismic events (Operational Design Earthquakes,) it is generally assumed that some friction can be developed. Full slip underestimates maximum thrust ((Lanzano, Hashash et al., 2001, Teraphan, 2007).

As Mirko et al.(2011:14) note: "*A full-slip condition is usually adopted to obtain the extreme values of the bending moment and shear force in the tunnel lining, whereas the no-slip assumption yields the maximum values of the thrust force acting on the lining. Since the shear force and the bending moment in full and no-slip conditions are slightly different (10 - 20%), while the thrust in no-slip condition can be much higher than in full-slip (100-200 times), for the sake of conservationism the no-slip condition has just been assumed as the reference boundary condition*".

In this model, interface property supported by PLAXIS software is used. R_{inter} is a coefficient used to relate the strength of the medium and the tunnel. A value of 1 indicates lining strength same as that of soil. It is obvious that two different types of materials don't have same strength. However, as stated in the previous paragraph and as it is customized in order to avoid complexity, no slip condition will be considered with R_{inter}=1. Besides this, the medium with which the tunnel under consideration traverses is rock. Moreno Pescara et al. (2011) stated that no slip condition is recognized to be the most suitable for rock formations.

4.3.3. Permeability

The area in which the Ashangi basalt dominates is taken as basalt (dense or fractured based on weathering) while the Kemise formation is taken as rhyolitic tuff, ignimbrite according to the report of Geological Survey of Ethiopia (Belay et.al., 2009).

As described by Lewis et.al. (2006:11): "*A wide range of values of hydraulic conductivity can occur for any one lithology, depending on both the degree of the fracturing and the size of the fractures*".

As measured data couldn't be obtained during this study, average values from suggested ranges of permeability coefficient from literature (Lewis et.al., 2006, cited in Lewis, 1989) are taken.

4.3.4. Constitutive model

Mohr Coulomb's elastic perfectly plastic model (Ti et al., 2009; Sandhya Rani et al., 2014) is widely used in different applications including mining, tunneling and unloading situations. Young's modulus, E, and Poisson's ratio, ν, are the parameters used to define the material behavior in the elastic range while the friction angle, ø, and cohesion, c, are the parameters for failure criteria. In addition, dilatancy angle, Ψ is used to model a realistic irreversible change in volume due to shearing. All the above five parameters are used to define the Mohr Coulomb constitutive model.

Due to the limited data and ease of use, the constitutive model for the ground medium used in this thesis is Mohr Coulomb model. Besides, the concrete invert also uses Mohr Coulomb constitutive model using parameters from Mohamad and Ibrahim (2015) which enables the computation of cohesion and internal friction angle. Linear elastic model is used for the linings.

4.4. Initial conditions

Initial stress conditions and initial pore water pressure, if any, are accounted for as initial conditions. The stretches considered in this thesis are expected to be rock resulting in a

different at rest earth pressure coefficient from the one determined using angle of internal friction. At rest earth pressure coefficient is taken as 0.5.

4.5. Loads

Loads applied on the tunnel are taken as per the recommendation of FHWA (2009) which in turn uses AASHTO LRFD specification (2005).

Dead loads in a structural system are considered using the weight of the respective material in the model but dead load of nonstructural components, wearing surface and utilities is ignored for simplicity and due to the belief that it will not be much as compared to the structural ones. The loads in Table 4.1 are considered in the analysis.

Table 4. 1: Loads considered in the analysis

Permanent loads considered for the tunnel linings according to LRFD specification			
Name	Symbol	Description	Remark
Dead load	DC	Self weight of structural & nonstructural components	Considered by directly inserting weights in PLAXIS
Horizontal earth pressure	EH	Horizontal earth pressure	Calculated in the initial condition of PLAXIS
Earth surcharge load	ES	Earth surcharge load	min 0.6kN/m2 (400psf) & 1.49kN/m2 (1000psf) if future development is possible
Vertical earth pressure	EV	Vertical earth pressure	Considered by directly inserting unit weight of the medium
Transient loads considered for the tunnel linings according to LRFD specification			
Name	Symbol	Description	
Earthquake	EQ	Earthquake load	Considered in dynamic analysis and applied as time history

In PLAXIS, earthquake load is introduced using prescribed displacement which will be multiplied by displacement multiplier in the calculation. The multiplier is the scaled acceleration time history while the prescribed displacement is assigned to be 1m.

4.5.1. Load combinations

Since the analysis in this thesis is drained analysis, applicable combination will be drained static load with seismic load. A seismic loading criterion for ODE which has been stated in section 2.6 is used.

4.6. Stage construction

Construction sequence has more effect than stiffness regarding ground deformations (Shlash et al., 2014). The following construction stages are used in this thesis.

1. Pipe umbrella activation
2. Top heading excavation
3. Lining activation at the crown & provisional invert activation
4. Bench excavation
5. Full primary lining activation
6. Invert construction
7. Final lining activation
8. Ballast activation
9. Sleeper activation
10. Dynamic load activation

Figures of the above construction stages are shown in Appendix D.

CHAPTER 5 RESULTS

5.1. Effects due to earthquake

5.1.1. Analytical solution

Analytic calculations are carried out using the formula provided by St. John and Zahrah (1987), Wang (1993) and Wang and Munfakh (2001). This section considers only the effect of earthquake.

5.1.1.1. Longitudinal deformation

Longitudinal deformation is analyzed using free field deformation without accounting for soil structure interaction as long as the deformation doesn't exceed the allowable limit. The axial and curvature strain is given by (St. John and Zahrah, 1987):

$$\varepsilon_a = \frac{PGV_s}{V_s}\sin\phi\cos\phi = \frac{K^{'}PGV_s^{'}\sin\phi\cos\phi}{V_s} \tag{5.1}$$

Assuming same ratio exists between PGA and PGV values of selected motion and probabilistic seismic hazard analysis results;

$$K^{'} = \frac{K}{9.81*1.3} \tag{5.2}$$

$$\varepsilon_b = r\frac{PGA}{V_s^{\,2}}\cos^3\phi \tag{5.3}$$

Where ε_a - Axial strain

ε_b - Curvature strain

PGV_s - Peak particle velocity

PGV_s' - Peak particle velocity of selected motion

V_s - Apparent velocity of S wave

ø - Angle of incidence

r- Radius of tunnel

K' - Total scaling factor for PGV of selected ground motion

K - Total scaling factor for PGA of selected ground motion

PGA - Peak ground acceleration

As Nava-Tristán et al. (2008) notes maximum value of strain of an important tunnel or tunnels with high effective radius (> 2.0 m) must be calculated using the critical angle of incidence, $ø_c$ which is given as:

$$\phi_c = \arcsin\left[\frac{\left(\sqrt{8a^2 - 4a + 1}\right) - 1}{4a - 2}\right] \tag{5.4}$$

$$a = \frac{PGV_s V_s}{3PGAR_{eq}} \tag{5.5}$$

Where $ø_c$ - Critical angle of incidence

R_{eq} - Equivalent radius of tunnel

PGV_s, V_s, PGA and R_{eq} are as defined previously.

The axial force, Q, & bending moment, M_b, are calculated as follows.

$$Q = E_c A_C \varepsilon_a \tag{5.6}$$

$$M_b = \frac{E_c I_{Cl} \varepsilon_b}{R_{eq}} \tag{5.7}$$

Where A_c - Cross-sectional area

I_{cl}- Moment of inertia (for longitudinal deformation)

E_c - Modulus of elasticity of tunnel lining

ε_a, ε_b and R_{eq} are as defined previously.

The calculations are tabulated in table 5.1.

Table 5. 1: Analytic calculations

Parameter	Symbol	Value	Unit	Evaluation	Allowable limit	Remark
Equivalent radius	R_{eq}	4.35	m			
	a	1.03				
	sin φ	0.62				
Total scaling factor of PGV for selected n	K'	8.33				
critical angle of incidence	φ	39.05	°			
Peak particle velocity	PGV_s	0.234	m/s			
Apparent velocity of S wave	V_s	202	m/s			
PGA	a_g	3.53	m/s^2			
soil unit weight	γ	21.00	kN/m^3			
poisson's ratio of lining	ν_l	0.20				
poisson's ratio of medium	ν_m	0.25				
lining thickness	t	0.55	m			
moment of inertia(longitudinal)	I_{cl}	71.25	m^4			
moment of inertia(x-sectional)	I_{cx}	0.01	m^4			
xsectional area	A_c	15.02	m^2			
youngus modulus of lining	E_c	31000.00	MPa			
youngus modulus of medium	E_m	250.00	MPa			
concrete yield strength	f_c	25.00	MPa			
allowable concrete strain	ε_{allow}	0.0035				
Longitudinal strain						
Axial strain	ε_a	2.46E-04				
Curvature	ε_b	3.90E-06				
combined axial&curvature strain	ε_{ab}	2.50E-04		<	0.0035	**Ok**
Axial force	Q	1.15E+02	MN/m			
Bending moment due to curvature	M_l	1.98E+00	MNm/m			
Shear force due to bending moment	V_m	2.18E-01	MN			
Transversal strain						
Maximum free field ground shear strain	γ_{max}	1.16E-03				
Diametrical strain	$\Delta D/D_l$	5.79E-04				
Flexibility ratio	F	6.12E+00		<	20	**SSI is required**
Compressibility ratio	C	9.79E-02				
Full slip lining response coefficient	k_1	5.72E-01				
Diametrical strain accounting SSI	$\Delta D_{ssi}/D_l$	1.35E-03				
Bending moment induced strain	ε_m	2.67E-04				
No slip lining response coefficient	k_2	1.24E+00				
thrust induced strain	ε_T	3.66E-05				
Maximum bending moment	M_{max}	4.17E-01	MNm			
Maximum thrust force	T_{max}	6.25E-01	MN			
Maximum shear stress	ζ	1.16E-01	MN	<	5.83	OK
Stress from M_{max} & T_{max}	σ	9.41E+00	MPa	< >	17.71/1.275	OK for compression

5.1. 1.2. Transversal deformation

The maximum free field shear strain due to vertically propagating shear wave is given by (St. John and Zahrah, 1987):

$$\gamma_{max} = \frac{PGV_s}{V_s} \tag{5.8}$$

Where γ_{max} - Maximum free field shear strain, PGVs, and V_s are as defined previously.

Due to this maximum free field strain, the tunnel undergoes diametrical change which can be calculated assuming perforated or non perforated ground. If the lining stiffness is comparable with the ground stiffness, non perforated ground can be assumed. The relative stiffness against distortion is identified using flexibility ratio given by Equation 2.5, which is equal to 6.12 for this specific case. Therefore, diametrical change of the tunnel is calculated assuming nonperforated ground using the following formula provided by FHWA (2009).

$$\frac{\Delta D}{D_t} = \pm \frac{\gamma_{max}}{2} \tag{5.9}$$

Where ΔD - Diametrical change

D_t - Tunnel diameter

γ_{max} - Maximum free field shear strain

These principal shear strains occur on planes inclined at 45° from the horizontal as shown in Figure 5.1.

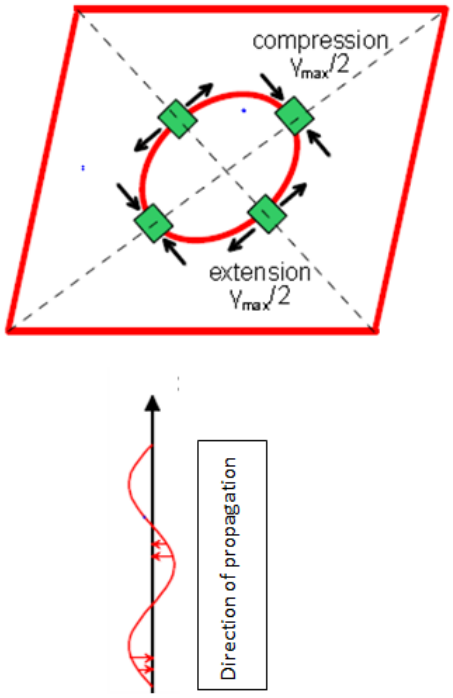

Figure 5. 1: Maximum free field shear distortion

(Bouckovalas and Kouretzis, 2011)

However, the flexibility ratio indicates the presence of considerable stiffness of the lining. This means that the lining is capable of resisting forces rather than conforming to the deformation of the ground. For such a case, soil structure interaction need to be considered. Therefore, taking soil structure interaction into account, the diametrical change of the tunnel will be calculated using the following formula (Wang and Munfakh, 2001).

$$\frac{\Delta D_{ssi}}{D_t} = \pm \frac{1}{3} K_1 F \gamma_{\max} \tag{5.10}$$

$$K_1 = \frac{12(1-\nu_m)}{(2F+5-6\nu_m)} \tag{5.11}$$

Where ΔD_{ssi} - Diametrical change accounting soil structure interaction

K_1 - Full slip lining response coefficient

F - Flexibility ratio

ν_m - Poisson's ratio of the medium

D_t and γ_{max} are as defined previously.

The resulting maximum bending moment, M_{max}, can be computed as follows (Wang and Munfakh, 2001).

$$M_{\max} = \pm\frac{1}{6} K_1 \frac{\varepsilon_m}{(1+\nu_m)} R_{eq}^2 \gamma_{\max} \tag{5.12}$$

Where ε_m - Bending moment induced strain (Transversal deformation)

M_{max} - Maximum bending moment

K_1, R_{eq}, ν_m and γ_{max} are as defined previously.

This maximum bending moment is calculated using a coefficient which considers full slip. As stated in section 4.3.2, full slip assumption underestimates thrust force. Thus, no slip lining response coefficient is used to calculate thrust force as follows (Wang, 1993).

$$K_2 = 1 + \frac{F[(1-2\nu_m)-(1-2\nu_m)C]-\frac{1}{2}(1-2\nu_m)2C+2}{F[(3-2\nu_m)+(1-2\nu_m)C]+C\left[\frac{5}{2}-8\nu_m+6\nu_m^2\right]+6-8\nu_m} \tag{5.13}$$

$$T_{\max} = \pm K_2 \frac{\varepsilon_m}{2(1+\nu_m)} R_{eq} \gamma_{\max} \tag{5.14}$$

Where K_2 - No slip lining response coefficient

T_{max} - Maximum thrust force

C - Compressibility ratio

F,ε_m, R_{eq}, ν_m and γ_{max} are as defined previously.

The resulting bending moment induced maximum fiber strain, ε_m, and maximum axial induced strain,ε_T, is given by (Wang and Munfakh, 2001):

$$\varepsilon_m = \pm\frac{1}{6}K_1\frac{E_m}{1+\nu_m}R_{eq}^2\frac{\gamma_{\max}t}{2E_cI_{cx}} \quad (5.15)$$

$$\varepsilon_T = \pm K_2\frac{E_m}{2(1+\nu_m)}R_{eq}\frac{\gamma_{\max}}{E_ct} \quad (5.16)$$

Where ε_T - Thrust induced strain

I_{cx} - Moment of inertia (for transversal deformation)

t - Thickness of the tunnel lining

E_m - Young's modulus of medium

E_c, K_1, K_2, I_{cx}, ε_m, R_{eq}, ν_m and γ_{max} are as defined previously.

The calculations are tabulated in table 5.1.

5.1.2. Result of numerical method

Shear forces, axial forces and bending moments at each node are the output of the numerical analysis as given in Appendix H .The maximum values of these nodal forces are shown in Figure 5.2, extracted from the output of the numerical analysis. A maximum axial force of 19,060 kN/m, shear force of 1,930kN/m and bending moment of 2,220kNm/m acts on the lining. Note that the forces include the static forces in addition to the dynamic forces. The maximum bending moment and axial force occur at the end of the pipe umbrella where stiffness difference manifests. The next maximum bending moment occurs on the straight portion of the tunnel near corner point where arching effect due to circular shape is absent. The second maximum axial force occurs at the corner point where stress concentrates.

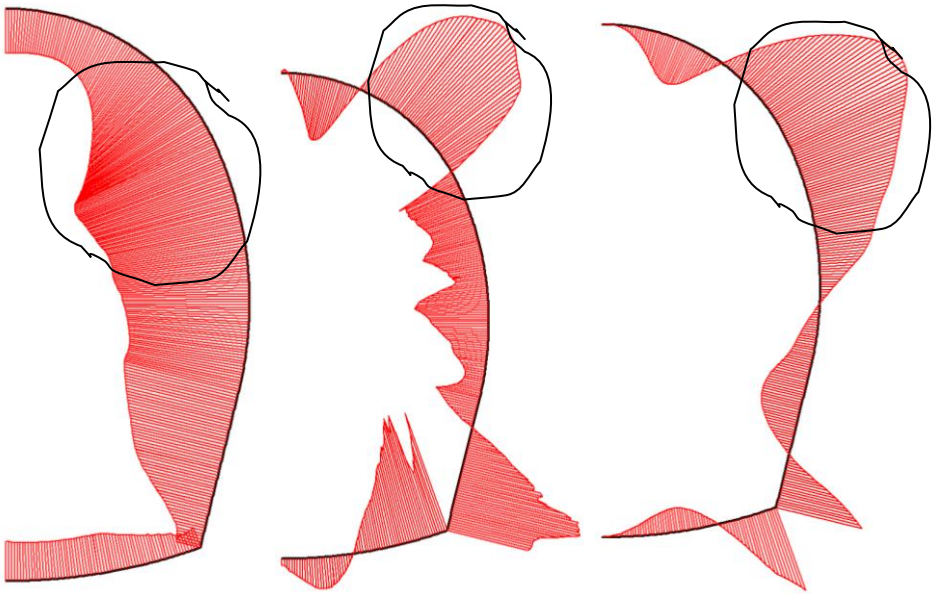

Figure 5. 2: Lining forces a) Axial force b) Shear force c) Bending moment

The maximum shear deformation is 322.63E-04.

CHAPTER 6 DISCUSSION

Comparing analytic solution with numerical method could be misleading since analytic solution is a simplified procedure associated with lots of assumptions. Numerical analysis result in better solution as it represents the existing situation in a better way. Besides, analytic solution is limited to elastic properties while the constitutive model used in the numerical modeling is Mohr Coulomb model (elastic perfectly plastic constitutive model).

The maximum shear deformation from analytic solution as referred from table 5.1 is ±1.16E-03 while numerical analysis results in a value of -322.63E-04. The closed form solution is expected to be conservative. However, the maximum shear strain obtained from the numerical analysis has been larger than the maximum shear strain of analytic solution. To understand the reason behind, another analysis using a design earthquake of magnitude 5 and 20km has been done. During selection of the design earthquake, the distance from source to site has been clearly defined while a single magnitude can't be obtained. Therefore the magnitude has been selected by considering maximum contribution. Considering this, for the additional analysis, altering the magnitude value while fixing the distance will be logical and based on this, magnitude of 5 and radius of 20km has been selected. From now onwards the design earthquake with magnitude of 5 and radius of 20km is termed as first design earthquake and this additionally selected design earthquake with magnitude of 5 and radius of 20km is termed as additional design earthquake.

Similar work has been made for the additional design earthquake. The analysis result in conservative analytic solution as maximum value is obtained using analytic solution, unlike the analysis of selected ground motion using the first design earthquake.

The major difference between the two selected ground motions is their duration. The significant duration, D_s, (5%-95%) of the selected ground motions for the first design earthquake and for the additional design earthquake are 16.3 sec and 5.5 sec respectively.

The response of foundation materials and structures is highly dependent on duration of ground shaking (Bommer and Martinez-Pereira, 1999). This shows that seismic response depends not only peak ground motion parameters but also on duration. The seismic hazard analysis performed in this thesis doesn't consider strong motion duration and there was no way to consider the duration in the analytic solution while the significant duration, D_s, (5%-95%) has been an input in the numerical analysis.

Significant duration defines a continuous time in which the motion may be considered as strong. As can be seen from the previous paragraph, the significant duration of the selected ground motion for the first design earthquake is almost three fold of the selected motion for the additional design earthquake. This implies the presence of higher energy for the selected ground motion of the first design earthquake.

Though the peak PGA values of both the selected motion are scaled to an equal peak ground acceleration, their shearing effect vary extremely. This agrees with the statement made by Bommer and Martinez-Pereira (1999) which describes the existence of great damage for larger durations though accelerations are equal.

Besides as stated by Bommer and Martinez-Pereira(1999), while using acceleration time histories, the duration of shaking of the selected ground shaking need to be consistent with the design scenario. Therefore a thorough seismic hazard assessment which includes estimation of duration of ground motion should be done to obtain realistic results.

The strain limit for concrete is given as 0.0035 (ES EN 1998-1, 2013) or 0.003 (Wang, 1993; USACE, 1997). The calculated longitudinal strain as referred from table 5.1 is 2.5E-04 which results in a lower value as compared to these threshold values.

The tunnel lining needs to be verified for ultimate limit state and serviceability limit state. Since seismic case is considered in this thesis, serviceability limit state verification of structures is not required. ES EN 1998-1 (2013) provides the following formulas for

ultimate limit state design compressive strength (f_{cd}) and design tensile strength (f_{ctd}) respectively.

$$f_{cd} = \alpha_{cc} \, f_{ck} / \gamma_c \tag{6.1}$$

$$f_{ctd} = \alpha_{cc} \, f_{ctk} / \gamma_c \tag{6.2}$$

Where f_{cd} - Design compressive strength

f_{ctd} - Design tensile strength

α_{cc} - Coefficient to account for long term effects on the compressive strength and of unfavorable effects resulting from the way the load is applied.

f_{ck} - Characteristic compressive cylinder strength

f_{ctk} - Characteristic axial tensile strength

γ_c - Partial factor for concrete

Therefore, these strength values for the shotcrete are calculated as 17.71MPa and 1.275MPa for f_{cd} and f_{ctd}, respectively, using α_{cc} of 0.85 and γ_c of 1.2. 1.2 is partial factors for concrete in case of accidental actions.

The values of normal forces and bending moments acting on the lining were taken from the result of numerical analysis (see Appendix H) so as to calculate the stresses on the lining. Since the lining has some thickness, when subjected to bending, the stress due to bending assumes compression and tension at either of the sides. Therefore intrados and extrados stresses are calculated using the following formula.

$$\sigma_{in} = \frac{N}{t} - \frac{6M_b}{t^2} \quad \text{And} \quad \sigma_{ex} = \frac{N}{t} + \frac{6M_b}{t^2} \tag{6.3}$$

Where σ_{in} - Intrados stress

σ_{ex} - Extrados stress

N - Normal force

M_b - Bending moment

t - Thickness of the tunnel lining

The calculations are tabulated in Appendix H. Before the application of the earthquake, the maximum compressive stress and tensile stress acting on the lining are 29,979.89 kN/m^2 and 16,545.51 kN/m^2 . The resistance of the support which was calculated above (17.71MPa for compression and 1.275MPa for tension) is exceeded. On the site of construction, fiber reinforcement or wire mesh or lattice girders or a combination of these are used. The support capacity of all these is not considered; rather only the capacity of plain concrete is considered. The steel only have a design capacity of 435MPa. However, considering the cross section of the reinforced concrete and specifying the tension and compression zone, support capacity must be calculated and verified for every load combinations.

The internal stresses seem to be large. The thickness of the lining could contribute to this as increasing thickness result in increased internal stresses. Besides this, the 3D arching effect may not be properly modeled. As stated by the British Tunneling Society and The Institution of Civil Engineers (2004), 30–50% of the deformation during construction occurs ahead of the face which will result in significantly reduced pressures acting on the lining than predicted from a two-dimensional analysis.

After applying the earthquake excitation, the maximum compressive stress and tensile stress in the lining become 76,632.69 kN/m^2 and 23,157.37 kN/m^2. This shows 155.61% and 39.96% increase in compressive and tensile stress, respectively, from the maximum stress values of static condition.

A maximum of 194% of compressive stress increase at a node located around the end of pipe umbrella (x= 48.03 and y= 43.8) is found. On the other hand a maximum of 124.23% of tensile stress increase is found at a node located around the crown (x=46.32 and y=45.3). At this node, the static compressive stress has been changed to tensile stress upon the application of earthquake. This ensures that the earthquake is exerting cyclic stress as expected where compressive stress and tensile stress due to earthquake adds to and deduct from static stresses.

Seismic verifications are made on lining stresses due to the earthquake only by comparing to the support capacity. The maximum compressive and tensile stress due to the earthquake are found to be 50,569.84kN/m^2 and 16,639.81 kN/m^2, respectively. These values are higher than the allowed stress or the support capacity of plain concrete. Therefore, analyzing the tunnel using reinforced concrete is required.

CHAPTER 7 CONCLUSIONS AND RECOMMENDATIONS

7.1. Conclusions

The aim of this research is to analyze the ground shaking effect on a tunnel located at Karakore. It focuses on the dynamic response. The static analysis is limited to computations of stress.

Ground shaking effects are considered based on the deformation caused by the ground shaking. These deformations are analyzed using both analytical and numerical solutions.

To model the real situation in an approximate way, time acceleration histories have been used in the numerical analysis carried out using PLAXIS software.

One of the major portions of the research is seismic hazard analysis for the specified tunnel area. Probabilistic seismic hazard analysis has been performed for return period of both 475 years and 2475 years. For the operating design earthquake corresponding to 475 years of return period, peak ground accelerations has been calculated by varying the assumption during calculating the top 30m shear wave velocity. PGA value of 0.36g has been obtained using an assumed single soil layer in which the tunnel is buried. 0.22g has been found while using intact rock property of the medium. Shear wave velocity for thickness of 30m below the tunnel level has been used and resulted in PGA value of 0.24g. PGA for MDE has been calculated for the case which uses intact rock property during shear wave velocity calculation and resulted in 0.87g.

Besides the probabilistic seismic hazard analysis, deaggregation has been performed since probabilistic seismic hazard analysis aggregates the effect of the entire possible earthquake hazard. The deaggregation process has been done for the assumed single layer which resulted in PGA value of 0.36g. The calculation results in two pairs of design earthquakes: one with magnitude of 5.6 and radius around 20km and the other with magnitude of 5.8 and radius around 33km.

There exists deformation upon the application of the excitation. The applied excitation results in maximum shear strain of -322.63E-04 using PLAXIS and ±1.16E-03 using simplified method. The numerical analysis gives maximum shear strain though the analytic solution is expected to be conservative. This could be due to the effect of strong motion duration. The analytic solution doesn't consider strong motion duration while the numerical analysis considers. Since significant duration is defined based on the energy content, the damage level is highly related with this parameter along with peak ground motion parameters. Besides consistency of strong motion duration with the design earthquake scenario has not been considered.

As compared to the maximum static condition stress, the ground shaking results in maximum compressive and tensile stress of 168.68% (50,569.84 kN/m^2) and 100.57% (-16,639.81kN/m^2) respectively. The maximum compression due to dynamic effect show 194% increase in compression near the end of the pipe umbrella and the maximum tensile stress alters the compressive stress to tensile stress and shows 124.23% increase of stress in magnitude at a maximum tensile stress node. After superposing the stress due to earthquake on the static condition stress for each node, the maximum compressive and tensile stress show an increase by 46,652.8 kN/m^2 (155.61%) and 6,611.86 kN/m^2 (39.96%).

Computations of maximum moment, thrust force, shear force and stress using simplified procedure results in reduced values as compared to the numerical analysis. The reason could be attributed to the chance that the soil could be sheared by the earthquake beyond the elastic peak. This is due to the assumption of elastic perfectly plastic model used for the numerical analysis which enables the consideration of plastic capacity.

Generally as compared to the static one, the maximum stress increase due to dynamic load is large for the considered ground motion record. Thorough probabilistic seismic hazard analysis which incorporates strong ground motion duration besides peak ground motion parameters should be done. The consistency of strong ground motion duration of selected

motion with design earthquake scenario need to be checked. Besides analysis should be rechecked for reinforced support.

7.2. Recommendations

The existing tunnel has been analyzed for seismicity using pseudo-static method. Considering the output of this thesis, it would be recommended to perform full dynamic analysis, incorporating strong motion duration.

Manual, report, publications and materials related with this topic and those which were referred during this thesis period show the existence of disparity on loading criteria and strength requirement. Standardization will lead to common agreement; therefore, it is important to have a code for seismic effects on underground structures.

Recommendations for future study

- It would be recommended to perform thorough seismic hazard analysis to estimate strong ground motion duration.
- Since the presence of train simultaneously with ground excitation could alter the response, it would be recommended to consider it.
- It is recommended to assess the sensitivity of the tunnel for changing lateral earth pressure coefficient and repeat the analysis if measured lateral earth pressure coefficients are obtained.
- It would be suggested to analyze using appropriate deconfinement ratio to account for 3D arching effect or to perform 3D analysis for better representation of arching and pipe umbrella effect.
- It would be recommended to analyze the tunnel for more number of selected ground motions.

REFERENCES

1. AASHTO(2005) *LRFDSI-3-II: AASHTO LRFD bridge design specifications*. 3rd edn. Washington, DC.
2. Anagnos, T. and Kiremidjian, A. S. (1988) A review of earthquake occurrence models for seismic hazard analysis. *Probabilistic Engineering mechanics,* 3(1).
3. Ardeleanu,L., Grecu, b. and Raileanu, v. (2012) Peak Ground Acceleration, Velocity and Displacement from Moderate Magnitude Under crustal Earthquakes Of Vrancea Region. *Romanian Reports In Physics,* 64(2), pp.555-570.
4. AREMA(2010) *ISSN 1542-8036: Manual for railway engineering.*
5. Ayele, A. (2017) Probabilistic seismic hazard analysis (PSHA) for Ethiopia and neighbouring region. *Journal of African Earth Sciences,* 134, pp. 257-264.
6. Baker, J. W. (2008) *An Introduction to Probabilistic Seismic Hazard Analysis (PSHA)*. Stanford University.
7. Bakker, K.J. (2003) Structural design of Linings for bored tunnels in soft ground. *HERON*, 48(1).
8. Bazzurro, P. and Cornell, C.A. (1999) Disaggregation of Seismic Hazard. *Bulletin of the seismological society of America*, 89(2), pp.501-520.
9. Belay, T., Tesfay, I., Ayalew, A., Yohannes, G. , Zewdie, T., Bekele, H. , Tadesse, M., Demisse, T. and Alemu, T. (2009) *Basic Geoscience Mapping Core Process: Geology of the were-ilu area*, Geologic Survey of Ethiopia, Memoir 25.
10. Bell, F.G. (2002) *Geological hazards-Their assessment, avoidance and mitigation*. 2nd edn. London: Routledge and Taylor & Frands e-Library
11. Bilotta, E., G. Lanzano, G. Russo, Santucci de Magistris F., Aiello, V., Conte, E. , Silvestri, F. and Valentino, M. (2007) Pseudostatic and dynamic analyses of tunnels In transversal and longitudinal directions. In: *Proceedings of the 4th International Conference on Earthquake Geotechnical Engineering,* Greece, June 25-28, 2007.
12. Bommer, J.J. and Martinez-Pereira, A. (1999) The effective duration of earthquake strong Motion. *Journal of Earthquake Engineering,* 3(2),pp. 127-172.

13. Boore, D. M. and Atkinson, G. M. (2008) Ground-Motion Prediction Equations for the Average Horizontal Component of PGA, PGV, and 5%-Damped PSA at Spectral Periods between 0.01 s and 10.0 s. *Earthquake Spectra,*24(1), pp. 99–138.
14. Boore, D. M. and Joyner, W.B. (1982)The empirical prediction of ground motion. *Bulletin of seismological society of America*, 72(6), pp-843-860.
15. Bouckovalas. G. and Kouretzis. G. (2011) Seismic Design of Underground Structures. Civil Engineering Department, National Technical university of Athens, Greece, October 2011.
16. BTS and ICEngineers (2004) *Tunnel lining design guide. Britain,* Thomas Telford Publishing.
17. Chen, C-H. and Hou, P-C. (1994) Response spectrum of ground shear strain. In: *Proceedings of the 10th world conference on earthquake Engineering*, Madrid, July 19-24, 1992. Balkema. Rotterdam.
18. Corigliano, M., Scandella, L., Lai, C. G. and Paolucci, R. (2011) Seismic analysis of deep tunnels in near fault conditions:a case study in Southern Italy. *Bulletin of Earthquake Engineering,* 9(4), pp. 975-995.
19. Douglas, J. (2011) *Ground-motion prediction equations*. s.l.: BRGM (BRGM/RP-59356-FR).
20. ES EN 19998-1 (2013): *Design of structures for earthquake resistance.*
21. Gaspari, G. M., Quaglio, G. and Floria. V.(2012) *Geotechnical Aspects of Underground Construction in Soft Ground . Rome, Italy. 16-18 may 2011. S.l.,CRC Press.*
22. Gonzalez, E. G. (1994): Seismic effects on tunnels across the Strait of Gibraltar. In*: Proceedings of the Tenth Earthquake Engineering World Conference*, Madrid, July 19-24, 1992. Balkema . Rotterdam.
23. Green, R. A. and Hall, W. J. (1994) *An overview of selected seismic hazard analysis methodologies.* Urbana, Illinois, s.n, (592).
24. Haselton, C.B., Whittaker, A.S., Hortacsu, A., Baker, J.W., Bray, J. and Grant, D.N. (2012) Selecting and Scaling Earthquake Ground Motions for Performing Response-

History Analyses. In*: Proceedings of the Fifteenth Earthquake Engineering World Conference*, Portugal, Sept 24-28, 2012.

25. Hashasha, Y. M.A., Hooka, J.J., Schmidtb, B. and Yaoa, J.C. (2001) Seismic design and analysis of underground structures. *Tunneling and Underground Space Technology*, 16, pp. 247-293
26. Htwe, Y. M. M. and WenBin, S. (2009) Gutenberg-Richter Recurrence Law to Seismicity Analysis of Southern Segment of the Sagaing Fault and Its Associate Components. *International Journal of Environmental, Chemical, Ecological, Geological and Geophysical Engineering*, 3(2).
27. Hung, C. J., Monsees, J., Munfah, N. and Wisniewski, J. (2009) *Technical Manual For Design And Construction Of Road Tunnels –Civil Element*s. One Penn Plaza, New York: Parsons Brinckerhoff, Inc. (FHWA-NHI-10-034).
28. Huyse, L., Cheri, R., and Stamatakos, J. A.(2003) Application of Generalized Pareto Distribution to Constrain Uncertainty in Low-Probability Peak Ground Accelerations. *Bulletin of Seismological Society of America*
29. Kamatchi, P., Ramana, G. V., Nagpal, A. K., and Iyer, N. R. (2013) Modelling Propagation of Stress Waves through Soil Medium for Ground Response Analysi. *Scientific research*,5,pp: 611-621. Available at: http://dx.doi.org/10.4236/eng.2013.57073 / [Accessed 22 Aug 2016].
30. Kevvadas, M. (2005) Numerical Analysis in the Design of Urban Tunnels: *The 11th international Conference of IACMAG*, Torino, Canada, 19-24 June 2005.
31. Kijko, A. (2003) Estimation of the Maximum Earthquake Magnitude, m_{max}. *Pure and Applied Geophysics, 161(8), pp.1655-1681.*
32. Kinde, S., Engida, S., Kebede, A. and Tesema, E. (2011) Notes and proposed guidelines on updated seismic codes in Ethiopia- Implications for large scale infrastructures. *Zede Journal* , 28
33. Kawashima, K. (2000) Seismic design of underground structures in soft ground: A review. *Geotechnical Aspects of Underground Construction in Soft Ground*. Rotterdam.

34. Kontoe, S., Zdravkovic, L., Potts, D. M. and Salandy, N. E. (2007)The Use Of Absorbing Boundaries In Dynamic Analyses of Soil-Structure Interaction Problems. In:*Proceedings of 4th International Conference on Earthquake Geotechnical Engineering*. Greece,June 25-28, 2007.
35. Kramer, S. L. (1996) *Geotechnical Earthquake Engineering*: USA: Prentice-Hall,Inc.
36. Lanzano, G. (2008) *Physical And Analytical Modeling Of Tunnels Under Dynamic Loadings.* Ph.D. Thesis. Università degli Studi di Napoli Federico II Facoltà di Ingegneria.
37. Lewis, M. A., Cheney, C. S. and ÓDochartaigh, B. É. (2006) *Guide to Permeability Indices*:British Geological Survey.
38. Lin, T. and Baker, J. (2011) Probabilistic seismic hazard deaggregation of ground motion prediction models. In: *Proceedings of the 5th international conference on earthquake Geotechnical engineering*. Santiago, Chile, January, 10-13, 2011.
39. Martin, J. and Perez C. J. (2009) Application of a generalized lognormal distribution to engineering data fitting. *Researchgate*
40. McGuire, R. K. (1995) Probabilistic Seismic Hazard Analysis and Design Earthquakes: Closing the Loop. *Bulletin of the Seismological Society of America*, 85(5), pp. 1275-1284.
41. Mohammed, J. (2017) Numerical Modelling For Circle Tunnel Under Static And Dynamic Loads For Different Depth. *Research Journal of Mining,* 1 (1),pp: 1-11
42. Mohamad, M.E. and Ibrahim, I.S.(2015) Interface shear strength of concrete to concrete bond with and without projecting steel reinforcement. *Jurnal Teknologi(Sciences & Engineering)*: 75(1), pp. 169-172
43. Moldovan, A. R. and Popa, A. (2012) Finite element modelling for tunneling excavation. *Civil Engineering and Architecture*, 55(1).
44. Morales-Esteban, A., Luis deJusto, J., lvarez, F.M.A. and Azanon, J.M. (2012) Probabilistic method to select calculation accelerograms based on uniform seismic

hazard acceleration response spectra. *Soil Dynamics and Earthquake Engineering* 43, pp. 174-185.

45. Nava-Tristán, Hernández, U. M., Sandoval, E. M. and Andrade, E. (2008) Seismic Guidelines for tunnels on Rock. In: *Proceedings of the 14th World Conference on Earthquake Engineering.* Beijing, China, October 12-17, 2008.
46. Nikam, S. and Bhagat, S. R. (2016) Dynamic Behavior of Underground Structures during Earthquake: A Critical Review. *International Journal of Engineering Research*: 5(1), pp: 116-119.
47. Owen, G. N. and Scholl, R. E. (1981) *Earthquake Engineering of Large Underground Structures*. FHWA/RD-80/195.
48. Paçi, E. (2014) Comparison of Analytical Solutions with Numerical Ones for Seismic Design of Tunnels in the Case of Heterogeneous Formations. *Journal of Civil Engineering and Architecture Research*: 1(2), pp:129-137.
49. Pavlovic, N. (2005) Seismic vulnerability of underground structures. In: *Proceedings of the 11th Association of Structural Engineers of the Philippines (ASEP) international convention*, Manila, Philippines.
50. Pescara, M., Gaspari, G. M. and Repetto, L. (2011) Design of underground structures under seismic conditions: a long deep tunnel and a metro tunnel. In: *Proceedings of colloquium on seismic design of tunnels*, ETH Zurich**.** Torino, Italy, 15 Dec2011.
51. Raju, L. G., Ramana, G. V. , Hanumantha, C. R. and Sitharam, T. G. (2004) Site-specific ground response analysis. *CURRENT SCIENCE*, 87(10)
52. Rani, S. R., Prasad, N. K. and Krishna, S. T (2014) Applicability Of Mohr-Coulomb & Druckerprager Models For Assessment Of Undrained Shear behaviour Of Clayey Soils. *International Journal of Civil Engineering and Technology (IJCIET)*,5(10), pp. 104-123.
53. Shaalan, O. A., Salem, T. N., El shamy, E. A. and Mansour, R.M. (2014) Dynamic analysis of two adjacent tunnels. *International Journal of Engineering and Innovative Technology (IJEIT)*, 4(4).

54. Singh, D. R., Mishra, A. K. and Agrawal, H. (2016) Fully grouted rock bolts: Application and performance evaluatio. In: *Proceedings of the International conference on advanced material technologies (ICAMT).* December 27-28, 2016.
55. Shlash, K.T., Salim, N.M. and Shaker, Z.H. (2014) Stress Analysis Around Tunnels During Construction Stages Using Finite Elements Method. *Journal of Engineering and Technology*, 32(6), pp. 1562-1578.
56. St John, C. M. and Zahrah, T.F. (1987) Aseismic Design of Underground Structure. *Tunneling and Underground space Technology*, 2, pp. 165-197.
57. Stewart, J. P., Chiou, S.J., Bray, J. D., Abrahamson, N. A., Graves, R. W. and Somerville, P. G. (2001) *Ground Motion Evaluation Procedures for Performance-Based Design. California:* Pacific Earthquake Engineering Research Center (PEER 2001/09).
58. Stewart, J.P., Douglas, J., Javanbarg, M., Bozorgnia, Y., N. A. Abrahamson, Boore, D. M., Campbell, K. W., Delavaud, E., Erdik, M. and Stafford, P. J. (2015) Selection of Ground Motion Prediction Equations for the Global Earthquake Model. *Earthquake Spectra, Earthquake Engineering Research Institute*, 31 (1), pp.19-45.
59. Ti, K. S.,. Huat, B.B.K., Noorzaei , J., Jaafar M.S. and Sew, G. S. (2009) A Review of Basic Soil Constitutive Models for Geotechnical Application. *Electronic journal of Geotechnical Engineering*, 14. Available at: http://www.ejge.com/2009/Ppr0985/Abs0985.htm/ [Accessed 26 Dec 2016].
60. Theodorakatou, A. (2007) *Sensitivity Analysis In Probabilistic Seismic Hazard Assessment*. Dissertation for Master Degree. European School for Advanced Studies In Reduction Of Seismic Risk.
61. Torcato, D. M. M. F.(2010*) Seismic behaviour of shallow tunnels in stratified ground.* Extended Abstract for Master Thesis. Instituto Superior Tecnico(IST).
62. USACE(1997) *EM 1110-2-2901: Engineering and Design: Tunnels and shafts in rock*. Washington, DC.

63. Vipin, K. S., Anbazhagan, P. and Sitharam, T. G. (2009) Estimation of peak ground acceleration and spectral acceleration for South India with local site effects-probabilistic approach. *Natural Hazards and Earth System Sciences*, 9, pp. 865-878.
64. Wang, J-N. (1993) *Seismic Design of Tunnels*. New York: Parsons Brinckerhoff Inc.
65. Wang, J-N. and Munfakh, G.A.(2001) Seismic design of tunnels. *Transactions on the built environment*, 57, WIT Press.
66. Wiemer, S. (2015) Earthquake Statistics and Earthquake Prediction Research. *Researchgate*. 21 September 2016.Available at: https://www.researchgate.net/publication/228610586/.
67. Yapı Merkezi (2014) *Basic design report*, (AWR-YM-X-BTR-GNRL-001-00).
68. Yapı Merkezi (2016) Tunnel 04. Excavation and support design, (AKH-YMI-DD-TTU04X-I-CE-REP-0003-2).

Appendix A

Contemporary earthquake data of the area

Hr	Mi	Secs	Lat	Lon	Dep	Mag	E	N
4	59	35.00	10.00	39.00	10.00	5.4	500000.000	1105412.520
10	52	1.20	10.40	39.40	10.00	5.4	543783.8623	1149666.055
11	39	57.00	10.57	39.73	10.00	4.5	579863.3861	1168528.154
11	59	9.00	10.50	39.50	10.00	4.5	554712.5615	1160738.628
19	24	2.00	10.41	39.88	10.00	5.4	596324.2572	1150877.796
19	26	5.50	10.40	40.00	10.00	5.4	609464.049	1149810.920
19	29	4.80	10.60	39.90	10.00	4.5	598453.4365	1171894.099
19	40	28.00	10.41	39.86	10.00	4.5	594134.9131	1150871.789
13	11	17.00	10.53	39.82	10.00	4.5	589721.7446	1164129.472
21	7	21.00	10.70	39.64	10.00	4.5	569987.1696	1182881.222
23	29	21.20	10.40	39.90	10.00	6.5	598516.7497	1149778.151
23	56	52.00	10.60	39.59	10.00	4.5	564540.2767	1171812.978
	1	46.00	10.44	39.66	10.00	4.5	572235.109	1154136.512
	8	57.00	10.37	39.96	10.00	4.5	605095.114	1146479.976
	21	19.00	9.79	39.71	10.00	4.5	577864.1431	1082276.360
	57	55.00	9.84	39.86	10.00	4.5	594301.2364	1087843.394
1	16	0.11	9.63	39.80	10.00	4.5	587776.4854	1064606.979
1	16	7.00	9.40	40.20	10.00	4.5	631757.8805	1039300.950
2	35	42.00	11.22	40.24	10.00	4.5	635370.7521	1240590.203
3	19	39.50	9.89	39.65	10.00	4.5	571262.3568	1093320.001
3	49	11.00	10.01	40.54	10.00	4.5	668791.1418	1106912.517
4	51	14.80	10.30	39.80	10.00	6.4	587597.4732	1138691.228
5	22	29.00	10.15	39.78	10.00	4.5	585447.492	1122099.624
5	44	53.00	10.22	39.92	10.00	5.8	600763.3915	1129880.201
6	17	16.00	10.62	39.77	10.00	4.5	584226.0405	1174067.511
7	2	52.00	10.15	39.89	10.00	5.7	597498.6379	1122130.576
7	21	49.90	10.68	39.74	10.00	4.5	580928.4948	1180694.138
22	19	34.00	10.38	39.98	10.00	4.5	607281.3879	1147592.463
23	32	36.00	10.49	39.85	10.00	4.5	593016.4399	1159715.078
2	5	34.00	10.24	39.81	10.00	4.5	588709.2332	1132059.434
15	20	31.00	10.38	39.86	10.00	4.5	594143.898	1147554.451
15	23	15.80	9.80	39.60	10.00	5.8	565798.2578	1083358.587
16	25	54.00	10.54	39.83	10.00	4.5	590813.0547	1165238.132
	41	43.00	10.29	39.72	10.00	4.5	578839.7506	1137564.713
17	46	43.00	10.83	39.56	10.00	4.5	561212.251	1197238.796
15	11	6.00	10.54	39.74	10.00	4.5	580965.3104	1165213.45
20	32	19.00	10.00	40.00	10.00	5.5	609600.7722	1105578.617
4	34	0.12	10.39	39.91	10.00	4.5	599614.6356	1148675.479
15	4	34.00	10.65	40.14	10.00	4.5	624690.3079	1177509.511
19	18	32.70	11.05	39.70	10.00	5.2	576459.5469	1221597.519
17	41	20.00	10.20	39.75	10.00	3.4	582148.0839	1127620.572
18	3	3.00	10.20	39.75	10.00	3.4	582148.0839	1127620.572
7	53	0.00	11.30	39.60	10.00	4.3	565480.2438	1249218.117
20	52	0.00	9.60	39.60	10.00	4.5	565837.2766	1061245.123
		0.00	10.00	39.80	10.00	4.0	587679.1017	1105518.817
15	47	44.00	11.03	39.71	9.00	5.3	577557.1262	1219388.522
7	7	53.07	10.00	39.60	10.00	4.3	565758.442	1105472.309
16	5	18.00	10.20	39.80	13.00	4.9	587624.9481	1127633.692
	44	37.00	11.20	39.70	10.00	3.8	576420.4442	1238184.38
21	35	21.20	10.52	39.75	13.00	5.2	582064.7852	1163004.532
22	12	45.00	10.6	40.00	10	4.8	609393.6976	1171927.47
16	10	0.00	10.48	38.93	10	4.1	492339.8391	1158484.637
6	23	2.04	11.08	39.62	14	5.2	567714.0847	1224895.535
2	56	0.00	9.75	39.50	10	4.1	554839.7821	1077812.366
22	26	0.00	10.7	41.10	7	4.9	729689.1174	1183590.428
6	51	0.00	10.5	41.00	10	4.2	718889.4065	1161391.535
17	3	0.00	10.6	41.00	10	4.3	718818.6714	1172454.591
17	13	0.00	9.9	40.65	10	4.0	680911.2874	1094804.156
18	54	0.00	9.8	40.60	10	4.2	675480.6074	1083717.069
7	35	0.00	10	40.70	10	3.8	686338.2254	1105892.654
8	10	38.08	11.33	39.61	10	5.2	566564.6894	1252537.733
2	29	0.00	10.6	40.00	10	4.8	609393.6976	1171927.47
12	8	36.03	9.47	39.61	10	4.9	566959.9539	1046873.414
19	11	35.09	11.48	39.64	15	5.6	569801.8472	1269131.729
8	43	28.40	9.89	41.08	7	4.7	728082.3583	1093961.882
23	17	52.90	9.94	41.08	5	4.6	728047.7655	1099493.482
17	54	2.10	9.93	41.04	7	4.6	723667.259	1098359.946
20	47	0.49	9.91	41.05	6	4.6	724777.7529	1096154.099
4	52	17.84	10.67	40.11	6	4.3	621400.6666	1179709.351
	21	38.33	9.74	40.63	5	4.3	678803.7488	1077096.594
18	31	31.57	10.54	40.21	6	4.3	632395.0103	1165373.557
19	14	47.03	10.48	40.30	5	4.1	642271.573	1158777.401
17	56	8.27	9.52	40.11	7	4.2	621832.5558	1052537.983
3	39	8.11	10.22	40.78	5	4.6	694976.9376	1130274.154

Appendix B

pga4nl calculation for site amplification

pga4nl										
	Magnitude scaling			Distance function	ln pga4nl			pga4nl		
	Strike slip	Normal	unspecified		Strike slip	Normal	unspecified	Strike slip	Normal	unspecified
M	$F_M(M)$	$F_M(M)$	$F_M(M)$	$F_D(R_{JB},M)$						
5	-1.319	-1.570	-1.353	-4.098	-5.417	-5.668	-5.451	0.004	0.003	0.004
5.1	-1.255	-1.507	-1.290	-4.042	-5.297	-5.548	-5.332	0.005	0.004	0.005
5.2	-1.194	-1.445	-1.229	-3.985	-5.179	-5.431	-5.214	0.006	0.004	0.005
5.3	-1.135	-1.386	-1.169	-3.929	-5.064	-5.315	-5.098	0.006	0.005	0.006
5.4	-1.078	-1.329	-1.112	-3.872	-4.950	-5.201	-4.985	0.007	0.006	0.007
5.5	-1.022	-1.274	-1.057	-3.816	-4.838	-5.090	-4.873	0.008	0.006	0.008
5.6	-0.969	-1.220	-1.004	-3.760	-4.729	-4.980	-4.763	0.009	0.007	0.009
5.7	-0.918	-1.169	-0.953	-3.703	-4.621	-4.873	-4.656	0.010	0.008	0.010
5.8	-0.869	-1.120	-0.903	-3.647	-4.516	-4.767	-4.550	0.011	0.009	0.011
5.9	-0.822	-1.073	-0.856	-3.591	-4.412	-4.664	-4.447	0.012	0.009	0.012
6	-0.777	-1.028	-0.811	-3.534	-4.311	-4.562	-4.345	0.013	0.010	0.013
6.1	-0.734	-0.985	-0.768	-3.478	-4.211	-4.463	-4.246	0.015	0.012	0.014
6.2	-0.693	-0.944	-0.727	-3.421	-4.114	-4.365	-4.149	0.016	0.013	0.016
6.3	-0.654	-0.905	-0.688	-3.365	-4.019	-4.270	-4.053	0.018	0.014	0.017
6.4	-0.617	-0.868	-0.651	-3.309	-3.925	-4.177	-3.960	0.020	0.015	0.019
6.5	-0.582	-0.833	-0.616	-3.252	-3.834	-4.085	-3.869	0.022	0.017	0.021
6.6	-0.549	-0.800	-0.584	-3.196	-3.745	-3.996	-3.779	0.024	0.018	0.023
6.7	-0.518	-0.769	-0.553	-3.139	-3.658	-3.909	-3.692	0.026	0.020	0.025
6.8	-0.504	-0.755	-0.538	-3.083	-3.586	-3.838	-3.621	0.028	0.022	0.027
6.86	-0.504	-0.755	-0.538	-3.049	-3.553	-3.804	-3.587	0.029	0.022	0.028

Appendix C

Material data

Soil data sets parameter

Mohr-Coulomb		Ballast	Dynamic rock B	Invert	Pipe umbrella	Rock B
Type		Drained	Drained	Drained	Drained	Drained
Υ_{unsat}	[kN/m³]	20	22.89	24	22.89	22.89
Υ_{sat}	[kN/m³]	20	24.53	24	24.53	24.53
k_x	[m/s]	0.001	0.001	0	0.001	0.001
k_y	[m/s]	0.001	0.001	0	0.001	0.001
k_0	[-]	0.5	0.5	0.5	0.5	0.5
c_k	[-]	1.00E+15	1.00E+15	1.00E+15	1.00E+15	1.00E+15
E_{ref}	[kN/m²]	150,000	2.5E+11	31,000,000	16,600,000	250,000
v	[-]	0.3	0.2	0.15	0.25	0.25
G_{ref}	[kN/m²]	57,692.31	1.02E+12	13,478,260.87	6,640,000	100,000
E_{oed}	[kN/m²]	201,923.08	2.72E+12	32,732,919.26	19,920,000	300,000
c_{ref}	[kN/m²]	0.01	500	1,448.35	5000	500
Ø	[°]	48	25	63.66	28	25
Ψ	[°]	18	0	0	0	0
E_{inc}	[kN/m²/m]	0	0	0	0	0
y_{ref}	[m]	0	0	0	0	0
$c_{increment}$	[kN/m²/m]	0	0	0	0	0
$R_{inter.}$	[-]	0.67	1	0.67	1	1

Plate data sets parameter

no.	Identification	EA	EI	w	n
		[kN/m]	[kNm²/m]	[kN/m/m]	[-]
1	final lining	1.71E+07	4.30E+05	12.65	0.2
2	provisional invert	2.25E+06	4218.8	3.45	0.2
3	primary Lining 807-864	7.75E+06	40365	5.75	0.2

Anchor data sets parameter

no.	Identification	EA [kN]	|Fmax,comp| [kN]	|Fmax,tens| [kN]	L spacing [m]
1	sleeper	1.55E+07	1.00E+15	1.00E+15	0.6
2	rock bolt anchor	6.90E+05	1.00E+15	1.00E+15	1

Appendix D

Construction stages

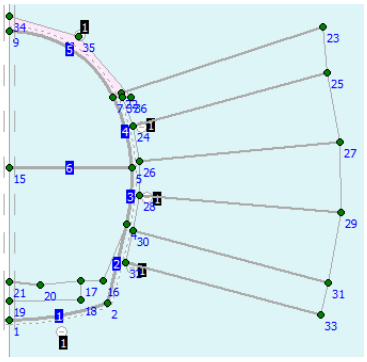

Pipe umbrella activation

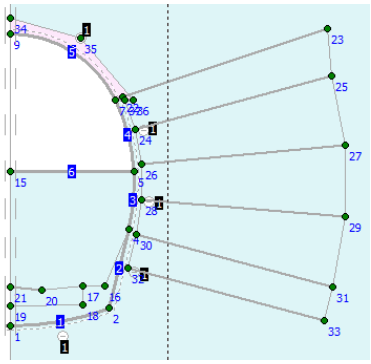

Top heading excavation

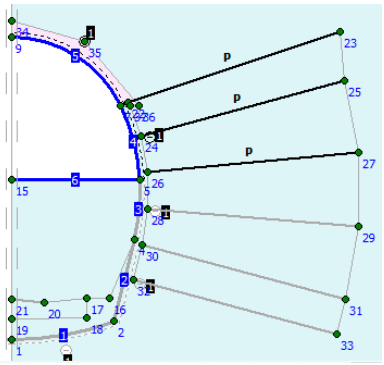

Provisional invert and crow lining activation

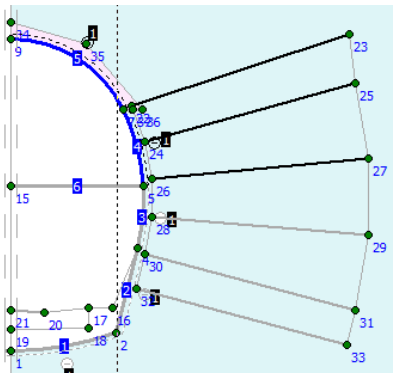

Bench excavation

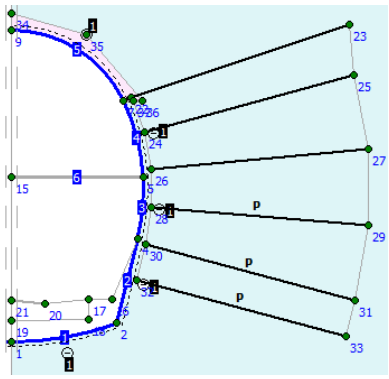

Full primary lining

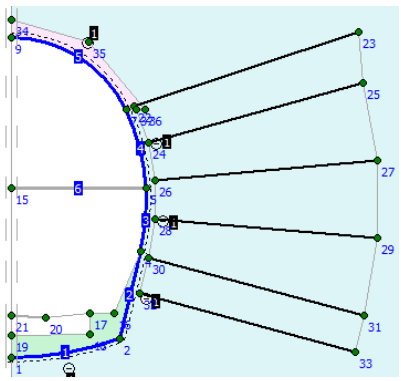

Invert

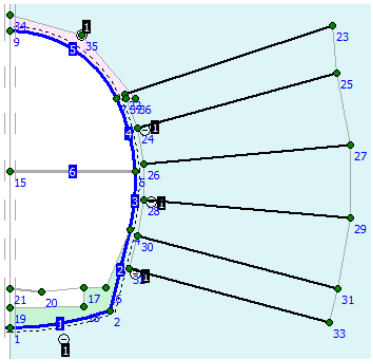

Final lining activation

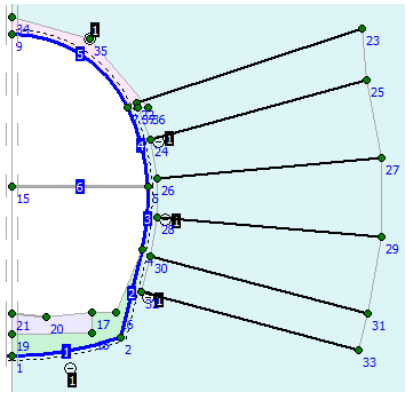

Activation of ballast

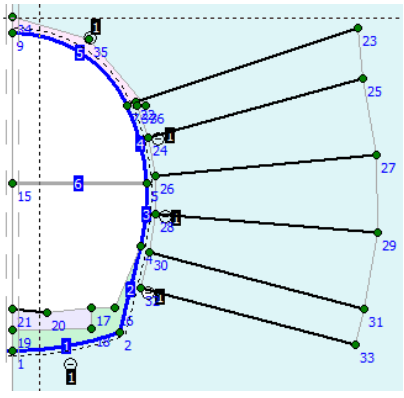

Activation of sleeper

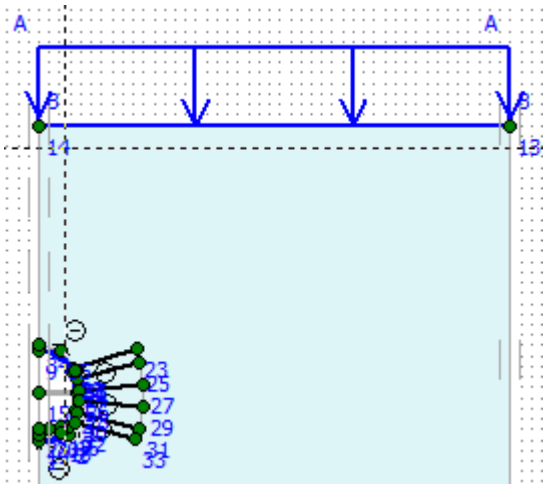

Surcharge load

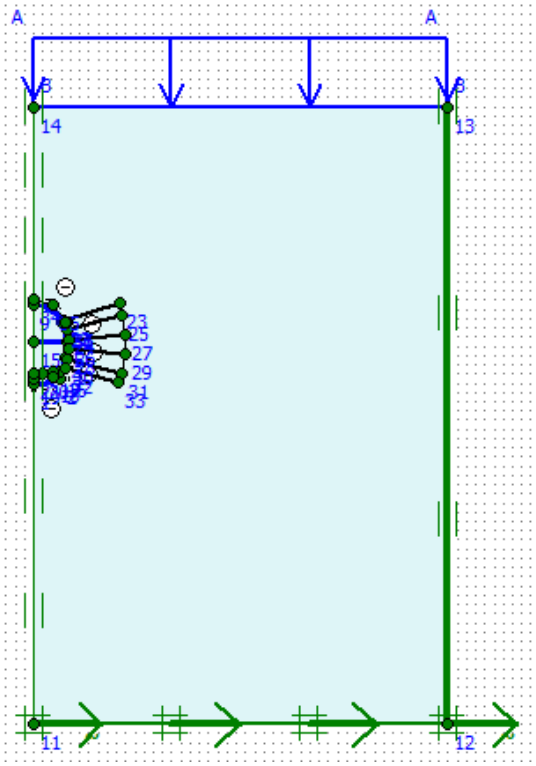

Earthquake load

Appendix E

Incremental shear strain due to earthquake

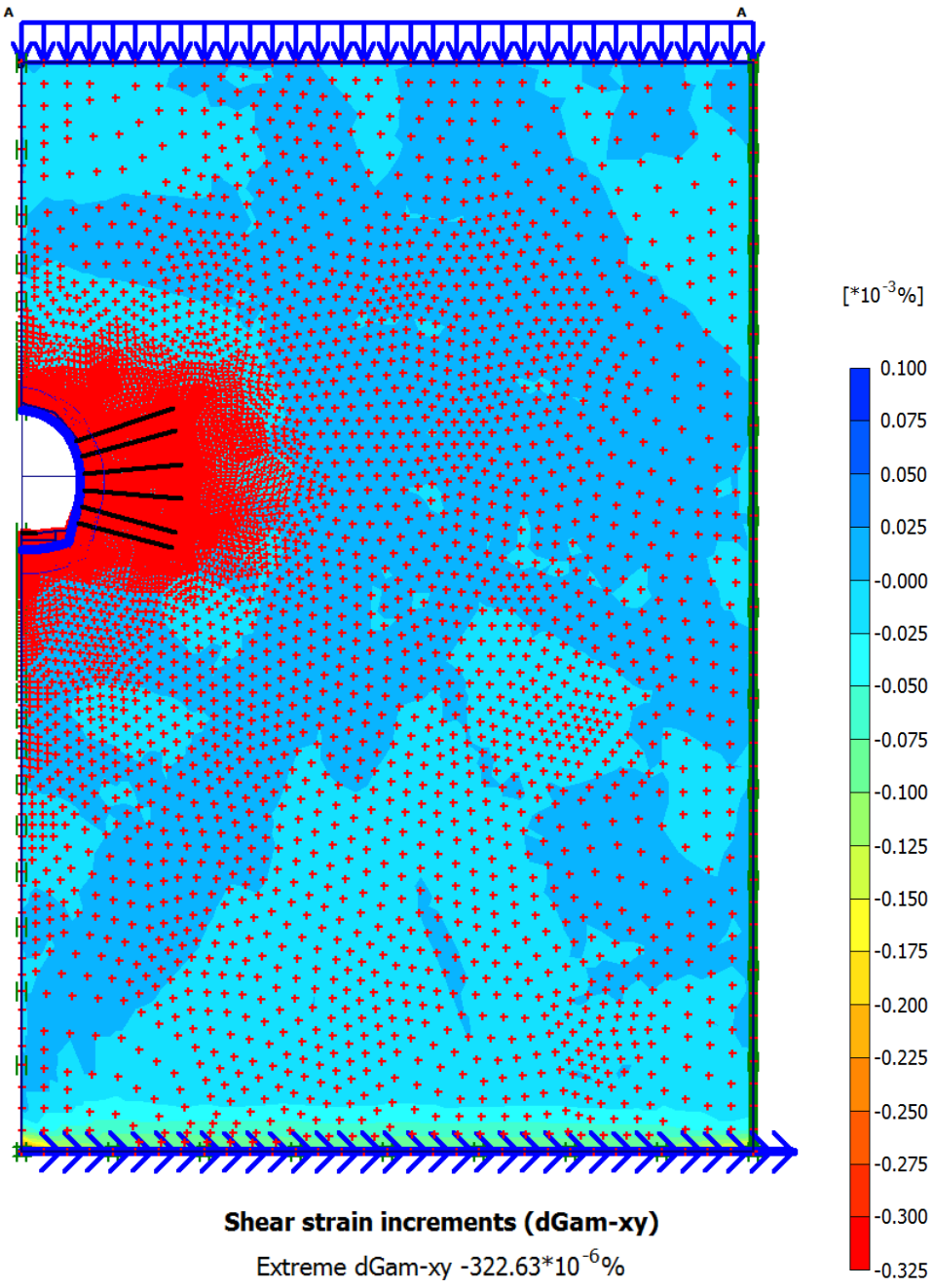

Appendix F

Horizontal acceleration

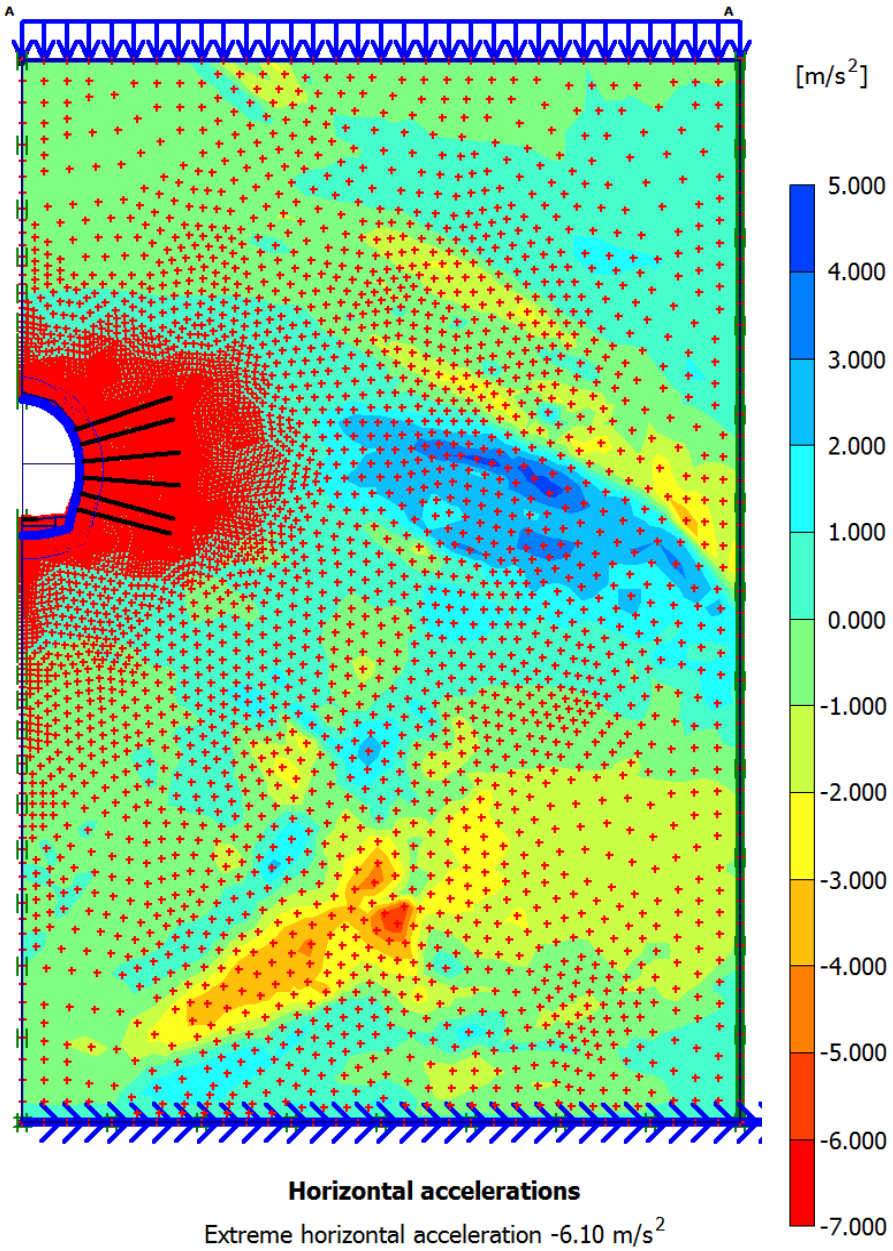

Appendix G

Deformed shape

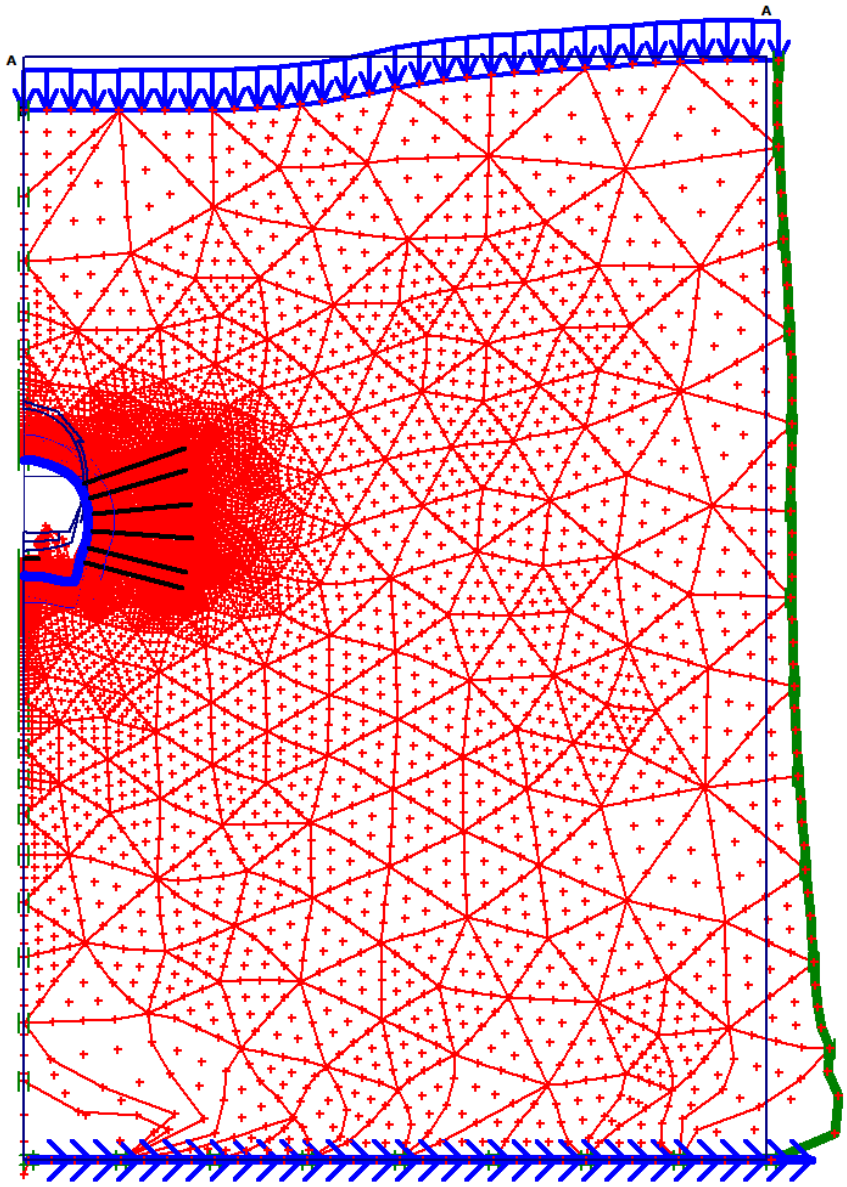

Deformed mesh

Extreme total displacement $102.39*10^{-3}$ m
(displacements scaled up 50.00 times)

Appendix H

Lining stress calculation

	After EQ							Before EQ					Difference in forces			Difference in stress	
						Normal stress at extrados	Normal stress at inttrados				Normal stress at extrados	Normal stress at inttrados					
Node	X	Y	N	Q	M	σ_{ex} = N/t+6M/t^2	σ_{in} = N/t+6M/t^2	N	Q	M	σ_{ex} = N/t+6M/t^2	σ_{in} = N/t+6M/t^2	N	Q	M	σ_{ex}	σ_{in}
	[m]	[m]	[kN/m]	[kN/m]	[kNm/m]	[kN/m^2]	[kN/m^2]	[kN/m]	[kN/m]	[kNm/m]	[kN/m^2]	[kN/m^2]	[kN/m]	[kN/m]	[kNm/m]	[kN/m^2]	[kN/m^2]
12093	48.09	43.63	-18727.9	-941.3	-2109.61	75894.27	-7792.81	-2620.5022	-68.236869	-1067	25927.02	-16397.92	-16107.40	-873.06	-1042.67	49967.25	8605.11
12089	48.07	43.67	-18538.3	-756.14	-2146.76	76286.43	-8874.37	-2624.0908	-51.711013	-1070	25986.08	-16443.93	-15914.23	-704.43	-1077.17	50300.35	7569.56
12088	48.06	43.71	-18353.7	-579.89	-2176.05	76531.70	-9790.85	-2630.1579	-30.112677	-1071	26033.00	-16468.79	-15723.58	-549.77	-1104.65	50498.70	6677.94
12087	48.03	43.75	-18173.4	-407.69	-2197.67	76632.69	-10547.69	-2638.2347	-3.9095536	-1072	26062.85	-16469.27	-15535.14	-403.78	-1125.51	50569.84	5921.58
12109	48.01	43.79	-17996.5	-234.7	-2211.77	76590.67	-11149.01	-2647.8526	26.430664	-1072	26070.81	-16442.25	-15348.60	-261.13	-1140.09	50519.86	5293.24
12109	48.01	43.79	-17995.5	-217.47	-2211.77	76588.86	-11150.79	-2647.6368	25.553979	-1072	26070.41	-16442.64	-15347.83	-243.02	-1140.09	50518.44	5291.85
11843	47.99	43.83	-17816	-43.369	-2217.47	76375.65	-11590.05	-2657.4152	57.612025	-1070	26052.13	-16388.80	-15158.62	-100.98	-1147.60	50323.51	4798.75
11842	47.97	43.87	-17633.1	127.573	-2215.62	76006.34	-11885.98	-2667.5735	90.64063	-1067	26006.17	-16305.90	-14965.53	36.93	-1149.00	50000.18	4419.91
11841	47.95	43.91	-17446.6	297.047	-2206.3	75482.50	-12040.18	-2678.1269	124.38096	-1062	25931.92	-16193.28	-14768.51	172.67	-1144.39	49550.58	4153.10
11847	47.93	43.94	-17256.6	466.745	-2189.57	74805.17	-12053.73	-2689.09	158.57417	-1056	25828.87	-16050.36	-14567.56	308.17	-1133.86	48976.31	3996.62
11847	47.93	43.94	-17256.7	463.295	-2189.57	74805.34	-12053.56	-2689.2542	158.23408	-1056	25829.17	-16050.06	-14567.48	305.06	-1133.86	48976.17	3996.50
11853	47.9	43.98	-17062.5	632.085	-2165.57	73976.26	-11930.73	-2701.375	192.22523	-1048	25698.83	-15875.65	-14361.15	439.86	-1117.55	48277.43	3944.93
11852	47.88	44.02	-16864.4	800.159	-2134.15	72992.77	-11667.62	-2714.6799	225.8459	-1039	25541.19	-15669.63	-14149.74	574.31	-1095.29	47451.58	4002.01
11851	47.86	44.05	-16662.9	964.23	-2095.46	71859.14	-11266.61	-2729.195	259.08481	-1028	25356.69	-15432.34	-13933.75	705.15	-1067.24	46502.45	4165.74
12207	47.83	44.09	-16458.6	1121.01	-2049.72	70580.45	-10730.86	-2744.9469	291.93066	-1016	25145.77	-15164.15	-13713.69	829.08	-1033.58	45434.68	4433.29
12207	47.83	44.09	-16458.7	1116.84	-2049.72	70580.50	-10730.85	-2744.6543	288.55145	-1016	25145.24	-15164.68	-13714.00	828.29	-1033.58	45435.26	4433.83
12149	47.81	44.13	-16257.9	1252.41	-1997.75	69184.75	-10064.96	-2762.5515	327.72058	-1003	24909.82	-14864.18	-13495.39	924.69	-995.12	44274.94	4799.21
12148	47.78	44.16	-16055.9	1370.41	-1940.16	67674.96	-9290.00	-2780.8975	360.15496	-987.5	24642.86	-14530.51	-13274.97	1010.25	-952.66	43032.10	5240.50
12147	47.76	44.2	-15852.8	1466.18	-1877.9	66071.03	-8424.32	-2799.8892	380.25128	-971.2	24354.83	-14173.41	-13052.96	1085.93	-906.67	41716.20	5749.09
12153	47.73	44.23	-15649.3	1535.1	-1812.01	64394.06	-7487.46	-2819.7237	382.40622	-954.4	24057.64	-13804.10	-12829.59	1152.69	-857.58	40336.42	6316.64
12153	47.73	44.23	-15648.7	1537.54	-1812.01	64392.93	-7488.65	-2819.0359	381.72121	-954.4	24056.39	-13805.35	-12829.64	1155.82	-857.58	40336.54	6316.70
12143	47.7	44.27	-15443.4	1572.24	-1743.84	62667.47	-6509.48	-2838.0713	352.51413	-938.3	23771.44	-13451.18	-12605.37	1219.73	-805.52	38896.03	6941.70
12142	47.68	44.3	-15237	1602.62	-1674.24	60911.57	-5504.40	-2855.9819	319.3471	-923.6	23511.74	-13126.35	-12380.99	1283.27	-750.65	37399.83	7621.95
12141	47.65	44.34	-15029.4	1631.57	-1603.32	59127.64	-4475.19	-2872.775	283.63747	-910.4	23279.80	-12833.34	-12156.65	1347.93	-692.97	35847.84	8358.15
12191	47.62	44.37	-14821	1662.02	-1531.16	57317.26	-3422.86	-2888.458	246.80259	-898.7	23077.76	-12574.27	-11932.50	1415.21	-632.43	34239.51	9151.41
12191	47.62	44.37	-14820.1	1663.36	-1531.16	57315.82	-3424.39	-2888.3975	248.69317	-898.7	23077.65	-12574.38	-11931.75	1414.67	-632.43	34238.17	9150.00
11955	47.59	44.4	-14610.5	1701.41	-1457.42	55472.10	-2343.02	-2902.108	219.25596	-888.5	22899.65	-12346.53	-11708.39	1482.15	-568.93	32572.45	10003.51
11954	47.56	44.44	-14396.2	1740.47	-1381.97	53585.84	-1236.15	-2914.2078	196.70542	-879.4	22741.27	-12144.16	-11481.96	1543.76	-502.57	30844.57	10908.01
11953	47.53	44.47	-14176.7	1780.54	-1304.78	51655.86	-104.20	-2924.4944	181.02415	-871.1	22596.22	-11961.69	-11252.21	1599.52	-433.64	29059.64	11857.50
12405	47.5	44.5	-13951.7	1821.62	-1225.85	49680.98	1052.40	-2932.7653	172.19479	-863.4	22458.21	-11793.60	-11018.92	1649.42	-362.41	27222.78	12846.01
12405	47.5	44.5	-13950.5	1818.66	-1225.85	49678.95	1050.29	-2933.0559	171.79803	-863.4	22458.73	-11793.08	-11017.49	1646.86	-362.42	27220.22	12843.36
12408	47.47	44.53	-13717.6	1854.21	-1145.34	47658.65	2223.58	-2939.7189	169.86554	-856	22322.67	-11632.78	-10777.90	1684.34	-289.38	25335.98	13856.36
12407	47.44	44.56	-13476.2	1884.29	-1063.35	45593.47	3410.91	-2945.189	172.36419	-848.5	22184.08	-11474.30	-10531.02	1711.92	-214.88	23409.39	14885.21
12406	47.41	44.59	-13226.5	1907.01	-980.214	43490.48	4605.94	-2949.3992	179.00645	-840.8	22039.26	-11314.17	-10277.12	1728.00	-139.43	21451.22	15920.12
12425	47.38	44.63	-12968.7	1920.49	-896.292	41357.24	5801.85	-2952.2828	189.50481	-832.7	21884.57	-11148.99	-10016.47	1730.99	-63.57	19472.67	16950.84
12425	47.38	44.63	-12969	1920.21	-896.294	41357.81	5802.33	-2952.4952	188.54805	-832.7	21884.95	-11148.61	-10016.54	1731.66	-63.57	19472.85	16950.94
12431	47.35	44.66	-12704	1926.26	-811.968	39203.25	6992.95	-2954.6562	198.32207	-824.2	21720.71	-10976.50	-9749.30	1727.94	12.27	17482.54	17969.46
12430	47.32	44.69	-12433.5	1924.48	-727.521	37036.50	8176.15	-2956.5507	208.61276	-815.3	21547.30	-10796.21	-9476.93	1715.87	87.80	15489.20	18972.36
12429	47.28	44.71	-12158	1915.06	-643.319	34865.58	9345.49	-2958.1089	219.95605	-805.9	21363.82	-10607.06	-9199.94	1695.11	162.61	13501.76	19952.55
12668	47.25	44.74	-11878.1	1898.22	-559.723	32698.46	10494.57	-2959.2607	232.88785	-796	21169.22	-10408.27	-8918.82	1665.33	236.29	11529.24	20902.84
12668	47.25	44.74	-11878.7	1901.58	-559.725	32699.66	10495.68	-2959.3539	233.27954	-796	21169.39	-10408.10	-8919.37	1668.30	236.29	11530.27	20903.78
12664	47.22	44.77	-11595.4	1871.87	-477.038	30544.39	11620.57	-2960.2676	246.82857	-785.5	20962.88	-10198.27	-8635.10	1625.04	308.48	9581.52	21818.84
12663	47.18	44.8	-11311.7	1843.48	-395.584	28413.09	12720.49	-2962.032	266.37269	-774.3	20743.19	-9972.16	-8349.70	1577.11	378.70	7669.91	22692.65
12662	47.15	44.83	-11028	1815.14	-315.381	26306.39	13795.42	-2964.3469	290.57781	-762.1	20505.62	-9726.17	-8063.65	1524.56	446.71	5800.77	23521.59
12984	47.12	44.86	-10744.3	1785.55	-236.461	24225.25	14844.99	-2966.9127	318.10981	-748.8	20245.82	-9457.05	-7777.40	1467.44	512.30	3979.42	24302.04
12984	47.12	44.86	-10745.1	1783.93	-236.463	24226.70	14846.36	-2966.7284	316.79099	-748.8	20245.49	-9457.39	-7778.36	1467.13	512.30	3981.21	24303.75
12970	47.08	44.88	-10462.9	1754.64	-158.906	22175.30	15871.59	-2969.0854	346.60646	-734.2	19961.51	-9164.83	-7493.81	1408.04	575.32	2213.79	25036.43
12969	47.05	44.91	-10184.5	1721.98	-82.6674	20156.92	16877.55	-2970.9871	376.89765	-718.4	19650.25	-8846.66	-7213.49	1345.08	635.69	506.67	25724.21
12968	47.01	44.93	-9910.32	1684.54	-7.97228	18176.89	17860.64	-2972.4532	406.60376	-701.2	19312.23	-8503.31	-6937.87	1277.93	693.21	-1135.34	26363.94
12974	46.97	44.96	-9640.89	1640.92	64.93502	16240.93	18816.86	-2973.5035	434.66399	-682.7	18948.24	-8135.50	-6667.39	1206.25	747.67	-2707.31	26952.36
12974	46.97	44.96	-9640.9	1639.32	64.9338	16240.97	18816.86	-2973.3177	432.87339	-682.7	18947.90	-8135.83	-6667.59	1206.45	747.67	-2706.93	26952.69
12964	46.94	44.99	-9376.2	1589.92	135.7336	14355.41	19739.88	-2973.0803	459.88181	-663.1	18558.92	-7747.72	-6403.12	1130.04	798.88	-4203.52	27487.60
12963	46.9	45.01	-9115.89	1533.03	204.2244	12523.61	20625.07	-2971.2951	480.31295	-642.5	18146.33	-7341.62	-6144.59	1052.72	846.73	-5622.73	27966.69
12962	46.87	45.03	-8860.43	1468.89	270.0644	10753.23	21466.53	-2968.3166	494.0008	-621.1	17716.76	-6922.88	-5892.12	974.89	891.19	-6963.53	28389.41
13138	46.83	45.06	-8610.33	1397.72	332.9136	9051.90	22258.39	-2964.4996	500.77941	-599.3	17276.87	-6496.88	-5645.83	896.95	932.21	-8224.98	28755.26
13138	46.83	45.06	-8610.72	1396.98	332.9133	9052.61	22259.09	-2964.8161	500.36287	-599.3	17277.45	-6496.30	-5645.90	896.62	932.21	-8224.84	28755.39
12746	46.79	45.08	-8367.27	1318.18	392.4556	7428.98	22997.47	-2961.3716	498.40646	-577.4	16836.36	-6067.74	-5405.90	819.77	969.83	-9407.38	29065.21
12745	46.75	45.1	-8131.47	1229.6	448.3459	5891.68	23677.30	-2959.1136	487.67995	-555.7	16402.86	-5642.45	-5172.35	741.92	1004.07	-10511.19	29319.75
12744	46.72	45.13	-7903.79	1131.47	500.1461	4450.27	24290.78	-2958.3757	468.50265	-534.7	15985.09	-5227.36	-4945.41	662.97	1034.88	-11534.82	29518.14
12750	46.68	45.15	-7684.72	1024.02	547.4194	3114.32	24830.13	-2959.4916	441.19387	-514.8	15591.11	-4829.32	-4725.23	582.82	1062.18	-12476.79	29659.45
12750	46.68	45.15	-7684.74	1024.53	547.4198	3114.35	24830.17	-2959.3474	442.56229	-514.8	15590.85	-4829.59	-4725.40	581.96	1062.18	-12476.50	29659.76
12756	46.64	45.17	-7474.74	907.825	589.7962	1892.00	25288.87	-2962.3575	409.75659	-496.1	15225.66	-4453.45	-4512.38	498.07	1085.87	-13333.66	29742.32
12755	46.6	45.19	-7273.7	784.716	626.9214	790.11	25659.72	-2966.6798	375.27889	-478.9	14892.10	-4104.17	-4307.02	409.44	1105.79	-14101.99	29763.89
12754	46.56	45.21	-7081.92	655.969	658.5316	-185.56	25938.00	-2972.3097	339.70586	-463.2	14591.30	-3782.90	-4109.61	316.26	1121.71	-14776.87	29720.91
13486	46.52	45.23	-6899.68	522.356	684.3711	-1029.43	26119.17	-2979.2426	303.61423	-449.1	14324.27	-3490.66	-3920.44	218.74	1133.46	-15353.69	29609.83

	After EQ							Before EQ					Difference in forces			Difference in stress	
						Normal stress at extrados	Normal stress at inttrados				Normal stress at extrados	Normal stress at inttrados					
Node	X	Y	N	Q	M	σ_{ex} = N/t+6M/t^2	σ_{in} = N/t+6M/t^2	N	Q	M	σ_{ex} = N/t+6M/t^2	σ_{in} = N/t+6M/t^2	N	Q	M	σ_{ex}	σ_{in}
	[m]	[m]	[kN/m]	[kN/m]	[kNm/m]	[kN/m^2]	[kN/m^2]	[kN/m]	[kN/m]	[kNm/m]	[kN/m^2]	[kN/m^2]	[kN/m]	[kN/m]	[kNm/m]	[kN/m^2]	[kN/m^2]
13486	46.52	45.23	-6899.78	523.889	684.3717	-1029.26	26119.37	-2979.191	304.94614	-449.1	14324.17	-3490.75	-3920.59	218.94	1133.46	-15353.43	29610.12
13476	46.48	45.25	-6727.59	389.072	704.3798	-1739.20	26203.14	-2987.4126	272.17144	-436.4	14088.51	-3225.19	-3740.17	116.90	1140.83	-15827.71	29428.33
13475	46.44	45.27	-6565.57	255.467	718.5011	-2313.87	26188.66	-2996.7082	243.27411	-425.2	13881.58	-2984.46	-3568.86	12.19	1143.67	-16195.45	29173.12
13474	46.4	45.29	-6413.72	123.848	726.8143	-2754.84	26077.47	-3006.9054	218.44986	-415.1	13699.62	-2765.42	-3406.82	-94.60	1141.87	-16454.46	28842.89
13762	46.36	45.3	-6272.04	-5.0093	729.4063	-3063.85	25871.28	-3017.8317	197.89441	-405.9	13538.83	-2564.89	-3254.21	-202.90	1135.35	-16602.67	28436.17
13762	46.36	45.3	-6272.12	-4.2918	729.407	-3063.72	25871.43	-3017.8358	197.90158	-405.9	13538.83	-2564.89	-3254.29	-202.19	1135.35	-16602.55	28436.32
13514	46.32	45.32	-6140.49	-127.61	726.4947	-3245.29	25574.33	-3029.2155	182.39292	-397.6	13394.52	-2379.19	-3111.27	-310.01	1124.12	-16639.81	27953.52
13513	46.28	45.34	-6018.93	-244.22	718.3144	-3304.04	25191.07	-3041.0242	171.01688	-389.9	13262.60	-2204.33	-2977.91	-415.24	1108.21	-16566.64	27395.40
13512	46.24	45.35	-5907.25	-353.56	705.1851	-3246.69	24727.60	-3053.1238	163.6675	-382.6	13139.35	-2037.09	-2854.13	-517.23	1087.76	-16386.04	26764.69
13814	46.2	45.37	-5805.24	-455.1	687.4321	-3080.04	24189.99	-3065.3765	160.23881	-375.5	13021.10	-1874.28	-2739.86	-615.34	1062.92	-16101.15	26064.27
13814	46.2	45.37	-5805.33	-454.97	687.4324	-3079.88	24190.16	-3065.4452	159.79967	-375.5	13021.23	-1874.16	-2739.88	-614.77	1062.92	-16101.11	26064.32
13800	46.16	45.38	-5713	-547.33	665.4344	-2811.42	23585.97	-3078.0426	159.68335	-368.5	12905.41	-1712.53	-2634.96	-707.02	1033.93	-15716.84	25298.51
13799	46.12	45.4	-5630.14	-630.6	639.5732	-2449.13	22922.37	-3090.9509	161.66151	-361.5	12789.28	-1549.46	-2539.19	-792.26	1001.03	-15238.42	24471.83
13798	46.08	45.41	-5556.41	-704.43	610.2709	-2001.98	22207.12	-3104.0945	165.61464	-354.3	12671.02	-1383.40	-2452.32	-870.04	964.56	-14673.00	23590.52
13804	46.04	45.43	-5491.49	-768.47	577.9534	-1479.00	21448.07	-3117.3981	171.4232	-346.9	12548.82	-1212.83	-2374.10	-939.89	924.86	-14027.82	22660.90
13804	46.04	45.43	-5491.53	-768.62	577.9529	-1478.92	21448.14	-3117.4467	171.07477	-346.9	12548.91	-1212.74	-2374.09	-939.69	924.86	-14027.83	22660.88
13807	45.99	45.44	-5435.07	-822.12	543.051	-889.31	20653.21	-3130.8663	178.38372	-339.3	12421.50	-1036.53	-2304.20	-1000.51	882.31	-13310.81	21689.73
13806	45.95	45.45	-5386.81	-864.81	506.0248	-242.66	19831.05	-3144.5757	186.91016	-331.2	12287.64	-852.82	-2242.23	-1051.72	837.27	-12530.31	20683.87
13805	45.91	45.46	-5346.35	-896.51	467.3692	450.51	18990.77	-3158.5585	196.50115	-322.8	12146.43	-660.76	-2187.79	-1093.01	790.22	-11695.92	19651.53
14042	45.87	45.47	-5313.32	-917.05	427.5808	1179.64	18141.53	-3172.7983	207.00378	-314	11996.97	-459.52	-2140.52	-1124.06	741.59	-10817.32	18601.04
14042	45.87	45.47	-5313.49	-917.52	427.5797	1179.97	18141.81	-3173.0164	206.47186	-314	11997.36	-459.12	-2140.47	-1123.99	741.59	-10817.40	18600.93
13219	45.82	45.49	-5287.67	-926.14	387.1297	1935.34	17292.55	-3187.8055	218.39378	-304.7	11839.64	-247.62	-2099.86	-1144.53	691.83	-9904.31	17540.17
13218	45.78	45.5	-5268.56	-922.58	346.5497	2705.48	16452.90	-3203.1955	231.54585	-294.8	11672.07	-24.09	-2065.36	-1154.13	641.39	-8966.59	16476.99
13217	45.74	45.51	-5255.71	-906.48	306.4022	3478.43	15633.23	-3219.1856	246.03734	-284.4	11493.56	212.57	-2036.52	-1152.52	590.78	-8015.13	15420.66
13216	45.7	45.51	-5248.68	-877.47	267.2551	4242.13	14843.99	-3235.7752	261.9775	-273.2	11303.00	463.45	-2012.91	-1139.45	540.50	-7060.87	14380.53
13216	45.7	45.51	-5248.6	-878.52	267.2534	4242.02	14843.81	-3235.8336	262.42042	-273.2	11303.11	463.56	-2012.77	-1140.94	540.50	-7061.09	14380.25
13115	45.65	45.52	-5247.15	-832.88	229.6918	4984.40	14096.14	-3253.1984	279.0428	-261.4	11099.42	730.39	-1993.95	-1111.93	491.08	-6115.02	13365.75
13114	45.61	45.53	-5250.43	-776.24	194.3912	5690.55	13401.94	-3271.3361	297.60568	-248.8	10881.82	1013.94	-1979.10	-1073.85	443.14	-5191.27	12387.99
13113	45.57	45.54	-5258.06	-711.85	161.7257	6352.33	12767.90	-3290.1179	318.48526	-235.3	10648.22	1315.85	-1967.95	-1030.34	396.98	-4295.88	11452.05
13112	45.52	45.55	-5269.65	-642.96	132.0271	6962.46	12199.90	-3309.415	342.05772	-220.8	10396.39	1637.85	-1960.23	-985.02	352.82	-3433.93	10562.05
13112	45.52	45.55	-5269.29	-644.64	132.0248	6961.85	12199.19	-3309.3414	339.87947	-220.8	10396.25	1637.72	-1959.94	-984.51	352.81	-3434.41	10561.48
12526	45.48	45.55	-5284.4	-578.44	105.2167	7521.06	11694.94	-3329.3439	363.41678	-205.4	10127.02	1979.69	-1955.06	-941.85	310.60	-2605.96	9715.26
12525	45.44	45.56	-5302.02	-512.11	81.30358	8027.40	11252.66	-3349.8038	388.51051	-188.9	9837.34	2343.77	-1952.21	-900.62	270.20	-1809.94	8908.90
12524	45.39	45.56	-5322.05	-445.59	60.30177	8480.39	10872.52	-3370.6582	415.06877	-171.3	9525.94	2731.00	-1951.39	-860.66	231.59	-1045.55	8141.52
12523	45.35	45.57	-5344.42	-378.83	42.22945	8879.52	10554.74	-3391.8442	442.99966	-152.5	9191.54	3142.43	-1952.58	-821.83	194.72	-312.02	7412.30
12523	45.35	45.57	-5344.06	-378.83	42.22658	8878.92	10554.02	-3391.5386	440.46701	-152.5	9190.99	3141.88	-1952.52	-819.30	194.71	-312.07	7412.14
11987	45.31	45.57	-5368.21	-311.83	27.08531	9223.15	10297.61	-3412.8596	470.66367	-132.5	8833.43	3576.97	-1955.35	-782.50	159.59	389.72	6720.64
11986	45.26	45.58	-5393	-244.49	14.88325	9510.24	10100.65	-3433.2247	495.51659	-111.3	8449.70	4034.75	-1959.77	-740.00	126.18	1060.54	6065.90
11985	45.22	45.58	-5418.17	-176.81	5.640019	9739.35	9963.09	-3452.7232	513.26378	-89.16	8046.06	4509.29	-1965.45	-690.07	94.80	1693.29	5453.79
11991	45.18	45.58	-5443.48	-108.8	-0.6238	9909.62	9884.87	-3471.4446	522.14322	-66.43	7629.24	4994.20	-1972.04	-630.95	65.80	2280.38	4890.68
11991	45.18	45.58	-5443.04	-116.03	-0.62689	9908.88	9884.01	-3469.4785	508.5864	-66.43	7625.66	4990.62	-1973.56	-624.61	65.80	2283.21	4893.39
11978	45.13	45.58	-5459.9	-35.155	-3.93198	10005.08	9849.10	-3486.5352	504.32171	-44.03	7212.50	5465.81	-1973.36	-539.48	40.10	2792.57	4383.29
11977	45.09	45.59	-5469.52	26.6357	-3.95706	10023.07	9866.10	-3497.3371	432.59464	-23.16	6818.17	5899.42	-1972.18	-405.96	19.20	3204.90	3966.67
11976	45.04	45.59	-5473.53	53.985	-2.10881	9993.71	9910.05	-3504.0807	280.15533	-7.27	6515.26	6226.85	-1969.45	-226.17	5.16	3478.45	3683.20
11975	45	45.59	-5473.56	31.5329	0.001483	9951.89	9951.95	-3508.9619	33.753917	0	6379.93	6379.93	-1964.60	-2.22	0.00	3571.96	3572.02
8037	48.64	41.53	-16174.8	-1059.9	-533.436	39989.22	18828.12	-1782.4207	-704.0346	-71.51	4659.22	1822.31	-14392.35	-355.90	-461.92	35330.00	17005.81
8043	48.63	41.57	-16243	-1034.7	-577.386	40985.06	18080.50	-1806.4066	-694.83127	-100.9	5286.25	1282.50	-14436.62	-339.91	-476.46	35698.81	16798.00
8042	48.63	41.61	-16322.2	-1014.2	-620.594	41986.07	17367.45	-1830.3184	-685.78291	-130	5905.63	750.08	-14491.90	-328.46	-490.63	36080.45	16617.37
8041	48.63	41.66	-16398.2	-977.43	-662.493	42955.28	16674.55	-1855.0776	-677.66086	-158.6	6519.46	226.27	-14543.13	-299.77	-503.85	36435.82	16448.28
8053	48.62	41.7	-16456.9	-903.33	-702.243	43850.35	15992.77	-1881.6055	-671.23643	-187	7130.06	-287.86	-14575.25	-232.09	-515.25	36720.29	16280.62
8053	48.62	41.7	-16459.8	-912.6	-702.243	43855.77	15998.19	-1883.4406	-677.25788	-187	7133.40	-284.52	-14576.40	-235.35	-515.25	36722.38	16282.71
8056	48.62	41.74	-16493.9	-839.18	-739.08	44648.28	15329.41	-1916.3113	-678.80777	-215.5	7759.03	-790.63	-14577.55	-160.37	-523.56	36889.25	16120.04
8055	48.62	41.78	-16531.8	-762.79	-772.797	45385.98	14729.59	-1944.2285	-677.95049	-244.1	8375.72	-1305.80	-14587.55	-84.84	-528.74	37010.26	16035.38
8054	48.61	41.82	-16560.5	-681.63	-803.192	46041.16	14178.99	-1967.9219	-677.14702	-272.6	8984.28	-1828.20	-14592.62	-4.48	-530.63	37056.88	16007.19
8079	48.61	41.87	-16567.1	-593.93	-830.04	46585.60	13658.38	-1988.1211	-678.85833	-301.1	9586.15	-2356.62	-14578.97	84.93	-528.98	36999.44	16015.00
8079	48.61	41.87	-16579.9	-584.24	-830.04	46608.92	13681.70	-1989.6339	-677.13402	-301.1	9588.90	-2353.87	-14590.29	92.90	-528.98	37020.02	16035.57
8082	48.6	41.91	-16523.1	-486.66	-852.379	46948.59	13135.23	-2014.0095	-671.58142	-329.4	10195.48	-2871.81	-14509.04	184.92	-522.97	36753.11	16007.03
8081	48.6	41.95	-16497.3	-438.66	-871.676	47284.59	12705.70	-2038.6374	-667.3836	-357.6	10798.98	-3385.75	-14458.69	228.73	-514.10	36485.61	16091.45
8080	48.59	41.99	-16510.3	-438.74	-889.959	47670.80	12366.64	-2063.0523	-662.9875	-385.6	11398.35	-3896.34	-14447.24	224.24	-504.41	36272.45	16262.98
8673	48.58	42.03	-16569.5	-485.44	-909.233	48160.71	12091.95	-2086.7891	-656.84005	-413.3	11992.16	-4403.83	-14482.69	171.40	-495.92	36168.55	16495.78
8673	48.58	42.03	-16496	-369.52	-909.233	48027.08	11958.32	-2087.3327	-657.67176	-413.3	11993.14	-4402.84	-14408.65	288.15	-495.92	36033.93	16361.16
8676	48.58	42.07	-16572.3	-493.73	-927.876	48535.52	11727.23	-2109.5918	-648.85053	-440.8	12578.55	-4907.31	-14462.66	155.12	-487.09	35956.97	16634.54
8675	48.57	42.12	-16619.3	-530.81	-949.42	49048.40	11385.46	-2131.3724	-639.07654	-467.9	13155.55	-5405.10	-14487.94	108.26	-481.54	35892.85	16790.56
8674	48.56	42.16	-16653.4	-532.82	-972.046	49559.23	10998.71	-2152.5825	-628.44654	-494.5	13723.00	-5895.43	-14500.85	95.63	-477.50	35836.23	16894.14
9049	48.56	42.2	-16690.9	-551.8	-994.604	50074.79	10619.43	-2173.1302	-617.05726	-520.7	14279.82	-6377.53	-14517.78	65.25	-473.87	35794.96	16996.96
9049	48.56	42.2	-16701.5	-564.3	-994.604	50094.04	10638.68	-2173.1798	-617.28201	-520.7	14279.91	-6377.44	-14528.32	52.98	-473.87	35814.13	17016.13
9055	48.55	42.24	-16757.6	-596.89	-1019.02	50680.21	10256.41	-2193.2888	-605.76391	-546.5	14826.54	-6850.95	-14564.28	8.87	-472.56	35853.66	17107.36
9054	48.54	42.28	-16819	-630.47	-1044.83	51303.94	9856.24	-2213.0804	-593.9798	-571.7	15363.10	-7315.53	-14605.97	-36.49	-473.14	35940.84	17171.77
9053	48.53	42.32	-16888.8	-665.51	-1072.08	51971.44	9442.51	-2232.5204	-581.88616	-596.4	15889.05	-7770.79	-14656.32	-83.62	-475.66	36082.39	17213.31
9285	48.52	42.36	-16969.8	-702.47	-1100.84	52689.06	9019.46	-2251.5746	-569.4395	-620.6	16403.86	-8216.32	-14718.27	-133.03	-480.20	36285.19	17235.78
9285	48.52	42.36	-16935.9	-686.47	-1100.84	52627.36	8957.76	-2251.6831	-569.3194	-620.6	16404.06	-8216.12	-14684.22	-117.15	-480.20	36223.30	17173.88
9288	48.52	42.4	-17071.5	-743.34	-1130.92	53470.63	8607.60	-2270.3491	-556.96598	-644.3	16907.74	-8651.92	-14801.16	-186.38	-486.61	36562.89	17259.52
9287	48.51	42.45	-17203.4	-792.03	-1163.26	54351.80	8206.03	-2288.8317	-544.03497	-667.5	17400.73	-9077.71	-14914.57	-248.00	-495.78	36951.07	17283.74
9286	48.5	42.49	-17330.2	-830.75	-1197.42	55259.98	7758.93	-2307.2354	-530.52322	-690.1	17882.55	-9492.61	-15022.96	-300.22	-507.34	37377.42	17251.53
9301	48.49	42.53	-17450.5	-857.71	-1232.97	56183.85	7272.62	-2325.6645	-516.4276	-712.1	18352.71	-9895.75	-15124.86	-341.28	-520.87	37831.13	17168.37

After EQ								Before EQ					Difference in forces			Difference in stress	
						Normal stress at extrados	Normal stress at inttrados				Normal stress at extrados	Normal stress at inttrados					
Node	X	Y	N	Q	M	σ_{ex} = N/t+6M/t^2	σ_{in} = N/t+6M/t^2	N	Q	M	σ_{ex} = N/t+6M/t^2	σ_{in} = N/t+6M/t^2	N	Q	M	σ_{ex}	σ_{in}
	[m]	[m]	[kN/m]	[kN/m]	[kNm/m]	[kN/m^2]	[kN/m^2]	[kN/m]	[kN/m]	[kNm/m]	[kN/m^2]	[kN/m^2]	[kN/m]	[kN/m]	[kNm/m]	[kN/m^2]	[kN/m^2]
9301	48.49	42.53	-17429.3	-822.16	-1232.97	56145.28	7234.04	-2325.8113	-513.63214	-712.1	18352.98	-9895.49	-15103.50	-308.53	-520.87	37792.29	17129.53
9304	48.48	42.57	-17532.1	-819.42	-1267.65	57020.09	6732.99	-2343.3537	-503.79874	-733.5	18809.29	-10288.00	-15188.74	-315.62	-534.16	38210.80	17021.00
9303	48.47	42.61	-17618.2	-788.27	-1301.46	57847.03	6219.04	-2360.1104	-492.10718	-754.5	19255.42	-10673.20	-15258.06	-296.16	-547.00	38591.61	16892.24
9302	48.46	42.65	-17698.7	-747.73	-1333.85	58635.83	5722.95	-2376.1154	-478.24527	-774.9	19689.50	-11049.08	-15322.55	-269.48	-558.98	38946.32	16772.03
9327	48.45	42.69	-17784.7	-716.8	-1364.54	59401.00	5270.66	-2391.4032	-461.90079	-794.6	20109.57	-11413.55	-15393.30	-254.90	-569.89	39291.43	16684.21
9327	48.45	42.69	-17775.4	-709.04	-1364.54	59384.04	5253.70	-2391.354	-463.12517	-794.6	20109.48	-11413.64	-15384.03	-245.91	-569.89	39274.56	16667.35
9330	48.43	42.73	-17867.4	-676.31	-1393.63	60128.59	4843.89	-2406.5286	-449.21501	-813.8	20517.69	-11766.68	-15460.90	-227.09	-579.80	39610.89	16610.57
9329	48.42	42.77	-17945.4	-652.95	-1421.55	60824.06	4431.81	-2420.9896	-434.32405	-832.4	20912.54	-12108.94	-15524.38	-218.63	-589.14	39911.52	16540.75
9328	48.41	42.81	-18026.6	-640.15	-1448.72	61510.59	4040.70	-2434.7628	-419.56692	-850.4	21293.88	-12440.20	-15591.84	-220.58	-598.34	40216.71	16480.90
9923	48.4	42.85	-18128.6	-639.08	-1475.57	62228.57	3693.51	-2447.8739	-406.05828	-867.7	21661.87	-12760.51	-15680.70	-233.02	-607.84	40566.70	16454.02
9923	48.4	42.85	-18103.3	-636.98	-1475.57	62182.67	3647.61	-2447.9931	-406.69289	-867.7	21662.09	-12760.29	-15655.33	-230.29	-607.84	40520.58	16407.90
9926	48.39	42.89	-18207.2	-642.64	-1502.52	62906.11	3302.03	-2459.6986	-391.71893	-884.5	22016.38	-13072.02	-15747.54	-250.93	-618.00	40889.73	16374.05
9925	48.37	42.93	-18279.6	-643.99	-1529.55	63573.91	2897.51	-2470.3887	-376.1114	-900.7	22356.21	-13372.97	-15809.25	-267.88	-628.88	41217.70	16270.48
9924	48.36	42.97	-18329.8	-648.9	-1556.75	64204.70	2449.20	-2480.3971	-359.85381	-916.2	22681.50	-13661.88	-15849.42	-289.05	-640.60	41523.20	16111.07
10323	48.35	43.01	-18367.1	-665.24	-1584.32	64819.13	1970.24	-2490.0575	-342.92968	-930.9	22992.20	-13937.44	-15877.02	-322.31	-653.38	41826.93	15907.69
10323	48.35	43.01	-18385	-665.18	-1584.32	64851.80	2002.91	-2490.704	-342.85029	-930.9	22993.37	-13936.27	-15894.34	-322.33	-653.38	41858.42	15939.18
10326	48.33	43.05	-18469.9	-677.83	-1612.52	65565.61	1597.73	-2499.6018	-326.11016	-945	23288.56	-14199.10	-15970.32	-351.72	-667.52	42277.05	15796.83
10325	48.32	43.09	-18526.4	-695.12	-1641.41	66241.19	1127.46	-2508.1823	-309.00674	-958.4	23569.16	-14448.49	-16018.20	-386.11	-683.05	42672.04	15575.96
10324	48.31	43.13	-18582.5	-713.4	-1671.02	66930.56	642.04	-2516.5365	-291.59257	-971	23834.95	-14683.91	-16065.93	-421.81	-700.03	43095.61	15325.95
10903	48.29	43.17	-18666.2	-729.04	-1701.37	67684.82	192.31	-2524.7554	-273.92016	-982.9	24085.74	-14904.82	-16141.46	-455.12	-718.49	43599.07	15097.13
10903	48.29	43.17	-18640.1	-721.17	-1701.37	67637.37	144.87	-2524.6847	-273.97424	-982.9	24085.62	-14904.94	-16115.43	-447.19	-718.49	43551.75	15049.81
10906	48.28	43.21	-18719.6	-754.57	-1732.5	68399.35	-328.01	-2532.8573	-256.26375	-994	24321.62	-15111.23	-16186.76	-498.31	-738.47	44077.73	14783.22
10905	48.26	43.25	-18803.7	-770.22	-1764.57	69188.26	-811.34	-2540.6379	-238.40794	-1004	24542.15	-15303.47	-16263.02	-531.82	-760.13	44646.11	14492.13
10904	48.25	43.29	-18899.7	-778.82	-1797.21	70010.10	-1284.09	-2548.0207	-220.42976	-1014	24747.02	-15481.49	-16351.63	-558.39	-783.11	45263.08	14197.40
11008	48.23	43.33	-19015	-791.03	-1830.16	70873.57	-1727.94	-2555	-202.35218	-1023	24936.03	-15645.12	-16460.05	-588.68	-807.18	45937.55	13917.18
11008	48.23	43.33	-18885.3	-749.88	-1830.16	70637.74	-1963.77	-2554.9584	-202.29905	-1023	24935.95	-15645.19	-16330.38	-547.58	-807.18	45701.78	13681.42
11011	48.21	43.37	-18990.6	-809.69	-1863.15	71483.48	-2426.76	-2562.526	-184.23122	-1031	25110.91	-15792.64	-16428.07	-625.46	-832.04	46372.57	13365.88
11010	48.2	43.4	-19049.4	-832.65	-1897.71	72275.78	-3005.27	-2569.7513	-166.03471	-1038	25270.20	-15925.65	-16479.64	-666.62	-859.23	47005.58	12920.38
11009	48.18	43.44	-19058.4	-838.6	-1932.97	72991.51	-3688.39	-2576.6145	-147.67831	-1045	25413.57	-16044.06	-16481.74	-690.92	-887.89	47577.94	12355.67
11581	48.16	43.48	-19014.1	-847.36	-1968.34	73612.60	-4470.26	-2583.0957	-129.13083	-1051	25540.81	-16147.73	-16431.05	-718.23	-917.44	48071.79	11677.47
11581	48.16	43.48	-19027.2	-827.55	-1968.34	73636.24	-4446.60	-2583.0336	-130.29508	-1051	25540.70	-16147.85	-16444.12	-697.26	-917.44	48095.55	11701.24
11584	48.15	43.52	-18947.2	-843.06	-2003.51	74188.58	-5289.63	-2589.6036	-109.80761	-1056	25652.48	-16235.74	-16357.61	-733.25	-947.58	48536.10	10946.11
11583	48.13	43.56	-18859.7	-846.44	-2039.08	74734.98	-6154.16	-2595.7363	-93.110609	-1060	25748.07	-16309.03	-16263.99	-753.33	-978.89	48986.91	10154.88
11582	48.11	43.6	-18768.5	-839.76	-2074.59	75273.38	-7024.34	-2601.2773	-79.779834	-1064	25830.03	-16370.84	-16167.21	-759.98	-1010.77	49443.35	9346.49
12093	48.09	43.63	-18677.3	-825.08	-2109.61	75802.22	-7884.88	-2606.0724	-69.391037	-1067	25900.78	-16424.15	-16071.20	-755.69	-1042.67	49901.44	8539.28
7893	48.48	39.84	-14403.9	-656.98	466.7277	16931.56	35446.38	-2652.8388	-65.617397	585.64	-6792.74	16439.42	-11751.09	-591.36	-118.92	23724.30	19006.95
7853	48.49	39.88	-14441.2	-563.14	440.8575	17512.40	35000.96	-2630.1559	-75.323273	582.65	-6774.51	16338.72	-11811.02	-487.81	-141.79	24286.92	18662.25
7852	48.5	39.92	-14450.1	-489.36	418.4726	17972.54	34573.11	-2605.9445	-85.815614	579.22	-6750.57	16226.73	-11844.11	-403.54	-160.75	24723.11	18346.38
7851	48.51	39.97	-14437	-427.99	399.0028	18335.07	34163.28	-2581.5028	-97.392293	575.32	-6717.70	16104.98	-11855.54	-330.60	-176.32	25052.77	18058.30
7857	48.52	40.01	-14408.6	-371.38	381.9784	18621.08	33773.94	-2558.1291	-110.35118	570.91	-6672.61	15974.90	-11850.50	-261.03	-188.93	25293.69	17799.04
7857	48.52	40.01	-14417.3	-366.47	381.9784	18636.90	33789.77	-2561.4336	-110.39928	570.91	-6666.60	15980.91	-11855.90	-256.07	-188.93	25303.51	17808.86
7863	48.53	40.05	-14369.7	-338.06	366.9427	18848.61	33405.01	-2539.7661	-115.37255	566.17	-6611.97	15847.49	-11829.98	-222.69	-199.22	25460.58	17557.53
7862	48.54	40.09	-14329.2	-308.13	353.237	19046.79	33059.50	-2517.6496	-128.27651	560.94	-6548.63	15703.72	-11811.58	-179.85	-207.71	25595.42	17355.78
7861	48.55	40.13	-14296.1	-286.24	340.5855	19237.48	32748.31	-2497.1858	-139.05702	555.27	-6473.29	15553.96	-11798.90	-147.19	-214.68	25710.76	17194.34
7867	48.55	40.17	-14270.6	-281.99	328.5889	19429.14	32464.07	-2480.4763	-137.65994	549.3	-6385.26	15405.18	-11790.15	-144.33	-220.71	25814.40	17058.89
7867	48.55	40.17	-14240.1	-270.3	328.5889	19373.55	32408.48	-2475.4122	-150.51101	549.3	-6394.47	15395.97	-11764.65	-119.79	-220.71	25768.02	17012.51
7873	48.56	40.22	-14229.3	-278.98	316.841	19586.94	32155.84	-2455.5592	-168.21216	542.52	-6296.16	15225.47	-11773.71	-110.76	-225.68	25883.10	16930.37
7872	48.57	40.26	-14224.1	-283.32	304.9228	19813.99	31910.09	-2434.3669	-187.99574	534.95	-6184.40	15036.65	-11789.76	-95.32	-230.02	25998.39	16873.45
7871	48.58	40.3	-14237.7	-294.8	292.6096	20082.88	31690.53	-2411.6581	-209.92826	526.48	-6057.79	14827.45	-11826.03	-84.87	-233.87	26140.66	16863.08
8263	48.58	40.34	-14283	-324.9	279.5279	20424.77	31513.48	-2387.2555	-234.07629	517.04	-5914.87	14595.80	-11895.76	-90.82	-237.51	26339.65	16917.68
8263	48.58	40.34	-14268	-307.35	279.5279	20397.38	31486.09	-2382.5877	-236.94404	517.04	-5923.36	14587.31	-11885.37	-70.41	-237.51	26320.74	16898.77
8266	48.59	40.38	-14309.3	-342.05	265.6518	20747.79	31286.04	-2369.6303	-252.9023	506.63	-5740.40	14357.24	-11939.67	-89.15	-240.98	26488.19	16928.80
8265	48.59	40.43	-14357.5	-369.53	250.5225	21135.54	31073.62	-2348.0956	-273.05885	495.45	-5557.75	14096.28	-12009.42	-96.47	-244.92	26693.29	16977.34
8264	48.6	40.47	-14410.6	-397.72	234.1682	21556.51	30845.83	-2318.0189	-297.71574	483.31	-5371.68	13800.84	-12092.62	-100.00	-249.14	26928.19	17044.99
8276	48.61	40.51	-14466.7	-434.54	216.5141	22008.66	30597.65	-2279.4358	-327.17503	470.03	-5178.39	13467.25	-12187.30	-107.36	-253.51	27187.05	17130.40
8276	48.61	40.51	-14455.1	-418.17	216.5141	21987.43	30576.42	-2297.6421	-310.83797	470.03	-5145.29	13500.35	-12157.42	-107.34	-253.51	27132.72	17076.07
8275	48.61	40.55	-14530.3	-465.41	197.5899	22499.64	30337.91	-2268.9981	-326.47341	456.45	-4928.13	13179.04	-12261.33	-138.94	-258.86	27427.77	17158.88
8274	48.62	40.6	-14593.1	-490.32	177.2257	23017.70	30048.14	-2240.7624	-341.5366	442.24	-4697.55	12845.78	-12352.35	-148.79	-265.01	27715.25	17202.37
8273	48.62	40.64	-14649.3	-503.7	155.992	23540.98	29729.09	-2211.9022	-358.05482	427.34	-4454.56	12497.84	-12437.37	-145.65	-271.35	27995.54	17231.25
8283	48.62	40.68	-14704.7	-516.34	134.3185	24071.60	29399.93	-2181.3845	-378.05538	411.69	-4199.68	12131.99	-12523.29	-138.29	-277.38	28271.28	17267.94
8283	48.62	40.68	-14725.7	-524.29	134.3186	24109.83	29438.17	-2184.7604	-373.42415	411.69	-4193.55	12138.13	-12540.94	-150.87	-277.38	28303.38	17300.04
8289	48.63	40.72	-14761.6	-517.55	112.2635	24612.55	29065.98	-2153.1599	-392.85695	395.39	-3927.57	11757.24	-12608.44	-124.70	-283.12	28540.12	17308.74
8288	48.63	40.76	-14810.9	-534.72	89.88463	25146.11	28711.78	-2122.807	-413.80363	378.22	-3642.26	11361.56	-12688.11	-120.91	-288.34	28788.37	17350.22
8287	48.63	40.81	-14867.3	-566.26	66.51744	25712.12	28350.83	-2094.7717	-436.9423	360.11	-3334.05	10951.41	-12772.54	-129.32	-293.60	29046.17	17399.42
8467	48.64	40.85	-14924.4	-602.66	41.62056	26309.75	27960.81	-2070.124	-462.95109	340.97	-2999.22	10526.94	-12854.28	-139.71	-299.35	29308.97	17433.87
8467	48.64	40.85	-14923.2	-597.79	41.6206	26307.63	27958.69	-2077.3489	-443.51878	340.97	-2986.08	10540.08	-12845.89	-154.28	-299.35	29293.71	17418.61
8453	48.64	40.89	-14990.8	-635.49	15.35922	26951.29	27560.58	-2043.1796	-473.74318	321.39	-2659.82	10089.57	-12947.59	-161.74	-306.03	29611.11	17471.02
8452	48.64	40.93	-15061.8	-670.04	-12.448	27632.08	27138.28	-2016.4567	-494.65391	300.78	-2299.60	9632.17	-13045.39	-175.38	-313.23	29931.69	17506.11
8451	48.64	40.98	-15136.6	-701.86	-41.6698	28347.68	26694.67	-1994.8785	-513.23669	279.29	-1912.66	9166.76	-13141.77	-188.62	-320.96	30260.34	17527.91
8457	48.64	41.02	-15215.3	-731.35	-72.1808	29095.89	26232.51	-1976.143	-536.47723	256.99	-1504.41	8690.38	-13239.17	-194.88	-329.17	30600.29	17542.13
8457	48.64	41.02	-15212.5	-726.5	-72.1808	29090.75	26227.38	-1972.7446	-537.83063	256.99	-1510.59	8684.20	-13239.74	-188.67	-329.17	30601.34	17543.18
8463	48.65	41.06	-15282.3	-764.2	-103.925	29847.37	25724.73	-1951.3852	-562.39445	233.58	-1085.05	8181.00	-13330.94	-201.81	-337.51	30932.43	17543.73
8462	48.65	41.1	-15359.4	-797.59	-137.194	30647.36	25204.97	-1930.2785	-586.47678	209.11	-637.96	7657.15	-13429.11	-211.12	-346.30	31285.32	17547.82
8461	48.65	41.15	-15435.9	-826.98	-171.8	31472.80	24657.60	-1909.9806	-608.23555	183.66	-170.23	7115.61	-13525.88	-218.75	-355.46	31643.03	17541.99
8477	48.65	41.19	-15503.9	-852.69	-207.562	32305.87	24072.02	-1891.0475	-625.82873	157.38	316.75	6559.79	-13612.87	-226.86	-364.94	31989.12	17512.23

After EQ								Before EQ					Difference in forces			Difference in stress	
						Normal stress at extrados	Normal stress at inttrados				Normal stress at extrados	Normal stress at inttrados					
Node	X	Y	N	Q	M	σ_{ex} = N/t+6M/t^2	σ_{in} = N/t+6M/t^2	N	Q	M	σ_{ex} = N/t+6M/t^2	σ_{in} = N/t+6M/t^2	N	Q	M	σ_{ex}	σ_{in}
	[m]	[m]	[kN/m]	[kN/m]	[kNm/m]	[kN/m^2]	[kN/m^2]	[kN/m]	[kN/m]	[kNm/m]	[kN/m^2]	[kN/m^2]	[kN/m]	[kN/m]	[kNm/m]	[kN/m^2]	[kN/m^2]
8477	48.65	41.19	-15508.5	-845.44	-207.562	32314.25	24080.39	-1888.5286	-627.33944	157.38	312.17	6555.21	-13620.00	-218.10	-364.94	32002.08	17525.18
8483	48.65	41.23	-15546.7	-856.95	-243.72	33100.90	23432.65	-1873.2999	-644.39314	130.3	821.54	5990.46	-13673.43	-212.56	-374.02	32279.36	17442.19
8482	48.65	41.28	-15595.9	-882.43	-280.75	33924.84	22787.67	-1855.7847	-659.4173	102.53	1340.41	5407.90	-13740.16	-223.01	-383.28	32584.44	17379.76
8481	48.65	41.32	-15651.5	-914.93	-318.978	34784.01	22130.36	-1834.4328	-673.11641	74.155	1864.49	4806.18	-13817.02	-241.82	-393.13	32919.52	17324.18
8493	48.64	41.36	-15708.5	-947.52	-358.643	35674.55	21447.40	-1807.6939	-686.19495	45.224	2389.71	4183.72	-13900.84	-261.32	-403.87	33284.85	17263.68
8493	48.64	41.36	-15705.9	-958.42	-358.643	35669.73	21442.58	-1815.6883	-683.79679	45.224	2404.24	4198.26	-13890.20	-274.62	-403.87	33265.49	17244.32
8033	48.64	41.4	-15820.7	-985.14	-399.743	36693.66	20836.11	-1790.4494	-688.63092	16.001	2937.98	3572.74	-14030.24	-296.51	-415.74	33755.68	17263.37
8032	48.64	41.45	-15953.3	-1039.1	-443.031	37793.38	20218.59	-1774.6221	-689.0229	-13.35	3491.46	2961.71	-14178.67	-350.11	-429.68	34301.92	17256.88
8031	48.64	41.49	-16075.2	-1073.9	-487.975	38906.51	19548.84	-1777.5683	-684.06498	-42.61	4077.06	2386.83	-14297.65	-389.88	-445.37	34829.45	17162.01
8037	48.64	41.53	-16158	-1043.1	-533.436	39958.72	18797.62	-1808.6495	-672.84942	-71.51	4706.90	1870.00	-14349.34	-370.28	-461.92	35251.81	16927.62
5613	47.91	37.5	-2991.78	1214.33	-1405.51	33317.45	-22438.26	-3745.7034	1892.5607	-1168	29979.89	-16359.15	753.93	-678.23	-237.38	3337.56	-6079.11
5619	47.92	37.55	-2989.15	1248.11	-1352.45	32260.27	-21390.61	-3739.0918	1817.2573	-1088	28386.56	-14789.86	749.94	-569.15	-264.04	3873.71	-6600.75
5618	47.93	37.59	-3029.69	1256.03	-1298.63	31266.39	-20249.33	-3727.8088	1740.817	-1012	26849.27	-13293.61	698.12	-484.79	-286.69	4417.12	-6955.72
5617	47.94	37.63	-3104.01	1254.03	-1244.59	30329.80	-19042.47	-3713.1944	1666.0442	-938.7	25370.09	-11867.56	609.18	-412.01	-305.89	4959.71	-7174.91
6141	47.95	37.67	-3202.75	1258.04	-1190.7	29440.33	-17793.97	-3696.5888	1595.7433	-868.6	23950.35	-10508.21	493.84	-337.70	-322.06	5489.98	-7285.76
6141	47.95	37.67	-3195.93	1249.92	-1190.7	29427.93	-17806.37	-3697.3209	1596.1227	-868.6	23951.68	-10506.88	501.39	-346.21	-322.06	5476.25	-7299.49
6144	47.96	37.71	-3359.97	1291.45	-1135.94	28640.01	-16421.95	-3681.0241	1530.5501	-801.5	22589.94	-9204.39	321.06	-239.10	-334.46	6050.08	-7217.56
6143	47.97	37.75	-3571.26	1334.53	-1079.76	27910.03	-14923.62	-3664.0249	1470.3498	-737	21279.92	-7956.19	92.76	-135.82	-342.77	6630.11	-6967.43
6142	47.98	37.8	-3836.82	1423.26	-1020.54	27218.05	-13265.99	-3646.4597	1415.3932	-675	20017.96	-6758.11	-190.36	7.86	-345.55	7200.09	-6507.88
6161	47.99	37.84	-4163.63	1601.75	-956.023	26532.67	-11392.20	-3628.4654	1365.5514	-615.2	18800.45	-5606.03	-535.16	236.20	-340.78	7732.22	-5786.17
6161	47.99	37.84	-4114.14	1592.84	-956.023	26442.69	-11482.18	-3628.56	1365.207	-615.2	18800.62	-5605.86	-485.58	227.63	-340.78	7642.07	-5876.32
6167	48	37.88	-4462.18	1696.39	-885.647	25679.60	-9453.51	-3611.3487	1325.8746	-557.5	17623.07	-4490.90	-850.83	370.51	-328.19	8056.53	-4962.61
6166	48.01	37.92	-4784.07	1818.87	-809.769	24759.84	-7363.21	-3594.4657	1293.5324	-501.2	16475.86	-3405.08	-1189.61	525.34	-308.60	8283.98	-3958.13
6165	48.02	37.96	-5069.47	1898.21	-729.871	23694.00	-5259.57	-3578.0229	1266.6191	-446.2	15354.86	-2343.87	-1491.45	631.59	-283.72	8339.15	-2915.70
7005	48.03	38	-5308	1872.32	-648.252	22508.80	-3206.97	-3562.1321	1243.5734	-392.2	14256.36	-1303.15	-1745.87	628.75	-256.02	8252.44	-1903.82
7005	48.03	38	-5296.79	1845.8	-648.252	22488.41	-3227.37	-3561.5061	1241.8209	-392.2	14255.22	-1304.29	-1735.28	603.98	-256.02	8233.19	-1923.08
7011	48.04	38.05	-5734.15	1868.91	-568.108	21693.99	-842.52	-3545.1349	1217.3973	-339.4	13177.19	-285.79	-2189.02	651.51	-228.73	8516.80	-556.73
7010	48.05	38.09	-6103.53	1844.64	-488.378	20784.16	1410.48	-3527.6665	1189.7963	-287.6	12118.84	709.04	-2575.86	654.85	-200.76	8665.32	701.45
7009	48.06	38.13	-6473.45	1816.37	-409.555	19893.32	3646.50	-3509.2537	1158.842	-237.1	11083.74	1677.18	-2964.20	657.52	-172.43	8809.58	1969.32
7515	48.07	38.17	-6912.47	1827.44	-331.565	19144.63	5991.64	-3490.0494	1124.3581	-188.1	10075.53	2615.56	-3422.42	703.08	-143.51	9069.09	3376.09
7515	48.07	38.17	-6769.87	1698.02	-331.565	18885.35	5732.36	-3490.3747	1124.5192	-188.1	10076.12	2616.15	-3279.50	573.50	-143.51	8809.22	3116.22
7518	48.08	38.21	-7252.94	1708.01	-257.733	18299.22	8075.11	-3470.4509	1089.1875	-140.5	9096.22	3523.60	-3782.49	618.82	-117.26	9203.00	4551.50
7517	48.09	38.25	-7660.61	1595.24	-186.638	17630.28	10226.47	-3449.8385	1049.8422	-94.48	8146.41	4398.46	-4210.77	545.39	-92.16	9483.87	5828.02
7516	48.1	38.3	-7939.38	1416.73	-121.509	16845.34	12025.14	-3428.124	1006.1484	-50.27	7230.02	5235.89	-4511.26	410.58	-71.24	9615.32	6789.26
7528	48.11	38.34	-8035.76	1229.51	-64.8317	15896.39	13324.56	-3404.8938	957.7708	-8.054	6350.47	6030.97	-4630.87	271.74	-56.78	9545.93	7293.59
7528	48.11	38.34	-8241.81	1324.56	-64.8317	16271.03	13699.19	-3405.765	958.66801	-8.054	6352.05	6032.55	-4836.05	365.89	-56.78	9918.98	7666.64
7527	48.12	38.38	-8605.08	1168.32	-12.3647	15890.84	15400.34	-3382.6764	913.2845	32.168	5512.28	6788.36	-5222.40	255.03	-44.53	10378.56	8611.98
7526	48.13	38.42	-9016.2	1182.21	38.36382	15632.16	17154.03	-3359.1343	869.16741	70.47	4709.77	7505.27	-5657.07	313.04	-32.11	10922.39	9648.76
7525	48.14	38.46	-9368.24	1234.18	89.83187	15251.38	18814.95	-3335.9503	827.70364	106.94	3944.23	8186.49	-6032.29	406.48	-17.11	11307.14	10628.46
7621	48.15	38.51	-9554.24	1192.2	142.7882	14539.18	20203.51	-3313.9358	790.28012	141.68	3215.06	8835.61	-6240.31	401.92	1.10	11324.12	11367.90
7621	48.15	38.51	-9503.21	1061.16	142.7883	14446.40	20110.72	-3312.4664	789.80281	141.68	3212.39	8832.94	-6190.74	271.36	1.10	11234.00	11277.78
7624	48.16	38.55	-9866.55	1095.1	189.3942	14182.60	21695.76	-3290.3187	761.31374	174.99	2511.45	9453.35	-6576.23	333.79	14.40	11671.15	12242.41
7623	48.17	38.59	-10146.6	1073.5	236.0803	13765.69	23130.86	-3267.5381	734.54795	207.16	1831.96	10050.00	-6879.01	338.96	28.92	11933.73	13080.86
7622	48.18	38.63	-10361.4	1017.4	281.2045	13261.27	24416.49	-3243.884	706.1265	238.13	1174.74	10621.20	-7117.50	311.27	43.08	12086.53	13795.29
7634	48.19	38.67	-10529.2	947.823	323.3998	12729.49	25558.57	-3219.1155	672.67047	267.78	541.50	11164.37	-7310.10	275.15	55.62	12187.98	14394.20
7634	48.19	38.67	-10622.6	973.339	323.3998	12899.33	25728.42	-3218.6348	673.21806	267.78	540.63	11163.50	-7404.00	300.12	55.62	12358.70	14564.92
7633	48.2	38.71	-10783.3	906.239	363.7823	12390.50	26821.54	-3193.0921	631.07142	295.79	-61.35	11672.59	-7590.22	275.17	67.99	12451.85	15148.95
7632	48.22	38.76	-10934.8	840.934	401.3263	11921.18	27841.56	-3168.1299	591.28385	322.07	-627.98	12148.45	-7766.63	249.65	79.25	12549.16	15693.11
7631	48.23	38.8	-11079.1	778.44	436.1296	11493.38	28794.39	-3143.3582	551.76921	346.64	-1160.27	12590.66	-7935.78	226.67	89.49	12653.64	16203.73
7657	48.24	38.84	-11218.6	719.773	468.3026	11108.85	29686.14	-3118.3872	510.44137	369.47	-1658.63	12998.22	-8100.23	209.33	98.83	12767.47	16687.92
7657	48.24	38.84	-11227.2	709.891	468.3026	11124.48	29701.77	-3117.6721	513.35189	369.47	-1659.93	12996.92	-8109.54	196.54	98.83	12784.40	16704.85
7643	48.25	38.88	-11359.2	669.272	497.9786	10775.83	30530.35	-3095.7076	491.99677	391.09	-2128.54	13385.66	-8263.49	177.28	106.89	12904.37	17144.69
7642	48.26	38.92	-11497.6	619.885	525.702	10477.65	31331.94	-3073.3273	466.63981	411.71	-2578.34	13754.08	-8424.31	153.25	113.99	13055.99	17577.87
7641	48.27	38.96	-11638.7	564.879	551.1985	10228.33	32094.06	-3050.3751	436.49406	431.14	-3005.44	14097.72	-8588.28	128.39	120.06	13233.78	17996.34
7647	48.28	39.01	-11778.4	507.403	574.2345	10025.45	32805.00	-3026.6946	400.77254	449.15	-3405.77	14411.93	-8751.68	106.63	125.08	13431.22	18393.07
7647	48.28	39.01	-11773.5	510.723	574.2345	10016.67	32796.22	-3026.6145	403.9754	449.15	-3405.91	14411.79	-8746.93	106.75	125.08	13422.58	18384.43
7653	48.29	39.05	-11922.2	445.833	594.7624	9879.86	33473.74	-3000.6941	371.27818	465.76	-3782.40	14694.02	-8921.55	74.55	129.00	13662.26	18779.72
7652	48.3	39.09	-12066.3	383.316	612.6045	9787.87	34089.54	-2976.0296	344.34299	481.17	-4132.99	14954.91	-9090.26	38.97	131.43	13920.86	19134.63
7651	48.31	39.13	-12206	318.638	627.6905	9742.75	34642.87	-2951.9831	314.65256	495.33	-4457.45	15191.94	-9254.06	3.99	132.36	14200.21	19450.93
7673	48.32	39.17	-12341.9	247.265	639.8899	9747.73	35131.79	-2927.9169	273.68966	508.04	-4753.36	15400.33	-9413.95	-26.42	131.85	14501.10	19731.46
7673	48.32	39.17	-12338.4	261.645	639.8899	9741.48	35125.54	-2926.8919	278.63219	508.04	-4755.23	15398.47	-9411.54	-16.99	131.85	14496.70	19727.06
7669	48.33	39.21	-12499.1	172.477	649.1023	9850.84	35600.35	-2908.1297	261.7203	519.65	-5019.51	15594.53	-9590.95	-89.24	129.46	14870.35	20005.82
7668	48.34	39.26	-12640.9	102.134	655.0174	9991.45	35975.61	-2889.5801	243.53562	530.53	-5269.09	15776.65	-9751.36	-141.40	124.49	15260.53	20198.96
7667	48.35	39.3	-12776	37.5464	657.9667	10178.44	36279.59	-2871.0321	221.32443	540.53	-5501.16	15941.28	-9904.93	-183.78	117.44	15679.60	20338.31
7689	48.36	39.34	-12916.1	-34.359	658.1091	10430.37	36537.18	-2852.2748	192.33298	549.45	-5712.24	16084.14	-10063.80	-226.69	108.66	16142.60	20453.03
7689	48.36	39.34	-12909.9	-16.547	658.1091	10419.12	36525.93	-2849.3378	191.55862	549.45	-5717.58	16078.80	-10060.55	-208.11	108.66	16136.69	20447.12
7685	48.37	39.38	-13066.9	-108.48	655.2777	10760.79	36755.28	-2829.2078	171.63963	557.29	-5909.66	16197.69	-10237.71	-280.12	97.99	16670.45	20557.59
7684	48.38	39.42	-13205.5	-174.87	649.1847	11133.62	36886.40	-2810.0461	148.1862	564.14	-6080.36	16298.71	-10395.46	-323.06	85.05	17213.98	20587.68
7683	48.39	39.47	-13335.4	-230.41	640.3968	11544.09	36948.26	-2792.1528	127.32395	570.07	-6230.50	16383.78	-10543.24	-357.73	70.33	17774.58	20564.47
7699	48.4	39.51	-13466.3	-289.77	629.2876	12002.51	36965.99	-2775.8279	115.17853	575.22	-6362.46	16456.38	-10690.51	-404.95	54.06	18364.97	20509.61
7699	48.4	39.51	-13467.7	-291.56	629.2876	12005.06	36968.53	-2773.85	110.38596	575.22	-6366.05	16452.78	-10693.89	-401.95	54.06	18371.11	20515.75
7366	48.41	39.55	-13588.2	-340.41	615.733	12492.96	36918.74	-2762.4487	95.782461	579.64	-6474.43	16519.70	-10825.77	-436.19	36.09	18967.40	20399.04
7365	48.42	39.59	-13710.7	-390.91	599.9881	13028.00	36829.18	-2748.7519	80.449114	583.46	-6574.97	16570.43	-10961.97	-471.36	16.53	19602.97	20258.75
7364	48.43	39.63	-13830.8	-438.21	582.1668	13599.79	36694.01	-2732.8883	60.719639	586.5	-6664.13	16601.91	-11097.91	-498.93	-4.33	20263.93	20092.10
7363	48.44	39.67	-13944	-477.46	562.4458	14196.75	36508.64	-2714.9867	32.927754	588.55	-6737.43	16610.11	-11229.00	-510.39	-26.11	20934.17	19898.54

After EQ								Before EQ					Difference in forces			Difference in stress	
						Normal stress at extrados	Normal stress at inttrados				Normal stress at extrados	Normal stress at inttrados					
Node	X	Y	N	Q	M	σ_{ex} = N/t+6M/t^2	σ_{in} = N/t+6M/t^2	N	Q	M	σ_{ex} = N/t+6M/t^2	σ_{in} = N/t+6M/t^2	N	Q	M	σ_{ex}	σ_{in}
	[m]	[m]	[kN/m]	[kN/m]	[kNm/m]	[kN/m^2]	[kN/m^2]	[kN/m]	[kN/m]	[kNm/m]	[kN/m^2]	[kN/m^2]	[kN/m]	[kN/m]	[kNm/m]	[kN/m^2]	[kN/m^2]
7363	48.44	39.67	-13946.1	-479.56	562.4458	14200.57	36512.46	-2716.9132	34.135265	588.55	-6733.93	16613.61	-11229.17	-513.70	-26.11	20934.49	19898.85
7359	48.45	39.72	-14058.2	-518.98	540.9811	14830.16	36290.57	-2700.7357	11.544347	589.6	-6784.04	16604.90	-11357.46	-530.52	-48.62	21614.20	19685.67
7358	48.46	39.76	-14171.1	-556.88	517.8567	15494.10	36037.18	-2682.6699	-18.442494	589.41	-6813.29	16568.45	-11488.43	-538.44	-71.56	22307.39	19468.72
7357	48.47	39.8	-14285	-594.56	493.1015	16192.19	35753.24	-2664.6067	-46.140286	588.04	-6818.93	16508.41	-11620.39	-548.42	-94.94	23011.12	19244.83
7893	48.48	39.84	-14400.1	-633.32	466.7276	16924.54	35439.35	-2648.4368	-61.864059	585.64	-6800.74	16431.42	-11751.63	-571.45	-118.92	23725.28	19007.93
5375	45	37	-4865.04	89.5353	-5.7E-07	8845.53	8845.53	-2204.9337	13.64138	0	4008.97	4008.97	-2660.11	75.89	0.00	4836.56	4836.56
5374	45.04	37	-4859.31	102.44	4.034476	8755.08	8915.13	-2198.0066	24.274229	0.824	3980.03	4012.72	-2661.30	78.17	3.21	4775.05	4902.41
5373	45.09	37	-4805.19	137.192	9.297009	8552.31	8921.12	-2192.9885	34.903867	2.1183	3945.24	4029.27	-2612.21	102.29	7.18	4607.08	4891.85
5372	45.13	37	-4738.09	175.059	16.04494	8296.46	8932.95	-2190.5715	44.908225	3.859	3906.31	4059.40	-2547.52	130.15	12.19	4390.15	4873.55
5371	45.17	37	-4693.38	197.307	24.2872	8051.70	9015.16	-2191.448	53.665236	6.0143	3865.16	4103.74	-2501.94	143.64	18.27	4186.54	4911.41
5371	45.17	37	-4721.58	197.367	24.2872	8102.95	9066.41	-2192.0423	53.995293	6.0143	3866.24	4104.82	-2529.53	143.37	18.27	4236.71	4961.59
4834	45.22	37	-4697.4	226.043	33.51482	7875.97	9205.48	-2193.4791	63.006982	8.5648	3818.26	4158.02	-2503.92	163.04	24.95	4057.70	5047.45
4833	45.26	37	-4678.53	254.19	43.99126	7633.87	9378.98	-2196.2534	71.897293	11.506	3764.96	4221.41	-2482.28	182.29	32.48	3868.91	5157.56
4832	45.31	37.01	-4664.79	281.273	55.66858	7377.27	9585.61	-2200.2924	80.72384	14.834	3706.29	4294.77	-2464.50	200.55	40.83	3670.97	5290.84
4831	45.35	37.01	-4655.98	306.756	68.4921	7106.89	9823.93	-2205.5235	89.544236	18.545	3642.21	4377.88	-2450.45	217.21	49.95	3464.69	5446.05
4831	45.35	37.01	-4654.55	307.992	68.4921	7104.30	9821.34	-2205.3954	89.485908	18.545	3641.97	4377.65	-2449.16	218.51	49.95	3462.33	5443.69
4802	45.39	37.01	-4639.92	332.334	82.44257	6800.99	10071.44	-2211.7202	97.651703	22.632	3572.40	4470.22	-2428.20	234.68	59.81	3228.58	5601.22
4801	45.44	37.01	-4631.77	357.37	97.48217	6487.86	10354.92	-2218.7657	103.43767	27.025	3498.08	4570.16	-2413.00	253.93	70.46	2989.78	5784.76
4800	45.48	37.01	-4628.92	382.508	113.6121	6162.75	10669.67	-2226.5299	106.88426	31.62	3421.07	4675.40	-2402.39	275.62	81.99	2741.68	5994.27
4799	45.52	37.02	-4630.18	407.152	130.8262	5823.61	11013.41	-2235.0104	108.03194	36.312	3343.42	4783.89	-2395.17	299.12	94.51	2480.19	6229.52
4799	45.52	37.02	-4634.49	403.294	130.8262	5831.44	11021.24	-2234.9427	108.20116	36.312	3343.30	4783.77	-2399.54	295.09	94.51	2488.14	6237.47
4763	45.57	37.02	-4628.07	431.893	149.0839	5457.64	11371.72	-2244.0959	107.64433	41.022	3266.52	4893.83	-2383.98	324.25	108.06	2191.12	6477.89
4762	45.61	37.02	-4623.15	448.219	168.3	5067.54	11743.90	-2253.7824	105.64485	45.677	3191.80	5003.77	-2369.36	342.57	122.62	1875.74	6740.13
4761	45.65	37.02	-4623.42	455.235	188.0402	4676.49	12135.94	-2264.0088	102.28951	50.216	3120.37	5112.39	-2359.41	352.95	137.82	1556.12	7023.54
4767	45.7	37.03	-4632.61	455.903	207.9097	4299.09	12546.75	-2274.7819	97.665104	54.578	3053.43	5218.50	-2357.82	358.24	153.33	1245.66	7328.24
4767	45.7	37.03	-4628.05	457.945	207.9097	4290.82	12538.47	-2274.7746	97.719819	54.578	3053.42	5218.49	-2353.28	360.22	153.33	1237.40	7319.98
4204	45.74	37.03	-4631.56	455.383	227.7609	3903.44	12938.58	-2286.1005	92.04239	58.717	2991.91	5321.18	-2345.46	363.34	169.04	911.53	7617.40
4203	45.78	37.04	-4636.9	454.496	247.6733	3518.20	13343.25	-2297.9466	85.425292	62.59	2936.64	5419.53	-2338.95	369.07	185.08	581.56	7923.72
4202	45.83	37.04	-4647.46	442.494	267.2385	3149.34	13750.53	-2310.3393	77.901561	66.154	2888.47	5512.77	-2337.12	364.59	201.08	260.87	8237.76
4201	45.87	37.04	-4666.63	406.589	285.878	2814.47	14155.09	-2323.305	69.50423	69.37	2848.26	5600.12	-2343.32	337.08	216.51	-33.79	8554.96
4201	45.87	37.04	-4653.23	413.241	285.878	2790.12	14130.73	-2323.2964	69.512544	69.37	2848.24	5600.11	-2329.94	343.73	216.51	-58.12	8530.63
4181	45.91	37.05	-4676.12	383.972	303.241	2487.34	14516.73	-2336.857	60.304268	72.202	2816.72	5680.94	-2339.26	323.67	231.04	-329.38	8835.79
4180	45.96	37.05	-4686.63	353.525	319.3518	2186.90	14855.40	-2351.0237	50.261267	74.616	2794.60	5754.57	-2335.61	303.26	244.74	-607.70	9100.83
4179	46	37.06	-4689.63	317.627	333.9945	1901.91	15151.28	-2365.8083	39.378556	76.574	2782.66	5820.28	-2323.82	278.25	257.42	-880.74	9331.00
4185	46.04	37.06	-4689.96	272.006	346.8961	1646.61	15407.78	-2381.2228	27.651152	78.037	2781.65	5877.35	-2308.73	244.35	268.86	-1135.04	9530.43
4185	46.04	37.06	-4693.83	273.91	346.8961	1653.65	15414.82	-2381.1947	27.623884	78.037	2781.59	5877.29	-2312.63	246.29	268.86	-1127.95	9537.52
4175	46.09	37.07	-4716.77	232.758	357.9785	1475.55	15676.35	-2397.238	15.033179	78.971	2792.26	5924.97	-2319.53	217.72	279.01	-1316.71	9751.38
4174	46.13	37.07	-4736.81	181.681	367.0441	1332.17	15892.59	-2413.8274	1.4791706	79.334	2815.21	5962.35	-2322.98	180.20	287.71	-1483.04	9930.25
4173	46.17	37.08	-4752.03	121.693	373.6945	1227.93	16052.17	-2430.9649	-13.056277	79.085	2851.30	5988.57	-2321.06	134.75	294.61	-1623.37	10063.60
4619	46.22	37.09	-4760.52	53.8085	377.5439	1167.02	16143.97	-2448.6527	-28.591298	78.181	2901.39	6002.80	-2311.87	82.40	299.36	-1734.38	10141.17
4619	46.22	37.09	-4753.84	69.1538	377.5439	1154.87	16131.81	-2448.6063	-28.645009	78.181	2901.31	6002.71	-2305.23	97.80	299.36	-1746.44	10129.10
4615	46.26	37.09	-4782.53	-6.7978	378.9134	1179.87	16211.15	-2466.937	-45.175422	76.577	2966.46	6004.22	-2315.59	38.38	302.34	-1786.59	10206.93
4614	46.3	37.1	-4797.87	-84.88	376.9174	1247.35	16199.45	-2485.7079	-62.86306	74.225	3047.24	5991.70	-2312.16	-22.02	302.69	-1799.89	10207.75
4613	46.35	37.11	-4814.71	-164.46	371.4889	1385.65	16122.39	-2504.9415	-81.655028	71.078	3144.62	5964.26	-2309.77	-82.80	300.41	-1758.98	10158.14
4635	46.39	37.11	-4847.92	-244.89	362.5677	1622.98	16005.83	-2524.6603	-101.49843	67.09	3259.58	5921.00	-2323.26	-143.40	295.48	-1636.60	10084.82
4635	46.39	37.11	-4804.65	-233.78	362.5677	1544.31	15927.16	-2524.656	-101.46732	67.09	3259.57	5921.00	-2280.00	-132.31	295.48	-1715.26	10006.16
4638	46.43	37.12	-4817.38	-325.95	350.2726	1811.31	15706.42	-2544.7985	-122.48196	62.213	3392.94	5860.88	-2272.58	-203.47	288.06	-1581.62	9845.55
4637	46.48	37.13	-4808.49	-399.3	334.4372	2109.25	15376.18	-2565.3508	-144.47587	56.396	3545.68	5782.87	-2243.14	-254.82	278.04	-1436.43	9593.31
4636	46.52	37.13	-4782.06	-461.38	315.6112	2434.59	14954.70	-2586.3578	-167.5278	49.597	3718.73	5686.21	-2195.70	-293.85	266.01	-1284.14	9268.50
5223	46.56	37.14	-4742.13	-519.76	294.2426	2785.84	14458.27	-2607.8645	-191.71651	41.772	3913.04	5570.10	-2134.26	-328.04	252.47	-1127.21	8888.17
5223	46.56	37.14	-4726.07	-513.97	294.2426	2756.64	14429.07	-2607.8143	-191.69163	41.772	3912.95	5570.01	-2118.26	-322.28	252.47	-1156.31	8859.06
5219	46.6	37.15	-4673.81	-576.74	270.3576	3135.37	13860.30	-2629.7424	-216.73139	32.875	4129.28	5433.42	-2044.07	-360.01	237.48	-993.91	8426.88
5218	46.65	37.16	-4581.34	-623.2	244.2263	3485.54	13173.86	-2652.1055	-242.93611	22.856	4368.67	5275.35	-1929.23	-380.26	221.37	-883.12	7898.50
5217	46.69	37.17	-4475.86	-668.07	216.0282	3853.07	12422.78	-2674.8872	-270.20942	11.672	4631.92	5094.94	-1800.97	-397.86	204.36	-778.85	7327.84
5313	46.73	37.18	-4384.59	-726.06	185.7467	4287.75	11656.22	-2698.0714	-298.45497	-0.719	4919.84	4891.33	-1686.52	-427.61	186.47	-632.08	6764.88
5313	46.73	37.18	-4327.89	-695.01	185.7467	4184.65	11553.12	-2698.061	-298.32788	-0.719	4919.82	4891.31	-1629.82	-396.69	186.47	-735.17	6661.80
5309	46.77	37.18	-4264	-774.67	153.6589	4704.95	10800.51	-2721.7279	-327.42887	-14.35	5233.28	4663.91	-1542.27	-447.24	168.01	-528.33	6136.59
5308	46.82	37.19	-4189.33	-843.57	118.3666	5269.19	9964.73	-2745.7227	-357.38846	-29.28	5573.02	4411.42	-1443.61	-486.18	147.65	-303.83	5553.31
5307	46.86	37.2	-4102.65	-906.75	80.16973	5869.22	9049.51	-2770.1186	-388.13698	-45.53	5939.73	4133.43	-1332.53	-518.61	125.70	-70.51	4916.09
5323	46.9	37.21	-4002.76	-969.22	39.30047	6498.22	8057.25	-2794.989	-419.60471	-63.14	6334.08	3829.52	-1207.77	-549.62	102.44	164.15	4227.73
5323	46.9	37.21	-4023.33	-972.39	39.30047	6535.64	8094.67	-2794.9575	-419.59028	-63.14	6334.02	3829.46	-1228.38	-552.80	102.44	201.62	4265.21
5303	46.95	37.22	-3930.2	-1052	-4.69913	7239.03	7052.62	-2820.2997	-451.79627	-82.12	6756.73	3498.90	-1109.90	-600.22	77.43	482.30	3553.72
5302	46.99	37.23	-3864.11	-1137.1	-52.5783	8068.53	5982.78	-2846.104	-484.53835	-102.5	7208.57	3140.90	-1018.01	-652.51	49.96	859.97	2841.88
5301	47.03	37.24	-3783.22	-1200.6	-103.555	8932.55	4824.60	-2872.3038	-517.71698	-124.4	7689.61	2755.13	-910.91	-682.84	20.84	1242.94	2069.46
5345	47.07	37.25	-3645.67	-1215.6	-156.489	9732.42	3524.58	-2898.8326	-551.2326	-147.7	8199.91	2341.30	-746.84	-664.36	-8.80	1532.51	1183.28
5345	47.07	37.25	-3656.51	-1202.2	-156.489	9752.11	3544.27	-2898.9372	-551.87538	-147.7	8200.10	2341.49	-757.57	-650.31	-8.80	1552.01	1202.79
5341	47.11	37.26	-3541.97	-1256.7	-209.488	10595.08	2284.82	-2926.7422	-587.45847	-172.5	8742.87	1899.82	-615.23	-669.23	-36.99	1852.21	384.99
5340	47.16	37.27	-3453.11	-1371.3	-267.19	11578.01	978.75	-2955.3784	-626.91557	-199	9319.87	1426.96	-497.73	-744.37	-68.22	2258.13	-448.21
5339	47.2	37.28	-3422.3	-1446.6	-328.515	12738.36	-293.62	-2985.1071	-670.07039	-227.2	9934.55	920.38	-437.20	-776.53	-101.28	2803.81	-1214.00
5355	47.24	37.3	-3481.96	-1383.2	-391.063	14087.44	-1425.79	-3016.1897	-716.74665	-257.4	10590.32	377.64	-465.77	-666.46	-133.62	3497.12	-1803.43
5355	47.24	37.3	-3294.1	-1444.9	-391.063	13745.89	-1767.34	-3016.2005	-717.15258	-257.4	10590.34	377.66	-277.90	-727.79	-133.62	3155.55	-2145.00
5335	47.28	37.31	-3207.69	-1502.7	-454.859	14854.16	-3189.82	-3048.8418	-767.37241	-289.8	11290.93	-204.24	-158.85	-735.32	-165.08	3563.22	-2985.59
5334	47.33	37.32	-3151.71	-1619.9	-523.11	16106.11	-4645.35	-3083.5161	-823.69709	-324.4	12041.71	-828.93	-68.19	-796.24	-198.66	4064.39	-3816.43
5333	47.37	37.33	-3119.48	-1735.6	-596.119	17495.62	-6152.05	-3120.133	-885.57202	-361.7	12847.06	-1501.12	0.65	-849.99	-234.42	4648.57	-4650.93
5487	47.41	37.34	-3104.35	-1788.4	-673.378	19000.53	-7711.97	-3158.6025	-952.44259	-401.7	13711.23	-2225.40	54.25	-835.98	-271.64	5289.30	-5486.57

After EQ								Before EQ					Difference in forces			Difference in stress	
						Normal stress at extrados	Normal stress at inttrados				Normal stress at extrados	Normal stress at inttrados					
Node	X	Y	N	Q	M	σ_{ex} = N/t+6M/t^2	σ_{in} = N/t+6M/t^2	N	Q	M	σ_{ex} = N/t+6M/t^2	σ_{in} = N/t+6M/t^2	N	Q	M	σ_{ex}	σ_{in}
	[m]	[m]	[kN/m]	[kN/m]	[kNm/m]	[kN/m^2]	[kN/m^2]	[kN/m]	[kN/m]	[kNm/m]	[kN/m^2]	[kN/m^2]	[kN/m]	[kN/m]	[kNm/m]	[kN/m^2]	[kN/m^2]
5487	47.41	37.34	-3083.93	-1836	-673.378	18963.40	-7749.10	-3158.3397	-952.51356	-401.7	13710.75	-2225.88	74.41	-883.47	-271.64	5252.65	-5523.23
5483	47.45	37.35	-2886.05	-1584.3	-744.864	20021.53	-9526.80	-3198.4403	-1024.4839	-444.8	14637.91	-3007.21	312.39	-559.86	-300.06	5383.63	-6519.59
5482	47.49	37.37	-2825.13	-1734.8	-818.435	21370.03	-11096.82	-3239.3992	-1100.9656	-491.1	15631.33	-3851.70	414.27	-633.83	-327.30	5738.70	-7245.12
5481	47.53	37.38	-2798.08	-1860.2	-895.801	22855.36	-12680.54	-3281.1415	-1181.4312	-540.9	16693.97	-4762.54	483.07	-678.76	-354.92	6161.40	-7918.00
5497	47.58	37.39	-2701.78	-1533.4	-972.999	24211.48	-14386.82	-3323.5923	-1265.3531	-594.2	17828.64	-5742.85	621.81	-268.04	-378.80	6382.84	-8643.96
5497	47.58	37.39	-2614.59	-1615.9	-972.999	24052.94	-14545.36	-3323.3433	-1265.5463	-594.2	17828.19	-5743.31	708.76	-350.34	-378.80	6224.75	-8802.05
5477	47.62	37.41	-2364.7	-1157.6	-1032.28	24774.40	-16175.49	-3366.095	-1352.7703	-651.2	19037.50	-6797.15	1001.40	195.17	-381.03	5736.90	-9378.34
5476	47.66	37.42	-2244.83	-961.63	-1077.89	25461.14	-17298.12	-3408.4289	-1443.3514	-712.2	20323.52	-7929.23	1163.60	481.72	-365.68	5137.62	-9368.88
5475	47.7	37.43	-2214.23	-970.28	-1119.12	26223.27	-18171.54	-3450.2937	-1537.0331	-777.2	21688.32	-9141.79	1236.07	566.76	-341.94	4534.95	-9029.74
5603	47.74	37.45	-2232.13	-1125.8	-1164.49	27155.64	-19038.82	-3491.6378	-1633.5592	-846.3	23133.90	-10437.03	1259.51	507.71	-318.22	4021.74	-8601.79
5603	47.74	37.45	-2176.45	-1068	-1164.49	27054.41	-19140.05	-3491.0253	-1634.2316	-846.3	23132.78	-10438.14	1314.58	566.22	-318.22	3921.63	-8701.91
5606	47.78	37.46	-2268.94	-1239.3	-1215.36	28231.58	-19980.90	-3532.7523	-1732.8109	-919.6	24663.47	-11817.10	1263.82	493.54	-295.74	3568.11	-8163.80
5605	47.82	37.47	-2334.72	-1353	-1271.46	29463.96	-20974.06	-3572.5479	-1840.1594	-997.5	26280.50	-13289.41	1237.82	487.14	-273.97	3183.47	-7684.64
5604	47.87	37.49	-2426.33	-1510.4	-1333.99	30870.88	-22047.86	-3609.6279	-1955.7182	-1080	27988.88	-14862.96	1183.30	445.35	-253.77	2882.00	-7184.90
5613	47.91	37.5	-2596.27	-1812.4	-1405.51	32598.34	-23157.37	-3643.208	-2078.9283	-1168	29793.54	-16545.51	1046.94	266.50	-237.38	2804.81	-6611.86
			Maximum compressive stress			**76,632.69**	**36,968.53**				**29,979.89**	**16,613.61**	**1,314.58**	**1,731.66**	**1,143.67**	**50,569.84**	**29,763.89**
			Maximum tensile stress			**-3304.04**	**-23157.37**				**-6818.93**	**-16545.51**	**-16481.74**	**-1154.13**	**-1149.00**	**-16639.81**	**-9378.34**